Development of Bloodmeal Protein Thermoplastic Blends

A thesis

submitted in fulfilment

of the requirements for the degree

of

Doctor of Philosophy in Engineering

at

The University of Waikato

by

KU MARSILLA

THE UNIVERSITY OF
WAIKATO
Te Whare Wānanga o Waikato

2015

Abstract

This study investigated the compatibilization of Novatein® Thermoplastic Protein (NTP) blends with other polymers. NTP was blended with three different types of polymers; a petroleum-based polyolefin, (low-linear density polyethylene, LLDPE); a biodegradable synthetic polyester, (polybutylene succinate, PBS) and a bioderived, compostable polyester, (poly (lactic acid), PLA). It was a relatively straightforward process to produce a compatible blend of LLDPE and NTP using a compatibilizer, regardless of the obvious difference in chemical structure between these polymers. Blending NTP with PBS, on the other hand, was much more challenging. It required two compatibilizers, added at different stages of blending to produce a compatible blend. For blends with PLA, a novel copolymer, itaconic anhydride grafted PLA (PLA-g-IA) was produced to be used as a compatibilizer and initial results suggested that PLA-g-IA may be a successful approach.

Two different methods of compatibilization pathways were explored: the addition of a graft copolymer based on one of the components (in the case of NTP/LLDPE blends) or using compatibilizers that are not chemically the same as either component (in the case of NTP/PBS blends). Polyethylene grafted maleic anhydride (PE-g-MAH) was added to NTP/LLDPE blends and produced a blend with synergistic mechanical properties (the elongation at break exceeded the raw LLDPE properties). The water resistance of NTP was improved after blending with LLDPE, but it may compromise the compostability of the material. For NTP/PBS blends, two compatibilizers with different functional end-groups were

i

used; these were (poly-2-ethyl-2-oxazoline)(PEOX) and (polymeric diphenyl diisocyanate)(pMDI). Using either of the compatibilizers individually in blends containing 50 % NTP resulted in poor mechanical properties. Compatibilization was accomplished with the addition of both two compatibilizers at different stages of blend preparation; PEOX dissolved in water and added during NTP production, while pMDI was added during injection moulding. This approach led to a tensile strength greater than that of pure PBS (24 MPa compared to 22 MPa). Dissolving PEOX in water improved the dispersion of the NTP phase throughout the PBS matrix via hydrogen bonding between water, PEOX and NTP. The addition of pMDI during injection moulding stabilized and strengthened the interactions between PBS and NTP, thereby leading to a superior blend.

The compatibility between NTP and LLDPE or NTP and PBS were characterized using thermal and morphological properties as well as water resistance. Two T_gs were obtained for all blends, however, the addition of compatibilizers improved the adhesion between phases, evident from broader and lower height of T_g peaks. The morphology provided evidence of a homogenous dispersion of NTP in LLDPE. In NTP/PBS blends, the fracture mechanism changed from brittle to ductile with the addition of PEOX. Both NTP/LLDPE and NTP/PBS blends showed a phase inversion from a particle- dispersed morphology to a co-continuous morphology at compositions greater than 50% NTP. The water resistance also improved with the addition of LLDPE and PBS.

Reactive extrusion was used to produce a copolymer, itaconic anhydride grafted poly (lactic acid) (PLA-g-IA). Different initiator (dicumyl peroxide) and monomer (IA) concentrations were used to optimize the degree of grafting. 0.75% was the highest degree of grafting and showed minimal chain scission evident

from the polymer's intrinsic viscosity. The reaction kinetics of grafting and the effect of grafting on thermal and mechanical properties were investigated. Grafting increased the crystallization rate of PLA, increased the crystallinity and also raised the thermal decomposition temperature. The mechanical properties of PLA-g-IA blended with PLA were also improved.

Crystallization of PLA and PLA-g-IA were investigated during annealing at different annealing temperatures and durations using differential scanning calorimetry (DSC) and wide angle X-ray scattering (WAXS). The rate of crystallization increased after grafting and affected the formation of PLA crystals by increasing the lattice spacing at the (110) plane, suggesting an expanded helical structure of PLA. The crystallinity of PLA-g-IA was also higher than that of neat PLA.

Although polymer blending offers an attractive route to modify selected polymer properties, it is not always successful without the addition of compatibilizers. Despite the subtle differences in methods to incorporate compatibilizers, development of NTP blends with different polymers, whether a petroleum based polymer, synthetic biodegradable polyester or bioderived compostable polyester, offers material with improved mechanical properties and thermal stability. Water resistance is also improved, however, biodegradability will likely be compromised if the second polymer is not also biodegradable. These blends offer a potentially wider range of commercial NTP grades.

Acknowledgements

Doctoral study is truly a collective endeavor of learning. It always seems impossible until it is done. I have been blessed with support and encouragement from within networks of social relationships. Therefore, I would like to thank the many people who have supported me over the past years. First and foremost I would like to thank my chief supervisor Dr Johan Verbeek for his constant enthusiasm and tireless effort in supervising this project. I would like to thanks my co-supervisors, Dr Mark Lay and Professor Kim Pickering for their support over the duration of this project.

I would also like to thank School of Engineering technical officers who provided the technical assistance for my research especially Chris Wang, Brett Nichols, Yuanzi Zhang, Helen Turner and Lisa Lee. I would also like to convey my sincere thanks to the Department of Engineering Secretary Mary Dalbeth who was always ready to help me with a smile.

I have been blessed with being a part of a great research group, thank you and well-wishers to Jim Bier, Kavwa, Talia Hicks, Matt, Jussi, Herman, Anu and Chanelle. I would also like to acknowledge some of the short termers, Aarthi and Dennis for your comradery and help in the lab.

A special thank to my soul mate Raa Khimi and my daughter Raaesya Zahra. They are my inspiration and my driving force. I owe them everything and wish I could show them just how much I love and appreciate them. I wish to thank my parents, my in-laws, brothers and sisters for their pray and unconditional support. I would never have been able to accomplish any of my

Preface

This thesis is a PhD with publication submitted as a fulfillment of the requirements for the Doctor of Philosophy at The University of Waikato. This thesis include chapters comprising a thesis introduction which provides the contextual framework and overview of the thesis, a literature review, five journal papers, followed by a concluding discussion chapter highlighting the overall contribution of the published papers.

The journal papers are listed as follows:

1) Ku Marsilla, K.I., & Verbeek, C. J. R. (2013). Properties of Bloodmeal/Linear Low-density Polyethylene Blends Compatibilized with Maleic Anhydride Grafted Polyethylene. *Journal of Applied Polymer Science*, Volume 130, Issue 3, Pages 1890-1897

2) Ku Marsilla, K. I., & Verbeek, C. J. R. (2014). Mechanical Properties of Thermoplastic Protein From Bloodmeal and Polyester Blends. *Macromolecular Materials and Engineering.* Volume 299, Issue 7, pages 885–895

3) Ku Marsilla, K. I., & Verbeek, C. J. R. (2015). Compatibilization of Protein Thermoplastics and Polybutylene Succinate Blends. *Macromolecular Materials and Engineering.*, Volume 300, pages 161–171

4) Ku Marsilla, K. I., & Verbeek, C. J. R. (2015). Modification of poly (lactic acid) using itaconic anhydride by reactive extrusion. *European Polymer Journal.*,Volume 67, June 2015, pages 213–223

5) Ku Marsilla, K. I., & Verbeek, C. J. R. (2014). Crystallization of itaconic anhydride grafted poly (lactic acid). *Macromolecular Materials and Engineering* Submitted..

As first author for these papers, I prepared the initial draft manuscript, which was refined and edited in consultation with my supervisor, who has been credited as co-author.

Listed below are other publications that are not included in this thesis including a book chapter and conferences papers.

Book Chapter

Biodegradable Plastic from Blood Meal (2013)

Author/s: K.I. Ku Marsilla, C.J.R. Verbeek

Category: Chapter in A Book: (Diversity of Research for a Sustainable Challenging World: A compilation of research by Malaysian postgraduates in New Zealand)

Publisher: Chair of Malay Studies, Victoria University of Wellington

Conferences

Title: Properties of blends of Novatein thermoplastic protein from bloodmeal and polybutylene succinate Using Two compatibilizers (2013)

Author/s: K.I. Ku Marsilla, C.J.R. Verbeek

Category: Full paper conference (International Conference on Chemical Engineering and Process Engineering (ICCPE, 2013)

Publisher: International Journal of Chemical Engineering and Applications

Title: Preparation and Characterization of Itaconic Anhydride Functionalized Polylactic Acid using Reactive Extrusion (2013)

Author/s: K.I. Ku Marsilla, C.J.R. Verbeek

Category: Full paper conference (NZ Conference of Chemical and Materials Engineering 2013)

Title: Polymer Blends from Blood Based Plastic (2012)

Author/s: K.I. Ku Marsilla, C.J.R. Verbeek

Category: Full paper conference (International Malaysia Research Conference in Auckland 2012 & Sub-Conference: Saudi-Malaysia Research Studies Conference)

Title: Blends of Linear-low-density Polyethylene and Thermoplastic Bloodmeal using Maleic Anhydride Grafted Polyethylene as Compatibilizer (2012)

Author/s: K.I. Ku Marsilla, C.J.R. Verbeek

Category: Full paper conference (Quality of Life through Chemical Engineering, CHEMECA 2012)

Title: Development of Blood Meal Protein Thermoplastic (2011)

Author/s: K.I. Ku Marsilla, C.J.R. Verbeek

Category: Extended Abstract conference (SCENZ-IChemE annual conference in New Zealand, 2011)

Table of Contents

Chapter 1

Introduction

Introduction

Recent development of biodegradable polymers has greatly been driven by a desire to replace synthetic plastics. More recently, Novatein® Thermoplastic Protein (NTP) have been developed from by-products of animal rendering (bloodmeal) which do not compete with human food, such as raw materials used for biofuel production.[1] NTP is currently being commercialized by Aduro Biopolymers LP.[2]

Bloodmeal is produced by steam coagulating, dewatering and drying animal blood into a powder with at least 85 wt% protein and less than 10% moisture, and is used as a fertilizer or as a pet food additive in low quantities. Efficient utilization is required to reduce the impact on the environment and to increase income by finding higher value applications. Transformation of bloodmeal into NTP involves the addition of water (plasticizer), a denaturant (urea), a reducing agent (sodium sulfite, SS) and a surfactant (sodium dodecylsulfate, SDS).[3, 4] These additives break covalent crosslinking and reduce hydrophobic and hydrogen bonding between chains and allow the formation of new interactions after processing. The resulting material consolidates during extrusion, and can be injection moulded and formed into products. Products that can be produced from protein-based thermoplastics include seedling trays, biodegradable plant pots, vine clips, containers and pegs.

NTP is easily composted due to the hydrophillic nature of protein. It is sensitive towards moisture, capable of breaking down in a matter of weeks in high humidity, or even days when immersed in water. This makes NTP an ideal starting material as biodegradable-based polymers especially in polymer blends.[5]

However, the mechanical properties of NTP are not exceptional. One of the most apparent limitations of NTP is brittleness. Although water is an efficient plasticizer to increase toughness, during production and storage, water desorbs from the moulded plastic over time and makes the materials brittle. TEG has been used as plasticizer in addition to water, but it has been shown that the tensile strength and the modulus of the materials are lower than desirable.[6]

Blending is an interesting option that offers the possibility to develop new materials with more desirable properties. Among the reasons for the popularity of polymer blends is the versatility in tailoring the end products' properties; whether to produce synergistic combinations of two components, such as high modulus and toughness, improving water-resistance, biodegradability and recycling or to lower costs. For instance, in the packaging industry, excellent mechanical properties are required as well as, for example water-resistance. The hydrophilic nature of NTP could potentially be manipulated by blending it with hydrophobic polymers, offering an excellent combination of mechanical properties from two different polymers whilst maintaining some of its biodegradation. Although the rate of decomposition of the materials might be compromised, optimal formulation in terms of composition could minimize these concerns.

However, polymer blending is one of those things that is "easier said than done". Developing miscible blends has been proven to be a daunting task where the principal challenges include the variability in the morphology obtained, possible reduction in thermal stability and mechanical properties.

This study was done to explore the potential of blending NTP with other thermoplastics using extrusion to improve NTP's material properties. The

objective of this study was to investigate the influence of blending NTP with three different types of polymers:

1. blending with petroleum based polymers; low-linear density polyethylene (LLDPE)

2. blending with biodegradable synthetic polymers; polybutylene succinate (PBS) and

3. a bioderived, compostable polymer, namely polylactic acid (PLA).

More specifically, the goals of the study were to develop an understanding of interactions between NTP and other polymers that influences the mechanical, thermal properties, water sensitivity, and morphology of the blends. In achieving this goal, processing conditions, compatibilization, morphology and mechanical properties were key issues, central to all of the blends studied.

The objectives were addressed in six chapters including a critical literature review and five journal papers:

Chapter 2 contains a critical review of current research within the scope of this research. This includes an overview of biodegradable polymers, proteins, the theory of polymer blending, factors influencing blend properties and characterization of compatibility.

In Chapter 3, the potential of blending NTP with linear low density polyethylene (LLDPE) was assessed. LLDPE is among the most popular synthetic polyolefin products, especially in agricultural and farming industry for products such as plastic films, seedling trays and containers. LLDPE is not biodegradable but has an exceptional elongation at break. By blending LLDPE with NTP, a reduction in the brittleness of NTP can be expected. A commercial grade of compatibilizer, polyethylene-*graft*-maleic anhydride (PE-g-MAH) was used to

improve compatibility. The mechanical properties of the blends was modeled to evaluate performance.

In Chapter 4, the potential of blending NTP with a synthetic biodegradable polymer (PBS) was assessed with the motivation to produce a completely biodegradable blend. Here, PBS was chosen because it has a similar range of processing conditions to NTP. Processing methods and compatibilization were assessed in light of using two different compatibilizer; poly-2-ethyl-2-oxazoline (PEOX) and polymeric diphenyl diisocyanate (pMDI). NTP compositions (0-100%) and concentration of compatibilizers (5-10%) on mechanical properties was investigated to optimize mechanical properties.

In Chapter 5, different methods to incorporate compatibilizers in PBS/NTP blends were investigated, by using the same processing conditions used in Chapter 4. It was postulated that the sequence in which the compatibilizers were added could further change the performance of the blends.

In Chapter 6, the potential of blending NTP with synthetic bioderived and biodegradable polymer (PLA) was assessed. PLA was chosen because it has high tensile strength, almost double that of PBS. However, it has a high melting temperature (T_m), at which NTP will degrade. Therefore, a suitable processing temperature is required. Considering the efficiency of maleic anhydride (MA) copolymers in NTP/LLDPE blends, a similar type of copolymer was considered as compatibilizer, except PLA-graft-maleic anhydride is not commercially available. The first objective of this chapter was to produce an itaconic anhydride grafted PLA (PLA-g-IA) copolymer. Itaconic anhydride was chosen as an alternative to MA as it is less harmful and is extremely stable when reacted to proteins.[7] To the author's knowledge, this is a novel copolymer (PLA-g-IA)

using IA as reactive groups. Free radical grafting of itaconic anhydride (IA) onto PLA was carried out using dicumyl peroxide (DCP) as initiator in a twin screw extruder. This chapter discusses work conducted to prepare and characterize PLA-g-IA that has the potential as a compatibilizer in PLA/protein blends, in terms of grafting kinetics, thermal and mechanical properties of the copolymer.

The complexity of blending proteins with PLA required further study into the behavior of the graft-copolymer on its own. In Chapter 7, assessment of the effect of grafting on the crystallization behavior of PLA was carried out using wide-Angle X-ray scattering (WAXS) and differential scanning calorimetry (DSC). Insight into crystallization of PLA after grafting is required for understanding the behavior of PLA during blending with proteins.

After the experimental chapters, the thesis concludes with a brief discussion, threading the material covered in the individual chapters into a single "Concluding remarks" chapter, including comments regarding on-going work and recommendations.

References

1. Pickering, K.L.H., NZ), Verbeek, Casparus Johannes Reinhard (Hamilton, NZ), Viljoen, Carmen (Howick, NZ), Van Den, Berg Lisa Eunice (Hamilton, NZ), *PLASTICS MATERIAL*, 2010, NOVATEIN LIMITED (Hamilton, NZ): United States.

2. *Developing and manufacturing bio-derived polymers and materials for local and export markets."*. Available from: http://www.adurobiopolymers.com/.

3. Verbeek, C.J.R. and L.E. van den Berg, *Development of Proteinous Bioplastics Using Bloodmeal.* Journal of Polymers and the Environment, 2010. **19**(1): p. 1-10.

4. Verbeek, C.J.R. and L.E. van den Berg, *Mechanical Properties and Water Absorption of Thermoplastic Bloodmeal.* Macromolecular Materials and Engineering, 2011. **296**(6): p. 524-534.

5. Verbeek, C.J.R. and L.E. van den Berg, *Extrusion Processing and Properties of Protein-Based Thermoplastics.* Macromolecular Materials and Engineering, 2010. **295**(1): p. 10-21.

6. Bier, J.M., C.J. Verbeek, and M.C. Lay, *Thermal and Mechanical Properties of Bloodmeal‑Based Thermoplastics Plasticized with Tri (ethylene glycol).* Macromolecular Materials and Engineering, 2014. **299**(1): p. 85-95.

7. Fischer, L. and F. Peißker, *A covalent two-step immobilization technique using itaconic anhydride.* Applied Microbiology and Biotechnology, 1998. **49**(2): p. 129-135.

Chapter 2

Literature review: Polymer blends

Polymer Blends

2.1 Introduction

Polymer blending is a well-used technique for polymer modification and has been one of the most prolific research areas in polymer science and technology in the past five decades.[1] The development of polymer blends has attracted attention for two major reasons. Firstly, from the plastic industry's point of view, blending is a much more effective and cheaper method to improve properties compared to synthesizing new polymers. Secondly, from an environmental point of view, blending polymers may offer potential solutions to growing pollution problems. However, blending synthetic polymers with biodegradable polymers only leads to disintegration of the material, reducing it to small particles. On the other hand, biodegradation is the ability of a material to be decomposed by the action of bacteria or other living organisms, leaving no trace of their original composition. Biodegradable polymers are often very expensive, or have inferior mechanical properties. Blending these with cheaper alternatives may offer a solution to the aforementioned problems.

Polymer blends using biodegradable materials have been studied extensively, with increased interest in their application in the agriculture, food and electronic industries. The global biodegradable plastics market is expected to grow from 664 thousand metric tons in 2010 to 2330 thousand metric tons in 2016.[2] Amongst all market segments, the starch-based plastic market has the largest share in volume, while PLA-based plastics lead the market in terms of revenue. These markets are expected to continue growing, driving demand for sustainable, eco-friendly biodegradable plastics in the coming decade.

In the U.S., the natural polymer market has been predicted to expand 6.9% annually and rise from $3.3 billion in 2012 to $4.6 billion in 2016.[2] Starch, protein-based polymers, and marine-based polymers lead the market in bio-based polymers. However, for natural polymers, most materials require chemical modification before it can be processed into thermoplastics. Starch for example, needs plasticizers such as water, glycerol, urea or glycol as well as heat and shear (processing) to be converted into a thermoplastic material. These plasticizers improve processability and prevent degradation.[3] Beside that, most natural polymers are hydrophilic or water soluble. Although it improves degradability, the presence of water usually compromises mechanical properties.

The use of biodegradable polymers in practical situations are often limited. Blending offers several distinct advantages such as better mechanical properties, water resistance and cost reduction without reducing biodegradability. However, it is well known that one of the most significant challenges for blending two different materials is compatibility. Selection of component materials, the processing method and interaction between the materials are still somewhat unresolved issues. Significant research on these issues is essential to overcoming limitations and will lead to improvement in material performance as well as fostering development of new applications.

Table 1 provides a summary of the primary purpose of blending proteins with other polymers. These include modification to be suitable for packaging or medical applications as well as improving mechanical properties and water sensitivity. In addition, cost saving is often the main purpose of blending with with low cost polymers or fillers.

Table 1: Summary of different objectives for making blends

Base polymer	Second component	Objectives				
		Packaging	Mechanical Property	Water sensitivity	Medical	Cost reduction
Soy protein	PLA	[4]		[5]		
Starch	PLA		[6]			
Soy meal	PBS					[7]
Starch	PBAT	[8]				
Soy protein	PBAT		[9]			
Soy protein	PCL	[10]				
Starch	PBS		[11]			
Protein	PEG				[12]	

2.2   Proteins

The purpose of this section is to briefly review some of the important notes on protein structure and sources of proteins.

2.2.1 Protein Structure

Natural proteins are linear and unbranched and have a precise length with a molecular diversity consisting up to 20 amino acids joined by peptide bonds, forming a polypeptide chain. The 20 amino acids are linked into proteins by the condensation of two amino acids as illustrated in Figure 1. The peptide bond is synthesized when the carboxyl group of one amino acid molecule reacts with the amino group of the other amino acid molecule, causing the release of a molecule of water (H_2O).
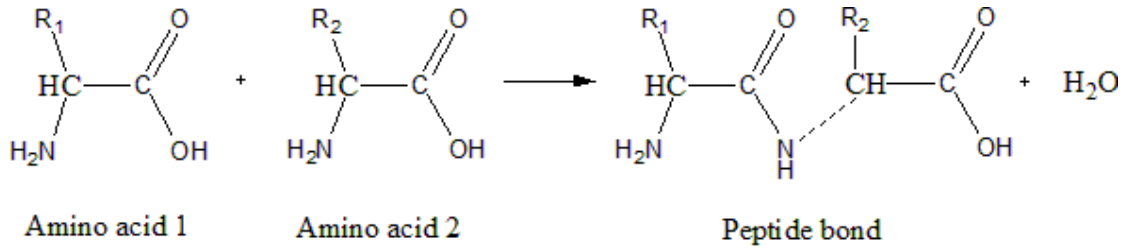
Figure 1:Condensation of two amino acids

Different amino acids interact differently with their environment and the physical properties of the protein are determined by the sequence of amino acid groups. Figure 2 shows the 20 different amino acids in the primary structure of a protein.

Cysteine and lysine are the most reactive amino acids. The cystine usually ionizes at slightly alkaline pH where it can react rapidly with alkyl halides to give stable alkyl derivatives. Cysteine residues play a valuable role by crosslinking proteins, which increase the rigidity of proteins. Amine group of lysine residues is active towards acylation, alkylation and amidination reactions

The amino acid functional groups can interact with other polymers to develop protein blends with enhanced properties such as toughness and strength. There are four targets functional groups for majority of crosslinking or chemical interactions as listed in Table 2.
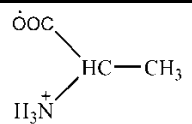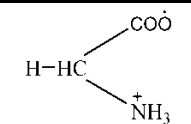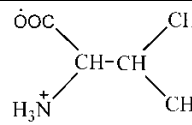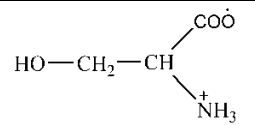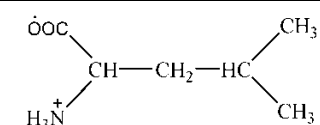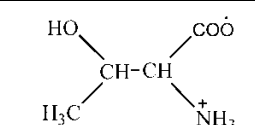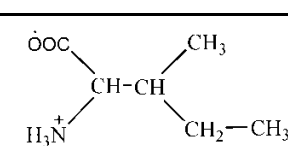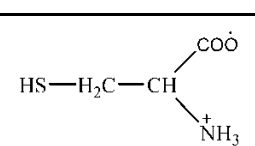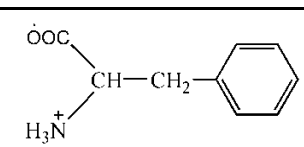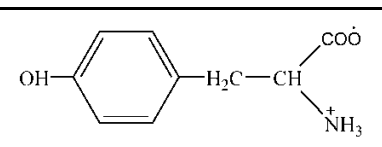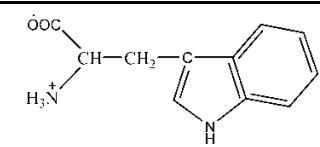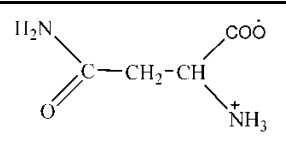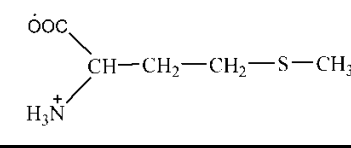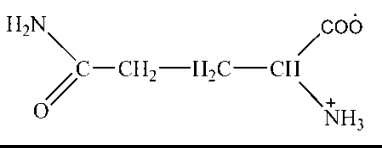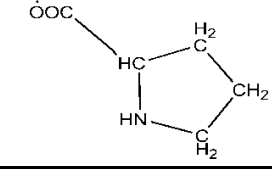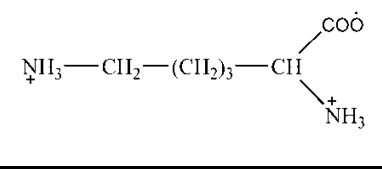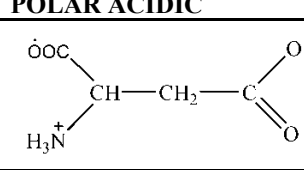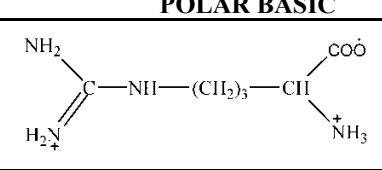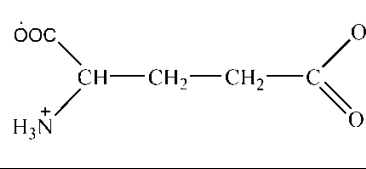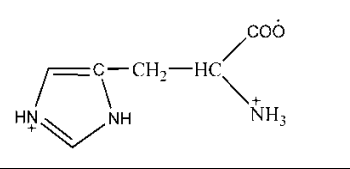
NONPOLAR, HYDROPHOBIC		POLAR, UNCHARGED	
Alanine	^-OOC $HC-CH_3$ H_3N^+	$H-HC$ COO^- NH_3^+	Glycine
Valine	^-OOC $CH-CH$ CH_3 H_3N^+ CH_3	$HO-CH_2-CH$ COO^- NH_3^+	Serine
Leucine	^-OOC $CH-CH_2-HC$ CH_3 H_3N^+ CH_3	HO $CH-CH$ COO^- H_3C NH_3^+	Threonine
Isoleucine	^-OOC $CH-CH$ CH_3 H_3N^+ CH_2-CH_3	$HS-H_2C-CH$ COO^- NH_3^+	Cysteine
Phenylalanine	^-OOC $CH-CH_2$ H_3N^+	OH H_2C-CH COO^- NH_3^+	Tyrosine
Tryptophan	^-OOC $CH-CH_2-C$ H_3N^+ N H	H_2N $C-CH_2-CH$ COO^- O NH_3^+	Asparagine
Methionine	^-OOC $CH-CH_2-CH_2-S-CH_3$ H_3N^+	H_2N $C-CH_2-H_2C-CH$ COO^- O NH_3^+	Glutamine
Proline	^-OOC HC $C H_2$ CH_2 HN $C H_2$	$NH_3^+-CH_2-(CH_2)_3-CH$ COO^- NH_3^+	Lysine
POLAR ACIDIC		POLAR BASIC	
Aspatic acid	^-OOC $CH-CH_2-C$ O H_3N^+ O	NH_2 $C-NH-(CH_2)_3-CH$ COO^- H_2N^+ NH_3^+	Arginine
Glutamine acid	^-OOC $CH-CH_2-CH_2-C$ O H_3N^+ O	$C-CH_2-HC$ COO^- HN^+ NH NH_3^+	Histidine

Figure 2: 20 amino acids in protein structure

13

Table 2: Four chemical targets account for the majority crosslinking and chemical interaction [13]

Target side		Explanation
Primary amines	(-NH2)	this group exists at the N-terminus of each polypeptide chain and in the side chain of lysine (Lys) residues
Carboxyl	(-COOH)	this group exists in the C-terminus of each polypeptide chain and in the side chains of aspartic acid (Asp) and glutamic (Glu)
Sulfhydryl	(-SH)	this group exists in the side chain of cysteine (Cys). Often, as part of a protein's secondary or tertiary structure, cysteine is joined together between their side chains via disulfide bonds
Carbonyls	(RCHO)	these aldehyde groups can be created by oxidizing carbohydrate groups on glycoprotein

Protein structure is broadly categorised into four structural forms; called primary, secondary, tertiary and quaternary structures (Figure 3). An increase in temperature, pressure, pH or the addition of certain chemicals can disrupt the folded state of proteins, resulting in unfolding of higher order structural forms of proteins (denaturing). Proteins are only marginally stable at best and the folded conformations are balanced by many interactions between amino acids.

Primary protein structure
is the sequence of a chain amino acids

Tertiary protein structure
occurs when certain attractions are present between alpha helices and pleated sheets

polypeptide chain

polypeptide chain

polypeptide chain

heme

Secondary protein structure
occurs when the sequence of amino acids are linked by hydrogen bonds

Quaternary protein structure
is a protein consisting of more than one amino acid chain

Figure 3: Four levels of protein structure

The primary structure refers to the sequence of amino acid residues in the polypeptide chain. Secondary structures are ordered structures constructed by internal hydrogen bonding between amino acid residues. It will become stabilized in a position where amine groups become close enough to form hydrogen bonds with carboxyl groups on another chain, or further along the same chain. The two main secondary structures are α-helices and β-sheets, and are the most stable structures. The tertiary structure is the three dimensional conformation of a single protein molecule. The structure is stable when chains are locked in place by disulfide bonds formed among two cysteine amino acids. The structure that have less disulfide bonds are usually rigid but still bendable, tough and can oppose rupture such as hair and wool while structures that have more disulfide bonds are

stronger, stiffer and harder.[13] The quaternary structure is the arrangement of more than two peptide chains, forming an entire unit of ultimate shape. A range of intermolecular interactions listed below exist holding the variety of chains together.

i. Hydrophobic interactions. These interactions are to minimize interactions of the non-polar amino acids with water.

ii. Hydrogen bonding between NH and C=O moieties of functional groups. The secondary and tertiary structures are stabilized by hydrogen bonding between polar amino acids.

iii. Ionic interactions can occur between positively charged side chains and negatively charged side chains.

iv. Covalent disulfide linkages to other groups. These linkages maintain tertiary structures. These bonds are only broken at high temperatures, acidic pH or in the presence of reductants.

The quaternary structure is stabilized by noncovalent interactions and disulfide bonds as the tertiary structure. There are two foremost categories of proteins, based on their quaternary structure, i.e., fibrous (keratin, wool) and globular protein (insulin, hemoglobin).[13]

2.2.2 Sources of proteins

2.2.2.1 Protein from plants

Plant protein is one of the major biopolymers from agricultural feedstocks. Table 3 lists the source, composition and major protein group from different plants. Henry Ford pioneered the use of soy protein in plastics and fibers in 1930s.[14] He patented an invention of panels in automobile bodies made from

soy meal with the addition of phenol or urea to increase strength and resistance to moisture. Later, it has been used as food ingredient, film formation, composites and food packaging. The United States is one of the major producers of soybeans in the world. It is available commercially in three different grades from soybean processing plants: soy protein isolate (90% protein), soy protein concentrate (65-72% protein content) and soy flour (54% protein). Soy protein (SP) is hydrophilic due to presence of a high proportion of glutamic and aspartic acid compared to other proteins. [15]

SP consists of both polar and non-polar side chains. Between these, there are strong intra- and inter-molecular interactions, such as hydrogen bonding, dipole–dipole, charge–charge, and hydrophobic interactions. The strong charge and polar interactions between side chains of soy protein molecules restricts segment rotation and molecular mobility, which increase stiffness, yield point, and tensile strength of SP films.[16] Molecular conformation can be altered with the help of physical [17, 18], chemical[19, 20] or enzymatic agents.[21]

Whey is the by-product of cheese and casein manufacture that contains approximately 7% dry matter. In general the dry matter includes 13% protein, 75% lactose, 8% minerals, approximately 3% organic acids, and less than 1% fat.[22] Whey Protein Concentrate (WPC, protein concentration 65–80% in dry matter) or whey protein isolate (WPI, protein concentrations over 90% in dry matter) can be obtained through a membrane filtration process followed by spray drying.

Strong interactions within whey protein (WP) involving intermolecular and intramolecular associations in conjunction with crosslinking via disulfide

bonds usually produce brittle materials. The amount of amine groups in WP is very low, (mainly on the side chains of lysine). This limits the potential of crosslinking WP with other polymers. Kurniawan L *et al* [23] used excess amount of poly (ethylene oxide) diglycidyl ether (PEODGE) which was added to graft the PEODGE onto WP via reactions between the epoxy groups in PEODGE and the amine groups of WP. The ungrafted amount of PEODGE was then coupled with the grafted PEODGE segments by the addition of ethylene diamine (EDA).

Pure protein isolate from gluten is obtained by washing off the soluble component (mostly starch). It has good elastic properties because of disulfide-linked glutenin chains, making it a good candidate for film formation.[24] Zein is extracted from maize gluten meal (corn) with hydrophobic properties, characterized by high percentage of proline. The most popular application of zein is in the textile fiber market.[25]

Sunflower meal is a by-product obtained after oil extraction from sunflower seeds. The high amount of histidine and arginine in sunflower meal increases its nutritive value that potentially can be used as additives in the food industry.[26] Peanut protein is extracted from defatted flour which provides the food industry with a new high protein food ingredient for product formulation. Peanut proteins with high oil and water binding ability are widely use in meats, sausages and breads, while proteins with high emulsifying and foaming capacity are good for salad dressing, bologna, soups, confectionery, frozen desserts and cakes.[27]

Table 3: Protein from plants

Sources	Protein content	Amino acid residues	Ref.
Gluten	80%	glutenin	[28]
Corn zein	65%	glutamine, proline, alanine, and leucine	[29]
Soy protein	90 %	glutamic acid, aspartic acid, leucine, arginine	[30]
Sunflower seed	30-50 %	lysine,isoleucine,arginine, histidine	[26]
Peanut	85%	arginine, histidine	[31]

2.2.2.2 Protein from animals

Protein from animal by-products such as bovine bloodmeal, fish, gelatin and collagen can be processed to form thermoplastics, fibers, films and coatings with interesting properties. Gelatin for example, has been produced on a large scale and used widely in the pharmaceutical and food industries. Gelatin film from mammals have the highest mechanical properties compared to fish gelatin film.[32] Meat bone meal which contain 50% protein, 9.5% fat, 10.1% calcium, and 4.8% phosphorus are being considered in adhesive for poly-wood industry [33] and sand replacement in cement based materials.[34] In other research, milk protein is effective in delaying browning reactions on the surface of sliced fruits.[35] Dragline silk is one of the strongest fibers produced by spiders. The fiber is stronger and is one-tenth the weight of the high tensile steel and consists of mainly hydrophobic amine groups such as glycine and alanine.[36] However, the mass production of the silk is too expensive and time consuming and limits its widespread applications.

2.3 Bioderived polymers

Generally, biopolymers can be classified into three categories according to their synthesis process; natural polymers, synthetic polymers from natural sources and polymers from microbial fermentation (Table 4).[37]

Table 4: Classification of main biodegradable polymers

Types of polymers	Classification	Ref.
Natural polymers	polysaccharides (e.g starch, cellulose, chitosan), proteins	[13, 38-42]
Synthetic polymers from natural sources	polylactic acid (PLA), polybutylene succinate (PBS)	[43-46]
Polymers from microbioal fermentation	poly(hydroxybutyrate) (PHB), Poly(hydroxy-alkanoate) (PHA)	[47, 48]

2.3.1 Poly lactic acid (PLA)

PLA is a biodegradable plastic that is produced from the ring opening polymerization of lactide, a dimer of lactic acid. Lactic acid (2-hydroxy propionic acid) is produced via fermentation. Currently, corn is used as raw material for lactic acid production but other potential starting materials such as corn stalks, wheat bran, cassava, cellulose, barley starch, potato starch, beet molasses, rye flour, and carrot processing waste are also considered.[49]

Interestingly, other sources of carbohydrates such as kitchen waste, fish meal and paper sludge are also being considered.[50-54] PLA presents great potential for industrial and commodity applications due to its good mechanical properties, biodegradability, transparency and sustainable biomass resources. These include packaging and automotive applications, similar to polyethylene terephthalate (PET), polystyrene (PS) and polycarbonate (PC).[55] However, the use of PLA for the cases may be limited because of its high T_g (60 ^{o}C), high brittleness and poor barrier properties.[43]

Plasticization have been employed to improve brittleness of PLA including the use of polyethylene glycol (PEG), triethyl citrate (TEC), tributyl citrate (TBC), and glycerol. The thermal and mechanical performance of PLA plasticized with different modifiers are listed in Table 5. PEG was found to be efficient in decreasing T_g with improved mechanical properties. In addition, the crystallization temperature of PLA also decreases without affecting the melting point significantly.[56, 57] However, plasticizer leaching was observed in PLA/ tributyl O-acetylcitrate (ATbC) materials but was improved with the addition of maleic anhydride grafted PLA.[58] Soy protein concentrate (SPC) existed as large SPC agglomerates in SPC/PLA blends when glycerol was used as plasticizer which turned into stretched threads with certain degree of interconnectivity when extra water was added.[5] Although plasticizers provide substantial reduction of T_g and adequate mechanical properties, higher amount of the plasticizers are needed (10- 30 wt% wt) which sometimes leads to a phase separation.

Table 5: Thermal and mechanical properties of PLA plasticized with different modifiers

Modifiers	Concentration (wt%)	T_g (^{o}C)	Tensile (MPa)	Strain (%)	Modulus (GPa)	Ref.
PLA	-	60	48-110	2.5-100	3.5-3.8	[59]
PEG (1000g/mol)	10	37.9	51	3.06	3.3	[57]
	20	32.9	52	15.4	1.9	
PEG (20 000g/mol)	10	57.4	28	2.5	2.42	[60]
ATbc	17	58	40.9	5	1.39	[61]
TBC	10	42	38.5	0.025	2.4	[58]
Glycerol	10	53.9	45.5	1.2	3.96	[5]
Glycerol+extra water	10 +20	55	39.7	1.21	3.56	

2.3.2 Polybutylene succinate (PBS)

PBS is a thermoplastic polymer of the polyester family that is biodegradable with properties that are comparable to polypropylene (PP). PBS is usually synthesized via polycondensation of succinic acid and 1,4-butanediol (BDO). Succinic acid can be obtained from fermentation of renewable feedstocks, such as glucose, starch or xylose as well as hydrogenation of maleic anhydride to succinic anhydride, followed by hydration to succinic acid.[62] The advantages of PBS are excellent biodegradability, thermoplastic processability and balanced mechanical properties. It has been used in foaming and food packaging application. However, the main problem is the high fermentative cost to produce succinic acid. It also possess some limitations in medical applications due to its hydrophobicity.[63]

PBS has a melting point of around 90 – 120 °C and a glass transition temperature of about -45 °C to -10 °C. It has a tensile strength of 34 MPa with elongation at break around 560 %. In comparison to PLA, PBS is tougher and easier to process, but has poor thermal stability and slow crystallization rate. The slow crystallization rate of PBS resulted in multiple melting peaks (DSC), interpreted as melt-recrystallziation of different PBS crystals.[64, 65] These different crystals affect the physicochemical properties of PBS, such as its melting point.

Development of PBS composites [66, 67], physical blending [44] and chemical treatment [68]   are areas of interest. Jute fibres were used as reinforcement filler in PBS/jute fibre composites where the mechanical strength and modulus reach an optimum value at 20 wt% fiber.[67] Blending PBS with PLA improved tensile strength and elastic modulus. Addition of 20% PBS in PLA changed the brittle properties of PLA to ductile from 24% to more than 200%.[69] Mechanical properties of PBS nanocomposites were improved after compatibilization with PBS-g-MA through improved dispersion of organo-montmorillonite (OMMT) filler in PBS matrix. However, the presence of alkylammonium groups on the OMMT surface catalyzed the degradation, leads to a reduction in the thermal stability.[68]

2.3.3 Novatein Thermoplastic Protein from bloodmeal (NTP)

Bloodmeal is a dry, inert powder made from blood used as a high-nitrogen fertilizer and a high protein animal feed. It is one of the highest non-synthetic sources of nitrogen coming from meat processing. Bloodmeal is different from meat bone meal in that bloodmeal contains a much higher amount of nitrogen, while meat bone meal contains phosphorus. Beef bloodmeal contains more lysine,

threonine, valine, leucine, tyrosine, and phenylalanine while pork blood meal contained more histidine, arginine, proline, glycine, and isoleucine.[70] The structure of these amino acids can be found in Figure 2. Cysteine and lysine are the most reactive amino acids. Cysteine residues play a valuable role by crosslinking proteins, which increase the rigidity of proteins while the amino group of lysine residues is active towards acylation, alkylation and amidination reactions.

2.3.3.1 NTP production

The steps involved in production of NTP are shown in Figure 4. Transformation of bloodmeal into NTP involves addition of additives. The additives are water, a protein denaturant (urea), a reducing agent (sodium sulfite, SS) and a surfactant (sodium dodecylsulfate, SDS).[38] These additives are needed to break the covalent cross-links to allow formation of new interactions in order to stabilize the final structure. Urea disrupts hydrogen bonding while SS disrupts the cysteine-cysteine crosslinkages. However, changing the concentration and composition of these additives will compromise its mechanical properties. For example, materials containing low water and high SS had reduced tensile strength and elongation, compared to higher water content at the same SS content.[71] Although water is an efficient plasticizer, water desorbs from the moulded plastic over time and the material becomes brittle and loses its toughness.

During extrusion processing, there are many thermal events that occur in the material at the temperatures as shown in Figure 5. At temperature around 100-120 $^{\circ}$C, denaturing, disassociation, unraveling and alignment of the protein chain occurred which allow it to flow and form new interactions during cooling.

Other than that, evaporation of water and additives also occur at this stage, which could possibly lead to aggregation of the protein.
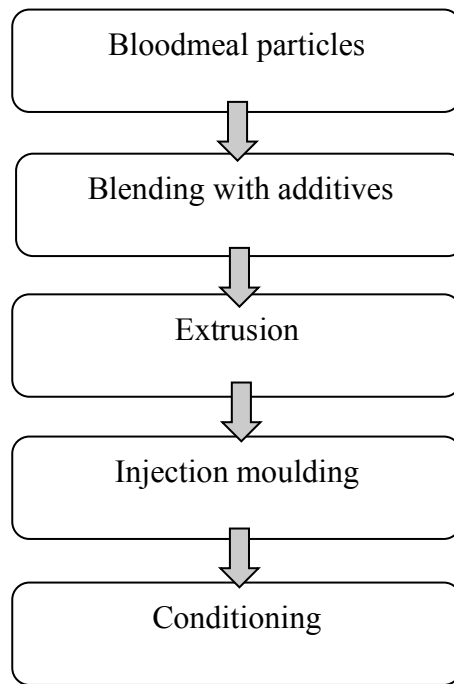
Figure 4: Production steps of NTP
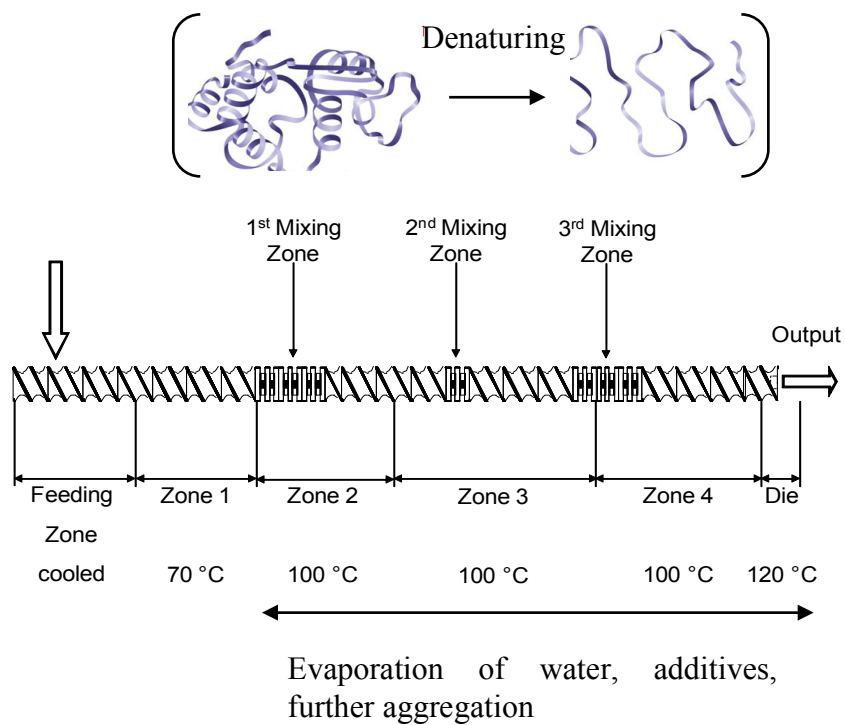
Figure 5: Thermal events occur in protein at typical extrusion temperatures

Excessive aggregation can cause physical crosslinking, increased viscosity and further limit processing.[72] Therefore, the majority of reactions in proteins need to occur just before, or just after, exiting the die. Injection-molding conditions do not influence the mechanical properties of NTP to a large extent. The observed changes are relatively small, which means that the protein-based material is robust enough for injection molding.[73]

Tri-ethylene glycol (TEG) was employed as a plasticizer in NTP. The mechanical properties of conditioned NTP at different TEG contents are listed in Table 6. Without TEG, the strength was at maximum, but it had poor energy to break. Increasing the TEG content slightly improved the energy to break but sacrificed its strength. TEG accumulated, migrated and evaporated upon heating.[74] Plasticizer migration and evaporation occured very slowly, which will affected the properties if exposed to high temperatures for pro- longed periods.

Table 6: Mechanical properties of NTP with varying TEG contents [74]

TEG content (pph)	Stress at max load (MPa)	Strain at break (mm/mm)	Secant Modulus (MPa)	Energy to break (MPa)
0	15.6	0.01	1799	0.1
10	11.3	0.28	710	2.8
20	5.7	0.53	251	2.8
30	3.7	0.43	126	1.4

Without plasticizers, the T_g of NTP is near its decomposition temperature. Plasticizers improve processability by increasing the free volume and alter the forces that hold the chains together. Although TEG had a plasticizing effect in

NTP and reduced the T_g, the tensile strength dropped, but increased its ductility.[74]

2.3.3.2 Thermal properties of NTP

NTP showed two transitions in the temperature range of -100-120 ^{o}C. The first transition was characterized as the T_g (~60 ^{o}C) where the second was the β-transition associated to relaxation transition temperature of NTP (-20 ^{o}C).TEG had significant impact on the T_g than the peak at β-tansition where the damping peak (DMA) at T_g was broadened and shifted to a lower temperature.[74]

2.3.3.3 Physical properties of NTP

NTP is in a denatured state and the typical secondary structures consist of clusters of crystalline α-helices and β-sheets distributed in a random coil protein structure and the proportion is affected with processing. To have a better strength, it is desirable to increase the β-sheet content as it has stronger hydrogen bonding interactions compared to α-helices.[72] Additives had a large influence on the amount of random coils and β-sheets, which processing might also affect the proportion of β-sheets.[75] Without TEG prior to extrusion, the formation of additional β-sheets was observed and decreased when TEG was increased due to effect of additional free volume induced by the plasticizer that prevented tight packed interactions from occurring. During extrusion, chain rearrangement lead to an increase in β-sheets that are evenly distributed throughout a more disordered matrix. Further processing in injection molding had a less significant effect on chain rearrangement.[73, 75] In this study, NTP was used as the polymer base. Development of NTP blends offer a sustainable option over other natural materials competing with food sources.

2.4 Polymer blend physics

2.4.1 Miscibility and compatibility

A true thermodynamicically miscible blend is a mixture containing two or more components that form a single phase system, but this definition of miscibility may be rather ambiguous. In many instances, it is desirable to have two phases present, as long as the multicomponent systems can be manipulated for structure, polymer interactions and phase domain sizes. Figure 6 shows the terminology used that describes the differences between miscible, immiscible, compatible and incompatible blends. Towards achieving miscibility, the interfacial adhesion increases, resulting in single phase component. Immiscible blends usually form aggregates that are totally phase separated. In compatible blends, the mixing between two polymers has high interfacial tension giving a rough structure and poor adhesion. The interfacial tension is much higher with increasing particle size with uneven distribution in incompatible blends. Thermal and mechanical properties are other characterization methods to distinguish between these types of blends and will be discussed in the next section.
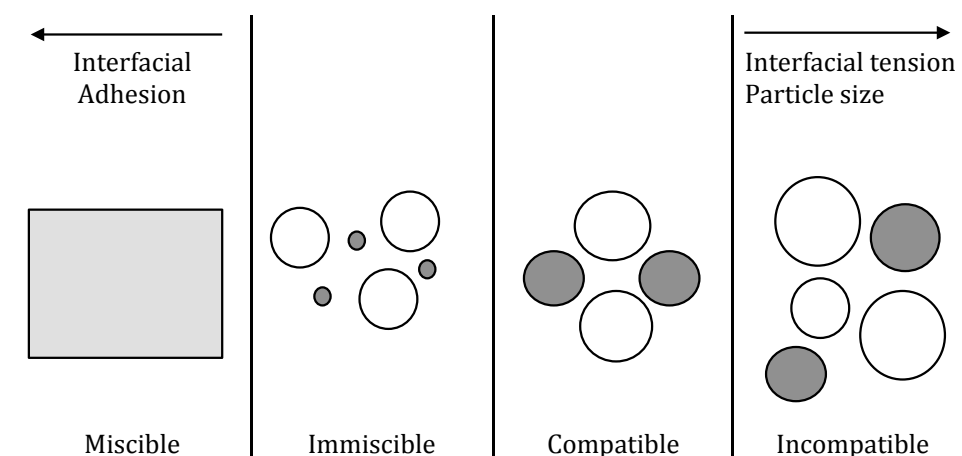
Figure 6: Blends terminology

2.4.2 Gibbs Free Energy of polymer blends

Miscibility is described as a necessary condition for two substances to mix at a certain temperature which is related to the enthalpic (ΔH_m) and entropic (ΔS_m) components through the relationship:

$$\Delta G_m = \Delta H_m - T\Delta S_m \tag{1}$$

where ΔG_m is the free energy of mixing, ΔH_m is the enthalphy of mixing and ΔS_m is the entropy of mixing with T being the absolute temperature. ΔH_m is a measure of the extent of interactions between molecules while ΔS_m is related to the increase in the total entropy of a compound system, when different material components are mixed. For miscibility to occur, the Gibbs free energy should be less than 0. Although this is a necessary criterion, it is not sufficient as for a stable one-phase system; criteria for phase stability of binary mixtures at a fixed temperature, T, and pressure, P, must also be met:

$$\Delta G_m < 0 \,, \left(\frac{\partial^2 \Delta G_m}{\partial \phi^2}\right)_{T,p} > 0 \tag{2}$$

The value of $T\Delta S_m$ is always positive since there is an increase in the entropy upon mixing. Therefore, the sign of ΔG always depends on the value of the enthalpy of mixing ΔH_m. In a polymer – polymer mixture the number of possible arrangements is much smaller than in a polymer – solvent system. Thus, the contribution of the volume of mixing to the free energy of mixing becomes significant. This results in limited solubility and other solubility behaviour such as phase separation at high temperatures and dissolution at lower temperatures. The Flory-Huggins model [76, 77] that was originally developed for polymer solutions can also be extended to polymer/polymer mixtures by introducing the concept of a reference segment volume (VR) that is approximated to the smallest polymer repeat unit (Equation 3).

$$\Delta G_{mix} = kTV \left[\frac{\varphi_A ln\varphi_A}{V_A} + \frac{\varphi_B ln\varphi_B}{V_B} \right] + \varphi_A \varphi_B \chi_{12} kTV/v_r \qquad (3)$$

where V = total volume, V_i = molecular volume of component i, φ_i = volume fraction of component i, k = Boltzman's constant, χ_{12} = Flory-Huggins interaction parameter and v_r = interacting segment volume (such as a repeat unit volume) or reference volume. For polymers, the assumption is made that the lattice is comprised of N cells with a volume of V. Each polymer molecule occupies volumes V_A and V_B, respectively. The volume fractions A and B are represented by the equations:

$$\varphi_A = \frac{V_A N_A}{V_A N_A + V_B N_B}; \quad \varphi_B = \frac{V_B N_B}{V_A N_A + V_B N_B} \qquad (4)$$

and
$$V = V_A N_A + V_B N_B \qquad (5)$$

The variables that one can control in polymer blends are usually temperature and composition. A lot of polymer pairs are only miscible when there is a lot more of one polymer than of the other. There will be a range of compositions for which the two polymers won't mix. At certain composition, a number of phases could be schematically presented in the free energy versus composition diagram for system with limited solubility (Figure 7). Immiscible blends is represented as (A), miscible system (B) and partially miscible system (C). In partially miscible systems, a single phase is present when the composition of polymer b is less than Φb_1 or more than Φb_2 where at that composition, it has a lower free energy than the two phase system. For composition between Φc and Φd, the system is unstable and the phases separate.

30

But the composition range over which the two polymers phase separate is not always constant, it also depends on temperature. Liquid-liquid and polymer-solvent mixtures (that are borderline in miscibility) usually exhibit an upper critical solution temperature (UCST) while polymer-polymer mixtures generally exhibit a lower critical solution temperature (LCST), as shown in Figure 8a.The range of miscibility gets smaller as temperature increases where at low temperatures, the UCST cannot be determined due to the glassy state restricting molecular motion (phase separation); and at higher temperatures, polymer degradation occurs before phase separation can be observed. Phase separation takes place when a single-phase system suffers a change of either composition, temperature or pressure that forces it to enter either the metastable or the spinodal region.
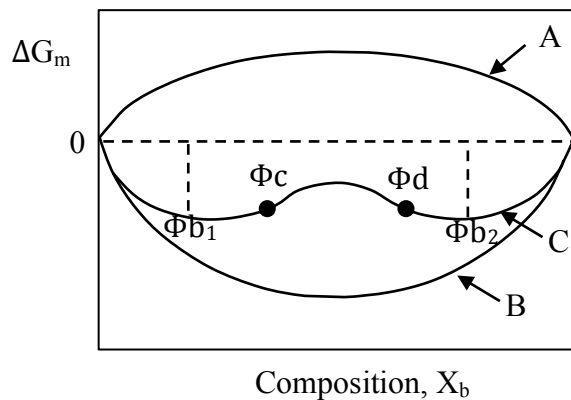
Figure 7: Schematic of free energy versus composition where A: immiscible system, B: fully miscible system and C: partially miscible system

At both USCT and LCST, there are two regimes for phase separation, the binodial and spinodial decomposition (Figure 8b). At the binodial conditions, phase separation occurs by nucleation and growth while spinodial decomposition arises from concentration fluctuation. The specific characteristics of the initial

stages of phase separation by these processes are noted in Table 7. At temperature T', for compositions between b and c, a single phase is metastable. In between c and d, the system is unstable for even the smallest concentration fluctuations and spinodial decomposition occurs (Figure 8c).

One strategy to enhance miscibility between two polymers is to force the enthalpic term to be negative by introducing specific interactions. In the context of true thermodynamic compatibilization, the presence of a third component mediates enthalpic interactions between the first two components, which in turn, creates a single homogeneous phase which is referred to as thermodynamic compatibilization.[78]

Table 7: Initial stages of phase separation [1]

Property	Nucleation and Growth	Spinodial Decomposition
size of phase separated region	increase with time	size constant
concentration of phase separated region	constant with time	increases with time
diffusion coefficient	positive	negative
phase structure	separated	interconnected
activation energy	required	not required
region of phase diagram	metastable or unstable region	only unstable region
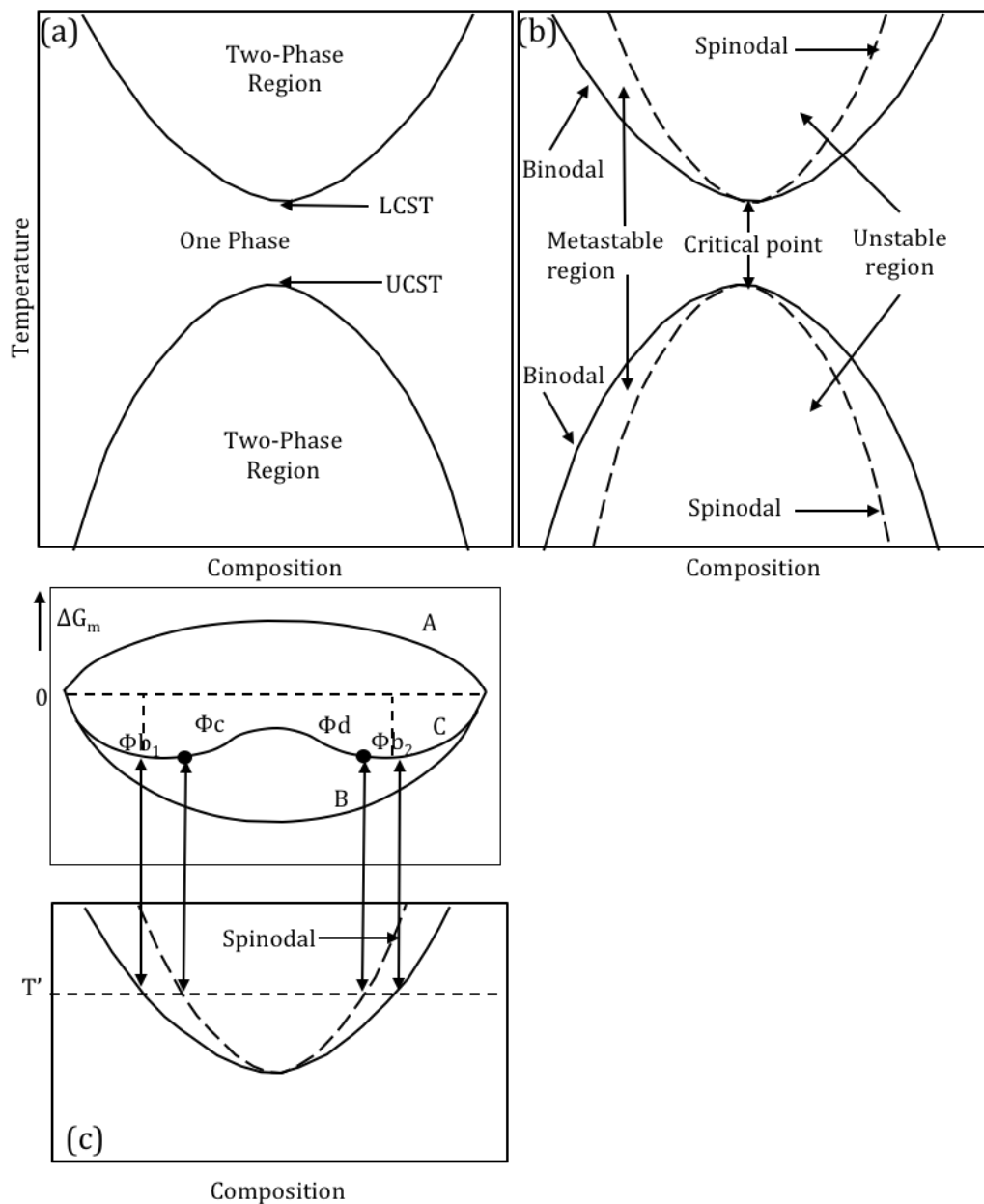
Figure 8: Phase diagram of binary polymer blend with illustration of LCST and UCST

2.5 Protein-based polymer blends

There are many factors that determine the properties of polymer blends, most important of which are the composition and compatibilizer. The properties of polymer blends depend greatly on interactions, which induced can be altered by

compatibilizers. The importance of composition and compatibilizer in determining the blend properties is discussed in the following section.

2.5.1 Composition

Generally, the mechanical properties of two-phase blends consisting of a continuous polymer phase and a dispersed phase follow the mixing rule. This concept does not only exist for blends, but may even be better known in the field of composite materials. Consider a simple model of continuous fiber composites as a solid block with the volume of each phase proportional to its relative abundance in the composite, as shown in Figure 9. The overall property in the direction parallel to the fibers (rules of mixtures) may be as high as

$$E_c = fE_f + (1 - f)E_m \tag{6}$$

where $f = \dfrac{V_f}{V_f + V_m}$, E_f is the material properties of fibers and E_m is the material properties of matrix. If the load is applied perpendicular to the fibers (inverse rules of mixtures), the properties of composites can be as low as

$$E_c = \left(\frac{f}{E_f} + \frac{1 - f}{E_m}\right)^{-1} \tag{7}$$
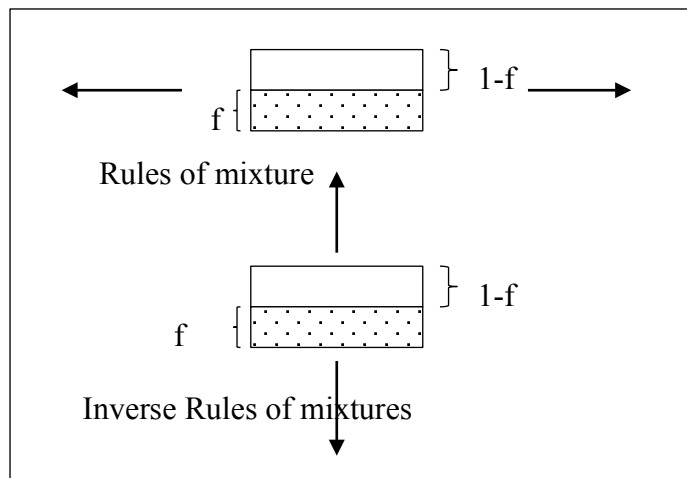
Figure 9: Parallel and perpendicular loading to fibers
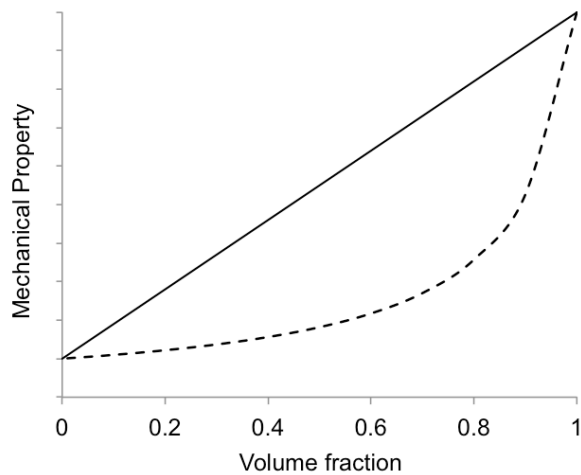
Figure 10: The mechanical property predicted by mixing rules and inverse mixing rules

The composite or blend's mechanical properties will fall between that of the mixing rule and inverse mixing rule, as shown in Figure 10. Changes in morphology may affect mechanical properties and can be related to a phase inversion with changes in composition. A phase inversion is when the blend's structure change from a matrix of polymer A containing a dispersed polymer B to a dispersed polymer A within matrix B. For example, the morphology of soy protein isolate and polycaprolactone blend (SPI/PCL) change from smooth surface to a rough and heterogeneous fracture surface as the PCL content increased and showed a bi-continuous phase at 60/40 (SPI/PCL) accompanied by an increased in toughness.[79]

It was observed that as the amount of protein increased in modified polyester blends, there was more interactions with the reactive groups in the protein that resulted in an increase in tensile strength, but blends containing more than 65% protein were difficult to injection mould.[80] The T_g of SPI in SPI/PCL blends decreased as PCL content increased (≤50% PCL) accompanied by

decreasing crystallinity (X_c), indicating that the crystallization of PCL in blends was difficult.[79] In a blend of SPI/PLA (80/20) with 10 phr triacetin (TA), a highly ordered porous matrix of SPI and homogenously dispersed PLA domains were formed to a complex coarsened phase structure for both SPI and PLA domains at 60/40.[81]

It is known that SPI is richer in protein than SPC, which also affected the properties of the blends. For example, SPC/PLA blends showed a fine co-continuous phase structure compared to SPI/PLA blends which presented severe phase coarsening. Due to higher protein content in SPI and its highly polar and hydrophilic nature compared to PLA which is hydrophobic, poor adhesion was observed. A high viscosity disparity between SPI and PLA further exaggerated this.[82] In other research of PLA and soluble eggshell membrane-protein (SEP), PLA is in a semi-crystalline state when SEP is added as a filler and changes to amorphous PLA when SEP content increased. Increasing SEP also improved the biocompatibility of the blends.[83]

2.5.2 Compatibilizers

In practice, polymer blends are said to be compatible if they exhibit two phases on a microscopic level but the interactions between polymer groups might be reasonable in a manner that provides useful properties of the multicomponent system. One of the strategies to improve compatibilization involves addition of at least one substance with a highly reactive group that can interact with more than one component of the blend.[84] There are two methods for blend compatibilization (Figure 11). The first is by addition of a third component or by reactive compatibilization.

36

2.5.2.1 Addition of a third component

Introducing a third component in binary blends reduces interfacial tension between components, improving the dispersion and enhancing the adhesion between phases. The compatibilizer should be miscible and have a high affinity for both phases (Figure 11). Polymeric methylene diphenyl diisocyanate (pMDI) and poly-2-ethyl-2-oxazoline (PEOX) are among the most used compatibilizers in protein blends. pMDI is the polymeric form of methylene diphenyl diisocyanate (MDI) and distillation of MDI yields pMDI. pMDI is highly reactive with hydroxyl functional groups to form urethane linkages [85] and the residues of untreated MDI are not expected in the blends due to high reactivity of the isocyanate groups.[86] Compatibility between SPI and PCL was improved with the addition of MDI in blends containing 50% of each component.[79]

Another compatibilizer often used in protein blends is poly(2-oxazoline), the properties of which can be tuned by changing the side chain of its monomer.[87, 88] In recent years, the use of poly (2-oxazoline) in biomedical applications has evolved as its biocompatibility and biodistribution are similar to polyethylene oxide (PEO).[87] PEO has been used widely in protein adsorption, protein conjugates and drug carriers. In PLA/SPC blends, hydrogen bonding between carbonyl groups in PEOX and hydroxyl and carboxylic end-groups (PLA) reduced SPC inclusion size and increased interfacial bonding between PLA and SPC. [89] The carboxyl groups and/or amino group functionalities present in proteins are capable of reacting with the oxazoline functional group. The reaction between the carboxylic and oxazoline groups will result in an ester-amide linkage and is a fast reaction.

Maleic anhydride and its isostructural derivatives such as fumaric, citraconic and itaconic acids are being widely used as a copolymer through graft modification of various thermoplastic polymers. Graft modification onto polyolefins, especially polypropylene (PP) started back in 1969s when maleic anhydride (MA) was grafted onto isotactic PP below its melting point.[90] Since then, much effort has been put to study the mechanism of grafting polyolefins under a variety of conditions.[91-94] Grafting has been done either in an extruder or an internal mixer.[95-100] By using an internal mixer, polymers need to be dissolved in suitable solvent at the appropriate temperature. To obtain a high yield, solution grafting is an effective method, however, costs and simple processing conditions favour reactive processing (using extrusion).

These maleic anhydride graft copolymers have been used as compatibilizers to improve interfacial adhesion between two polymers. The compatibility between synthetic polyolefin-MA group with soy protein and starch was improved evident from morphology, mechanical properties and thermal properties.[80, 101, 102] PLA-g-MA has been successfully used in starch and PLA blends. The maleation of PLA proved to be very efficient in promoting strong interfacial adhesion with hydroxyl group on starch.[99, 103]

Addition of third component	Substance with a highly reactive group	Affinity to A Affinity to B
	Copolymer	
Reactive compatibilization		
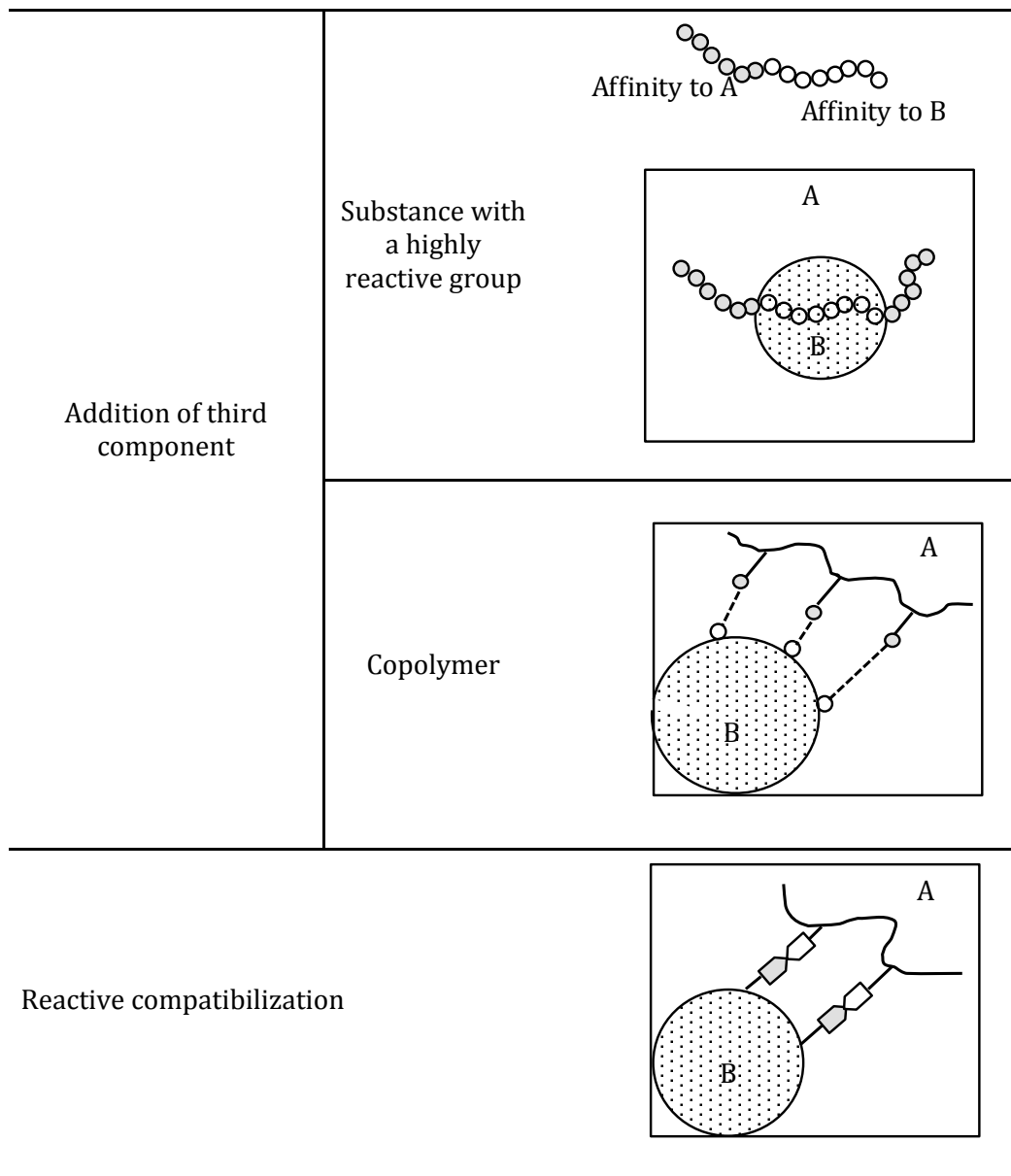
Figure 11: Methods for blends compatibilization

Only recently, PLA-g-MA with a degree of grafting between 0.25 - 0.9 % was used as compatibilizer in PLA/SP composites that improved the tensile strength and elongation at break of SP/PLA composites. A finer domain size of the soy protein concentrate (SPC) phase was observed, suggesting improved dispersion [104]. However, the use of graft-copolymers has a disadvantage

because it tends to form micelles in the bulk phase thereby increasing blend viscosity and reducing processability[105].

L.A. Utracki[105] listed three main factors that need to be considered in designing copolymers as compatibilizers:

1. to maximize miscibility of the appropriate part of its macromolecule with the specific polymeric component of the blends

2. to minimize its molecular weight to just above the entanglement molecular weight for each interaction segment and

3. to minimize its concentration in the blend

2.5.2.2 Reactive compatibilization

The second method is known as reactive compatibilization. From an economic point of view, this technique is more attractive than the addition of a third component.[106] The concept involves in-situ formation of a block- or graft copolymer at the interface between the phases of a polymer blend during melt-mixing.[107] Reactive extrusion has been shown to be a cost effective processing method as it is a continuous process which involves introducing reagents at optimum points in the reaction sequence. During extrusion, reagents are homogenized at a longer residence time for a high conversion. Batch mixers are also used, and have been found to be effective as it is easy to control processing parameters such as temperature, mixing time and mixing intensity via the rotation speed of motors.[98]

Reactive extrusion is an effective method for chemical modification of polyesters along with the production of compatibilized blends between biodegradable polyesters and fillers.[108] During chemical modification of

polyesters such as maleation, the reaction kinetics is dependant on the concentration of initiator and monomer, while a suitable screw configuration is required to meet residence time and mixing requirements to reach a high conversion. Also, polymerization needs to be fast enough if processing is in a continuous one-stage process.

Another advantage of using reactive extrusion is the formation of additional interactions between two phases at the interphase. During polymerization in an extruder, besides production of graft polymers, there are unwanted reactions such as chain scission, crosslinking and homopolymerization. The initiator radicals attack the polymer to generate macro-radicals that might form crosslinking which could produce a higher molecular weight polymer. Other advantages of crosslinking are that it can improve properties of the original polymer such as increased thermal stability, solvent resistance and mechanical properties. Using reactive extrusion, crosslinking is also possible through ionic bonds and physical crosslinking, i.e van der Waals or hydrogen bonds. In PLA, the crosslinked structure of triallyl isocyanurate (TAIC) promotes crystallization. Although this was achieved using a crosslinking agent, with further increase in crosslinking (from 12.1% to 41.2%), the onset crystallization temperature increased, resulting in the perfection of crystal lamellas.[109]

2.6 Characterization of compatibility

The methods commonly used in the literature to characterize compatibility are based on mechanical and thermal properties (T_g) as well as morphology. These are discussed in the following sections.

2.6.1 Mechanical properties

By way of example, the mechanical properties of various PLA/protein blends are shown in Table 8. Different factors that influence mechanical properties such as composition as well as type and amount of compatibilizer used are listed and discussed.

Table 8: Mechanical properties of PLA/protein blends

Material	Tensile strength (MPa)	Elongation at break (%)	Modulus (GPa)	Ref.
PLA/SPC, 70/30	44.7	1.54	4.17	[104]
PLA/SPC, 70/30, 2 phr PLA-g-MA	52.2	1.85	4.21	
PLA/wheat-straw, 70/30	57	1.8	4.5	[110]
PLA/wheat-straw, 70/30,5 phr PLA-g-MA	68	2	4.5	
PLA/SPC, 70/30	48.6	1.13	4.34	[89]
PLA/SPC, 70/30, 1 phr pMDI	60.3	1.46	4.52	
PLA/SPC, 70/30, 3 phr PEOX	53.8	1.26	4.42	
PLA/SPC, 70/30, 3 phr PEOX, 2 phr pMDI	73	2.29	4.41	
PLA/SPI, 30/70	12.4	1.3	3.96	[82]
PLA/SPI, 30,70, 5 phr PEOX	20.1	1.9	3.75	
PLA/SPC, 30/70	19.3	1.7	4.43	
PLA/SPC, 30/70, 5 phr PEOX	22.5	2.1	4.25	

Zhu *et al* [104] obtained a brittle material without any yield point as well as an increase in modulus due to the incorporation of rigid SPC. However, compatibilized PLA/SPC showed a 16.8% improvement in tensile strength, 20% in elongation at break and 1% in modulus when compared to uncompatibilized

blends. The tensile strength and elongation of both blends did not change when the amount of PLA-g-MA was increased. The improved interfacial adhesion was believed to be through the anhydride group in PLA-g-MA reacting with amine groups of the protein and hydroxyl groups of carbohydrates in SPC.

By using the same type of compatibilizer (PLA-g-MA), C. Nyambo *et al* [110] investigated different blending methods to prepare PLA/wheat starch (WS) blends; by reactive compatibilization and by conventional mixing (the conventional process of preparing PLA-g-MA via reactive extrusion and using it as compatibilizer to the PLA/WS composites) and found that the blends prepared through the conventional method showed 28% improvement in tensile strength over that at using reactive compatibilization. This was believed to be due to the presence of free radicals from the initiator that caused degradation of the materials. This observation is also consistent with studies using PLA/starch composites.[111] The tensile strength of blends with PLA-g-MA showed a 19.3% improvement accompanied with 11% increase in elongation at break. No changes was found in modulus.

Liu *et al* [89] used different types of compatibilizers (PEOX and pMDI) in PLA/SPC blends (70/30 wt%) and observed an increase in elongation at break from 11.5% - 100%, calculated from the lowest to the highest elongation at break value compared to uncompatibilized blends. Materials with pMDI showed a yield point and using dual compatibilizers had a synergetic effect on the tensile strength, elongation at break and modulus. By considering the nature of pMDI, which has a high reactivity with water, pMDI was added during injection moulding and compared with samples when pMDI was added during extrusion.

Samples with pMDI added during extrusion show no compatibilization effect on the composites.

Zhang *et al* [82] used PLA as a filler in PLA/SPI and PLA/SPC blends (30/70) using PEOX as compatibilizer. PLA/SPI showed a 62% improvement in tensile strength, 46 % improvement in elongation and a slight reduction (5.3%) in modulus compared to uncompatibilized blends. For PLA/SPC, better improvement were observed for tensile strength (16.5%), elongation at break (23%) as well as modulus (7.3%). The higher carbohydrate content in SPC compared to SPI may have been the reason for this observation. However, increasing PEOX showed only a slight improvement in strength.

Optimization of tensile properties of thermoplastic blends from SP and biodegradable polyester (PCL, PBAT and PBS) using the Taguchi experimental design method [112, 113] had concluded that between all factors (polyester type, urea content, SS content and glycerol content) selected, polyester type proved to have the dominant effect in determining the final properties of the blends.[114] PBS was found to improve the tensile properties through crosslinking with denatured protein. On the other hand, PCL significantly improved the elongation at break of PCL/SP. Increasing PCL content in SPI blends showed ductile properties and interfacial adhesion was improved with increasing MDI content.[79]

Other than using a third component as compatibilizer, polymers have been modified to create new functional groups on their backbone through grafting or crosslinking. Modified PBS containing urethane and free isocyanate groups (NCO) blended with SPI showed improved mechanical properties through

hydrogen bonding interactions between NCO groups and the functional side groups of SPI. When SPI was the matrix (70/30 wt%) at different NCO/OH ratios, the tensile strength increased from 4.81MPa to 18.2 MPa, accompanied by an increase in modulus, but elongation at break was less affected. PCL-g-MA was developed using graft polymerization and the tensile strength and percentage elongation were similar to ungrafted polymers, indicating that the polymers was not disrupted by copolymer and are capable of being an efficient compatibilizer.[115, 116]

Chemical modifications of proteins with epoxy groups have been trialed for the development of biomaterials for medical applications.[117, 118] The epoxy functional group is capable to react with amino groups in proteins.[23, 119] The reactive groups were further crosslinked by using a coupling agent ethylene diamine (EDA, a compound which contains two primary amine groups). Reduction in rigidity (storage modulus) was observed due to contribution of epoxy end groups but with more crosslinking, the storage modulus increased approaching the level of WP.

2.6.2   Thermal properties

2.6.2.1 The amorphous phase

Miscibility in polymer blends can be evaluated by the presence of one or more glass transition temperature (T_g) that can be measured by different thermal techniques such as differential scanning calorimeter (DSC) or dynamic mechanical analysis (DMA). For a miscible system, a single T_g is observed, intermediate of the two phases. For an ideal system, the relationship between T_g and the composition of the blend is predicted by the Flory-fox equation:

$$\frac{1}{T_{g\ (blend)}} = \frac{W_1}{T_{g1}} + \frac{W_2}{T_{g2}} \qquad\qquad (8)$$

where $T_{g,(blend)}$, T_{g1} and T_{g2} are the T_gs of polymer 1 and polymer 2 and W_1 and W_2 are the weight fractions of polymer 1 and 2 respectively. The T_g is the characteristic transition of the amorphous phase in polymers. Below the T_g, polymers are in the glassy state and polymer chains movement is fixed by intermolecular interactions. In miscible one-phase systems, macromolecules are statistically distributed on a molecular level and only one T_g occurs. In partly miscible systems, interaction between polymer chains of the two polymers cause a shift in T_g of the pure components towards each other. For immiscible blends, the components are completely separated in different phases and the T_g of pure components will remain at their original temperatures.

Generally, protein-based thermoplastics have two main relaxation peaks. The first is assigned to the T_g, (60-80 ^{o}C) and the other peak is attributed to a β-transition (-30 to -50 ^{o}C).[74] Interactions between proteins with other biodegradable polymers usually form stronger interactions through dipole-dipole, charge-charge or hydrophobic interactions. These interactions affect the T_g of both polymers as well as the damping peak (DMA). However, in most blends, comparison between these two T_gs is often limited due to the T_g and melting peaks of one or both polymers often overlapping.[80, 120]

Without any compatibilizers, the main transition of SPI in SPI/PBS (70/30) blends moved from 73 ^{o}C to a lower temperature, the damping peak was reduced and broader compared to pure SPI.[121] The same behavior was observed in PLA/SP blends. [104] With incorporation of a compatibilizer, interactions

between modified PBS (toluene-2, 4-diisocyanate (TDI)) and SPI did not significantly shift the T_g but further reduced the damping peak.[121] Similar observations were made in PLA/SP composites (70/30) using pMDI where the height of the main T_g peak was lower and broader than those with pure PLA and blends without compatibilizer.[89] An increase in T_g was observed in PLA/SPI (75/25) due to improved compatibility through formation of urethane linkages in the presence of NaHSO$_3$ and MDI.[122]

In blends of PBAT/SPC (70/30), increasing SPC reduced the T_g of PBAT by 15 ^{o}C and continuously decreased with increasing SPC loading.[120] Incorporation of PBAT-g-MA as a compatibilizer, further reduced the T_g of PBAT. In another study, the T_g of SPI blends decreased from 108.4 ^{o}C to 84 ^{o}C when PCL content increased up to 50 % in the presence of 2 % MDI.[79] However, the T_g of proteins can also be lowered by moisture absorption. If more protein is used in the blends, increasing moisture may lower the T_g and should not be confused with the effect of blending.[16, 82]

Unplasticized proteins should be considered as rigid fillers that would restrict chain mobility in blends thereby resulting in broadening and lowering damping peaks due to the interaction between phases. Interactions can be further increased by using compatibilizers. For example, increasing PLA-g-MA concentration was found to decrease the dampening peak height and was attributed to more effective adhesion between PLA/SPC (70/30 compositions).[104]

2.6.2.2 The crystalline phase

In general, there is a possibility that during blending there is competition between phase separation and crystallization. The rates of these two processes vary differently with temperature which will affect morphology and material properties. Considering blends with an amorphous and crystalline phase, as the blend is cooled from the melt, crystallization occurs, but decreases when the amount of amorphous phase increases. Diffusion of the amorphous component from the crystalline region depends on the interaction between these phases.

Crystallization consists of two major events defined as nucleation and crystal growth. Nucleation is the process of forming a nucleus, where molecules arrange themselves in a pattern characteristic of a crystalline solid, forming a site in which additional particles deposit as the crystal grows. Nucleation starts with small, nanometer-sized areas where, as a result of thermal motion, some chains or chain segments align. Those seeds can either dissociate, if thermal motion destroys the molecular order, or grow further, if the grain size exceeds a certain critical value.[123]

Nucleation and crystal growth continue to occur simultaneously where the rate of crystallization is driven by the existing supersaturation state of the solution. Depending on the conditions, the competition between crystal growth and nucleation results in the formation of different crystal sizes and shapes. The process of crystallization is completed when the crystal and remaining liquid reach equilibrium as the existing supersaturation state is exhausted.

In SP/PBS blends, soy protein induced and accelerated crystallization of PBS and the enthalpy of crystallisation for PBS in blends (with compatibilizer)

was higher than pure PBS which suggested a nucleation effect.[124] This was confirmed when modified PBS, containing urethane groups, had a lower crystallization temperature and showed a depression in crystallization after introduction of urethane groups. The same phenomenon has been observed for SP and PLA blends.[125]

SPC acted as a nucleation agent in PLA and promoted PLA crystallization but when pMDI was added in SPC/PLA blends, the cold crystallization (crystallization during cooling) temperature increased when pMDI concentration increased. The pMDI increased wetting between SPC and PLA, which increased the free energy needed for nucleation and therefore decreased the nucleation effect of SPC.[89]

These observations indicate that most natural polymers acted as nucleating agents and the addition of compatibilizer affected this behavior even further. Starch also played a role as a nucleating agent in blends.[126] In order to understand the crystallization mechanism between phases induced by a compatibilizer, further study of this mechanism is needed.

2.6.3 Morphology

The correlation between the viscosity of polymer phases, interfacial properties, blend composition and mixing conditions are the factors that influence morphology and ultimately the material properties. The process of blending in most mixing equipment involves melting, breaking chain structure, and coalescence where two phase domains of the same composition come together to form a larger phase domain. To study the morphology development during processing, samples at different locations along the screw of an extruder were

studied using compatibilized nylon (aPa)/polystyrene-maleic anhydride copolymer (PSMA/aPa) and uncompatibized nylon (aPa)/polystyrene (PS143/aPa) at 80/20 composition and the process is shown in Figure 12.[127]

During the initial mixing stage, the dispersed polymer is stretched biaxially into thin sheets within the matrix phase that further break up to mainly fibers and some small particles. The relaxation process afterwards, due to the low shear rate and shear stress, helps to further break the films of dispersed phase into fibers. The fibers are then stretched longer and thinner before coalescence. It is believed that the early mixing stage is controlled by droplet breakup, while the final stage is controlled by the balance between droplet breakup and coalescence.[128, 129]

Incorporation of compatibilizers only had a slight influence on the morphology. The film of dispersed phase are thinner compared to uncompatibilized blends. The breaking of the film into fiber was extensive and the particles were also smaller and more uniform in size. This led to faster morphology changes compared to uncompatibilized blends.
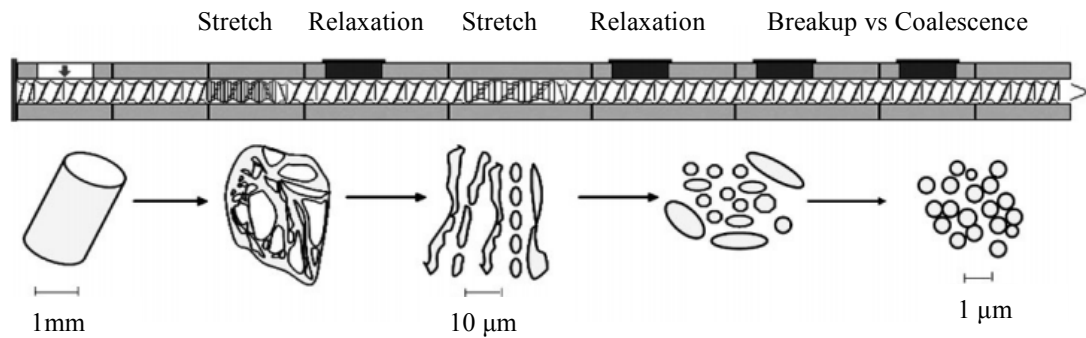
Figure 12: The flow field in extruder and the evolution of the dispersed phase down the length of the extruder

During processing, the major reduction of the dispersed phase's particle size occured at the initial stage (less than 2 minutes) during blending.[130] The size of the dispersed phase in compatibilized blends using copolymers will usually be very small if the reaction rate is much faster than the rate of change in morphology.

The morphology development during extrusion had a notable influence on the final properties of materials, which can be observed from the fracture surfaces or cross section of the samples.[131] In PLA/SPI blends, a clear and distinct phase fracture surface was observed when no compatibilizer was added to the blends where the dispersed SPI phase particles were large and nonuniform due to immiscibility. Adding 0.05 % $NaHSO_3$ resulted in much smaller SPI particles, but adding more compatibilizer (3 wt%) resulted in agglomeration of SPI particles due to breakage of disulfide bonds present in SPI induced by $NaHSO_3$. Despite the agglomeration of SPI, the compatibility between PLA and SPI were improved.[122]

In SPI/PCL blends, a rough and heterogeneous fracture surface was observed as PCL content increased with addition of compatibilizer.[10, 79] At

high PCL content, plastic flow [79] and a fibrillar structure [7] was observed indicating an increase in energy to break. Higher MDI concentrations led to improved compatibility between phases with no evidence of SPI particles.[79] Including glycerol led to good wetting with smaller protein particles resulting in a more homogeneous morphology.[132]

SPC showed irregularly shaped particles with a relatively large particle size distribution in SPC/Easter Bio Copolyester (This random copolymer is composed of adipic acid, terephtalic acid, and 1,4-butanediol). If SPC is exposed to moisture, significant secondary aggregation of the particles occured due its hydrophilic nature.[132] In other research, with addition of 7.5 % water, SPC changed the morphology of SPC from a rigid particulate filler to a ellipsoidal (Figure 13c) and fine threaded filler (Figure 13d-g), but the incusion of SPC was not sufficient to form deformability.[133]
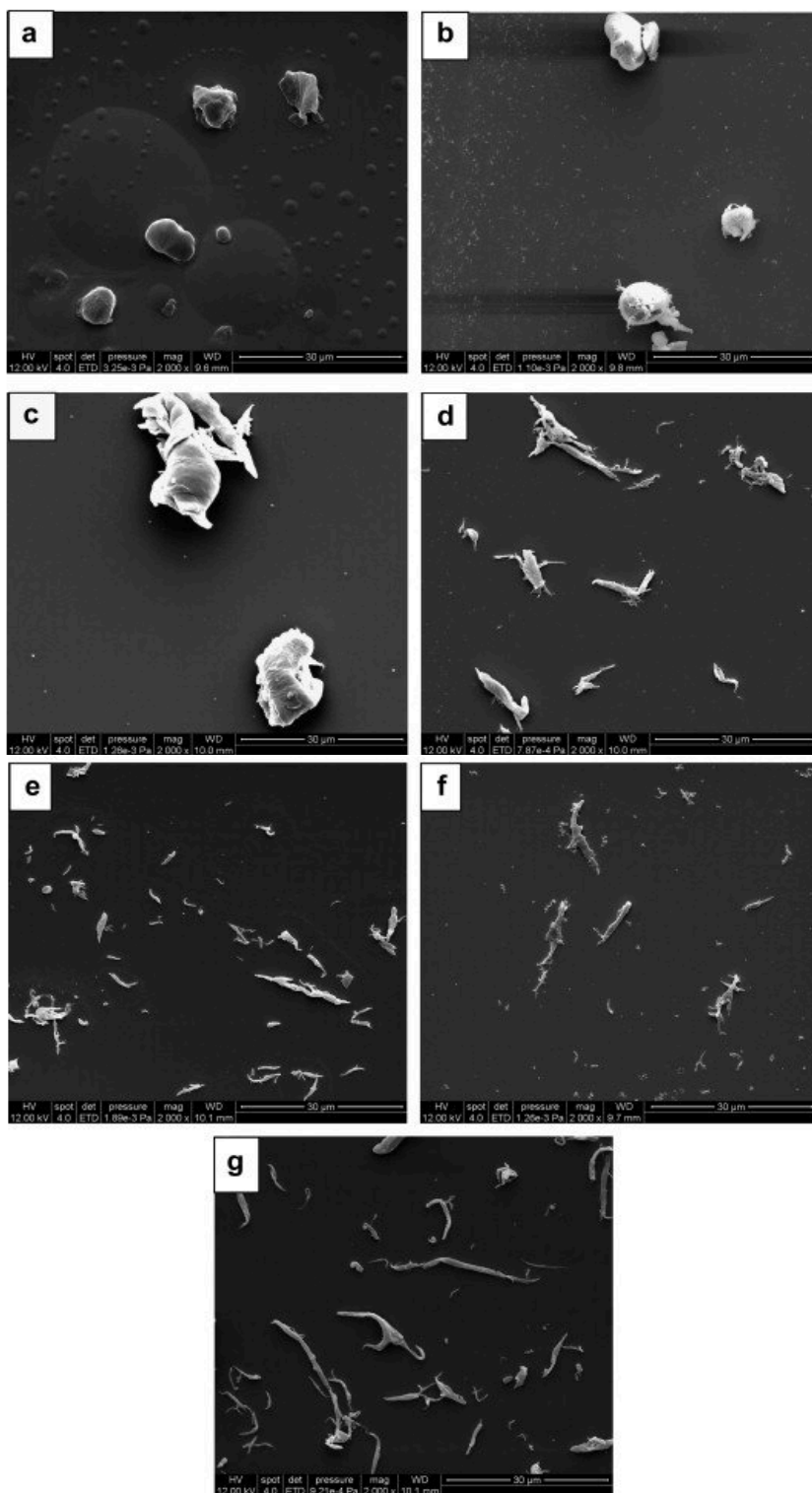
Figure 13: SEM micrographs showing the influence of water content in the pre-compounding SPC on the deformation of the SPC phase. a: Unprocessed SPC; b: SPC-0.6% H_2O; c: SPC-7.5 % H_2O; d, SPC-10% H_2O; e: SPC-12.5% H_2O; f: SPC-17.5% H_2O; g: SPC-22.5 % H_2O. *Reprinted with permission from Feng Chen, Jinwen Zhang, Polymer 2009, **50**, 3770-3770. Copyright (2009), Polymer Elsevier*

Another type of morphology that is frequently observed when changing composition is a co-continuous morphology. A co-continuous morphology is non-equilibrium morphology where both components form phases that are partially continuous and interpenetrating. Considerable attention has been given to co-continuous morphologies as it could give a maximum contribution to the modulus from each component simultaneously.[134] It enables each phase to share the load, providing sufficient stress transfer between the phases. It has been suggested that co-continuity occurs at the phase inversion point, which result in a significant increase in modulus of blends of polyethylene (PE) with polystyrene (PS) or polypropylene (PP).[135] SPC/PLA showed a co-continuous phase ranging from 30/70 to 70/30 with improved mechanical properties.[82] However, the condition to form a co-continuous blend are still not clear, whether it is actually a stable co-continuous structure or it is simply an unstable intermediate before change into dispersed morphology.

As a conclusion, the use of compatibilizer in multicomponent polymer mixtures is crucial in order to produce a compatible or miscible blend that provides morphological and thermodynamic stablility, higher tensile strength and ductility as well as relatively low cost. Development of completely biodegradable blends offer better advantages in development of polymers towards eco-friendly environment that could potentially cover a wide range of industry applications such as the coatings and adhesives industry, packaging, agricultural and medical applications.

References

1.   Robeson, L., *Historical Perspective of Advances in the Science and Technology of Polymer Blends.* Polymers, 2014. **6**(5): p. 1251-1265.

2.   MarketsandMarkets. *MarketsandMarkets: Global Biodegradable Plastics Market to be 2330 Thousand Metric Tonnes by 2016*. 2001 [cited 2012 11 April]; Available from: http://www.marketsandmarkets.com/PressReleases/biodegradable-plastics.asp.

3.   Verbeek, C. and J. Bier, *A Handbook of Applied Biopolymer Technology: Synthesis, Degradation and Applications*. Chapter 7: Synthesis and Characterization of Thermoplastic Agro-polymers. 2011: Royal Society of Chemistry. 197-237.

4.   González, A. and C.I. Alvarez Igarzabal, *Soy protein–Poly (lactic acid) bilayer films as biodegradable material for active food packaging.* Food Hydrocolloids, 2013. **33**(2): p. 289-296.

5.   Liu, B., et al., *Different Effects of Water and Glycerol on Morphology and Properties of Poly(lactic acid)/Soy Protein Concentrate Blends.* Macromolecular Materials and Engineering, 2010. **295**(2): p. 123-129.

6.   Yokesahachart, C. and R. Yoksan, *Effect of amphiphilic molecules on characteristics and tensile properties of thermoplastic starch and its blends with poly (lactic acid).* Carbohydrate Polymers, 2011. **83**(1): p. 22-31.

7.   Reddy, M.M., A.K. Mohanty, and M. Misra, *Biodegradable Blends From Plasticized Soy Meal, Polycaprolactone, and Poly(butylene succinate).* Macromolecular Materials and Engineering, 2012. **297**(5): p. 455-463.

8.   Stagner, J.A., V.D. Alves, and R. Narayan, *Application and performance of maleated thermoplastic starch‐poly (butylene adipate‐co‐terephthalate) blends for films.* Journal of Applied Polymer Science, 2012. **126**(S1): p. E135-E142.

9.   Chen, F. and J. Zhang, *In-situ poly (butylene adipate-< i> co</i>-terephthalate)/soy protein concentrate composites: Effects of*

compatibilization and composition on properties. Polymer, 2010. **51**(8): p. 1812-1819.

10. Choi, W.Y., C.M. Lee, and H.J. Park, *Development of biodegradable hot-melt adhesive based on poly-< i> ε</i>-caprolactone and soy protein isolate for food packaging system.* Lwt-Food Science and Technology, 2006. **39**(6): p. 591-597.

11. Zeng, J.-B., et al., *Bio-based blends of starch and poly (butylene succinate) with improved miscibility, mechanical properties, and reduced water absorption.* Carbohydrate Polymers, 2011. **83**(2): p. 762-768.

12. Mero, A., et al., *Synthesis and characterization of poly(2-ethyl 2-oxazoline)-conjugates with proteins and drugs: Suitable alternatives to PEG-conjugates?* Journal of Controlled Release, 2008. **125**(2): p. 87-95.

13. Gupta, P. and K.K. Nayak, *Characteristics of protein‐based biopolymer and its application.* Polymer Engineering & Science, 2014.

14. Johnson, A.M., D. J, *In Practical Handbook of Soybean Processing and Utilization*, ed. D.R. Erickson. 1995, Champaign, IL, : AOCS Press. 584.

15. Lodha, P. and A.N. Netravali, *Thermal and mechanical properties of environment-friendly 'green'plastics from stearic acid modified-soy protein isolate.* Industrial crops and products, 2005. **21**(1): p. 49-64.

16. Zhang, J., P. Mungara, and J. Jane, *Mechanical and thermal properties of extruded soy protein sheets.* Polymer, 2001. **42**(6): p. 2569-2578.

17. Kalapathy, U., et al., *Alkali-modified soy proteins: effect of salts and disulfide bond cleavage on adhesion and viscosity.* Journal of the American Oil Chemists' Society, 1996. **73**(8): p. 1063-1066.

18. Huang, W. and X. Sun, *Adhesive properties of soy proteins modified by urea and guanidine hydrochloride.* Journal of the American Oil Chemists' Society, 2000. **77**(1): p. 101-104.

19. Wang, Y., et al., *Soy protein adhesion enhanced by glutaraldehyde crosslink.* Journal of Applied Polymer Science, 2007. **104**(1): p. 130-136.

20. Franzen, K.L. and J.E. Kinsella, *Functional properties of succinylated and acetylated soy protein.* Journal of Agricultural and Food Chemistry, 1976. **24**(4): p. 788-795.

21. Liu, Y., et al., *Graft Copolymerization of Methyl Methacrylate onto Casein Initiated by Potassium Ditelluratocuprate(III).* Journal of Macromolecular Science, Part A, 2004. **41**(3): p. 305-316.

22. Bugnicourt, E., et al., *Processing and Validation of Whey-Protein-Coated Films and Laminates at Semi-Industrial Scale as Novel Recyclable Food Packaging Materials with Excellent Barrier Properties.* Advances in Materials Science and Engineering, 2013. **2013**: p. 10.

23. Kurniawan, L., G.G. Qiao, and X. Zhang, *Chemical modification of wheat protein-based natural polymers: grafting and cross-linking reactions with poly (ethylene oxide) diglycidyl ether and ethyl diamine.* Biomacromolecules, 2007. **8**(9): p. 2909-2915.

24. Shewry, P.R., et al., *The structure and properties of gluten: an elastic protein from wheat grain.* Philosophical Transactions of the Royal Society B: Biological Sciences, 2002. **357**(1418): p. 133-142.

25. Lawton, J.W., *Zein: A history of processing and use.* Cereal Chemistry, 2002. **79**(1): p. 1-18.

26. Ivanova, P., et al., *Amino acid composition and solubility of proteins isolated from sunflower meal produced in Bulgaria.* International Food Research Journal, 2013. **20**(6): p. 2995-3000.

27. Yu, J., M. Ahmedna, and I. Goktepe, *Peanut protein concentrate: Production and functional properties as affected by processing.* Food Chemistry, 2007. **103**(1): p. 121-129.

28. Mooney, B., *The second green revolution? Production of plant-based biodegradable plastics.* Biochem. J, 2009. **418**: p. 219-232.

29. Garratt, R., et al., *Studies of the zein‐like α‐prolamins based on an analysis of amino acid sequences: Implications for their evolution and three‐dimensional structure.* Proteins: Structure, Function, and Bioinformatics, 1993. **15**(1): p. 88-99.

30.   Poysa, V., L. Woodrow, and K. Yu, *Effect of soy protein subunit composition on tofu quality.* Food Research International, 2006. **39**(3): p. 309-317.

31.   Kholief, T., *Chemical composition and protein properties of peanuts.* Zeitschrift für Ernährungswissenschaft, 1987. **26**(1): p. 56-61.

32.   Avena‐Bustillos, R., et al., *Gelation, oxygen permeability, and mechanical properties of mammalian and fish gelatin films.* Journal of food science, 2011. **76**(7): p. E519-E524.

33.   Park, S.K., D. Bae, and N. Hettiarachchy, *Protein concentrate and adhesives from meat and bone meal.* Journal of the American Oil Chemists' Society, 2000. **77**(11): p. 1223-1227.

34.   Cyr, M. and C. Ludmann, *Low risk meat and bone meal (MBM) bottom ash in mortars as sand replacement.* Cement and concrete research, 2006. **36**(3): p. 469-480.

35.   Le Tien, C., et al., *Milk Protein Coatings Prevent Oxidative Browning of Apples and Potatoes.* Journal of Food Science, 2001. **66**(4): p. 512-516.

36.   Gosline, J., et al., *The mechanical design of spider silks: from fibroin sequence to mechanical function.* Journal of Experimental Biology, 1999. **202**(23): p. 3295-3303.

37.   Vroman, I. and L. Tighzert, *Biodegradable Polymers.* Materials, 2009. **2**(2): p. 307-344.

38.   Verbeek, C.J.R. and L.E. van den Berg, *Development of Proteinous Bioplastics Using Bloodmeal.* Journal of Polymers and the Environment, 2010. **19**(1): p. 1-10.

39.   Mucha, M., J. Piekielna, and A. Wieczorek, *Characterisation and morphology of biodegradable chitosan/synthetic polymer blends.* Macromolecular Symposia, 1999. **144**: p. 391-412.

40.   Correlo, V.M., et al., *Properties of melt processed chitosan and aliphatic polyester blends.* Materials Science and Engineering: A, 2005. **403**(1–2): p. 57-68.

41.   Bikiaris, D. and C. Panayiotou, *LDPE/starch blends compatibilized with PE‐g‐MA copolymers.* Journal of Applied Polymer Science, 1998. **70**(8): p. 1503-1521.

42. Janssen, L., Leszek Mościcki, *Thermoplastic Starch: A Green Material for Various Industries*. Eds ed. 2009: Wiley-VCH. Copyright. 35-52.

43. Madhavan Nampoothiri, K., N.R. Nair, and R.P. John, *An overview of the recent developments in polylactide (PLA) research.* Bioresource Technology, 2010. **101**(22): p. 8493-8501.

44. Bhatia, A., et al., *Compatibility of biodegradable poly (lactic acid)(PLA) and poly (butylene succinate)(PBS) blends for packaging application.* Korea-Australia Rheology Journal, 2007. **19**(3): p. 125-131.

45. Fan, D., et al., *Structure and properties of alkaline lignin-filled poly (butylene succinate) plastics.* Iranian Polymer Journal, 2011. **20**(1): p. 3-14.

46. Jacobsen, S. and H.G. Fritz, *Plasticizing polylactide—the effect of different plasticizers on the mechanical properties.* Polymer Engineering & Science, 1999. **39**(7): p. 1303-1310.

47. Parulekar, Y. and A.K. Mohanty, *Extruded Biodegradable Cast Films from Polyhydroxyalkanoate and Thermoplastic Starch Blends: Fabrication and Characterization.* Macromolecular Materials and Engineering, 2007. **292**(12): p. 1218-1228.

48. Poirier, Y., et al., *Polyhydroxybutyrate, a biodegradable thermoplastic, produced in transgenic plants.* Science, 1992. **256**(5056): p. 520-523.

49. Reddy, G., et al., *Amylolytic bacterial lactic acid fermentation — A review.* Biotechnology Advances, 2008. **26**(1): p. 22-34.

50. Kim, K., et al., *Production of lactic acid from food wastes.* Applied Biochemistry and Biotechnology, 2003. **107**(1-3): p. 637-647.

51. Zhang, B., et al., *Enhanced isomer purity of lactic acid from the non-sterile fermentation of kitchen wastes.* Bioresource Technology, 2008. **99**(4): p. 855-862.

52. Huang, L., et al. *Direct Fermentation of Fishmeal Wastewater and Starch Wastewater to Lactic Acid by Rhizopus Oryzae*. in *Bioinformatics and Biomedical Engineering, 2008. ICBBE 2008. The 2nd International Conference on*. 2008. IEEE.

53. Huang, L.P., et al., *Biotechnological production of lactic acid integrated with fishmeal wastewater treatment by Rhizopus oryzae.* Bioprocess and biosystems engineering, 2007. **30**(2): p. 135-140.

54. Budhavaram, N.K. and Z. Fan, *Production of lactic acid from paper sludge using acid-tolerant, thermophilic< i> Bacillus coagulan</i> strains.* Bioresource technology, 2009. **100**(23): p. 5966-5972.

55. Jamshidian, M., et al., *Poly-Lactic Acid: Production, Applications, Nanocomposites, and Release Studies.* Comprehensive Reviews in Food Science and Food Safety, 2010. **9**(5): p. 552-571.

56. Hassouna, F., et al., *New approach on the development of plasticized polylactide (PLA): Grafting of poly(ethylene glycol) (PEG) via reactive extrusion.* European Polymer Journal, 2011. **47**(11): p. 2134-2144.

57. Sungsanit, K., N. Kao, and S.N. Bhattacharya, *Properties of linear poly(lactic acid)/polyethylene glycol blends.* Polymer Engineering & Science, 2012. **52**(1): p. 108-116.

58. Hassouna, F., et al., *New development on plasticized poly(lactide): Chemical grafting of citrate on PLA by reactive extrusion.* European Polymer Journal, 2012. **48**(2): p. 404-415.

59. Carrasco, F., et al., *Processing of poly(lactic acid): Characterization of chemical structure, thermal stability and mechanical properties.* Polymer Degradation and Stability, 2010. **95**(2): p. 116-125.

60. Sheth, M., et al., *Biodegradable polymer blends of poly(lactic acid) and poly(ethylene glycol).* Journal of Applied Polymer Science, 1997. **66**(8): p. 1495-1505.

61. Courgneau, C., et al., *Effect of crystallization on barrier properties of formulated polylactide.* Polymer International, 2012. **61**(2): p. 180-189.

62. Xu, J. and B.H. Guo, *Poly (butylene succinate) and its copolymers: research, development and industrialization.* Biotechnology journal, 2010. **5**(11): p. 1149-1163.

63. Arphavasin, S., et al., *Enhanced osteogenic activity of a poly (butylene succinate)/calcium phosphate composite by simple alkaline hydrolysis.* Biomedical Materials, 2013. **8**(5): p. 055008.

64. Wang, X., J. Zhou, and L. Li, *Multiple melting behavior of poly(butylene succinate).* European Polymer Journal, 2007. **43**(8): p. 3163-3170.

65. Papageorgiou, G.Z., D.S. Achilias, and D.N. Bikiaris, *Crystallization Kinetics of Biodegradable Poly (butylene succinate) under Isothermal and Non‐Isothermal Conditions.* Macromolecular Chemistry and Physics, 2007. **208**(12): p. 1250-1264.

66. Ray, S.S., J. Bandyopadhyay, and M. Bousmina, *Thermal and thermomechanical properties of poly[(butylene succinate)-co-adipate] nanocomposite.* Polymer Degradation and Stability, 2007. **92**(5): p. 802-812.

67. Liu, L., et al., *Mechanical properties of poly(butylene succinate) (PBS) biocomposites reinforced with surface modified jute fibre.* Composites Part A: Applied Science and Manufacturing, 2009. **40**(5): p. 669-674.

68. Phua, Y., W. Chow, and Z.M. Ishak, *Reactive processing of maleic anhydride-grafted poly (butylene succinate) and the compatibilizing effect on poly (butylene succinate) nanocomposites.* Express Polymer Letters, 2013. **7**(4): p. 340-354.

69. Xu, J. and B.-H. Guo, *Poly(butylene succinate) and its copolymers: Research, development and industrialization.* Biotechnology Journal, 2010. **5**(11): p. 1149-1163.

70. Kramer, S.L., et al., *Amino acids in commercially produced bloodmeals.* Journal of Agricultural and Food Chemistry, 1978. **26**(4): p. 979-981.

71. Verbeek, C.J.R. and L.E. van den Berg, *Mechanical Properties and Water Absorption of Thermoplastic Bloodmeal.* Macromolecular Materials and Engineering, 2011. **296**(6): p. 524-534.

72. Verbeek, C.J.R. and L.E. van den Berg, *Extrusion Processing and Properties of Protein-Based Thermoplastics.* Macromolecular Materials and Engineering, 2010. **295**(1): p. 10-21.

73. Adamy, M. and C.J. Verbeek, *Injection‐Molding Performance and Mechanical Properties of Blood Meal‐Based Thermoplastics.* Advances in Polymer Technology, 2013. **32**(3).

74. Bier, J.M., C.J. Verbeek, and M.C. Lay, *Thermal and Mechanical Properties of Bloodmeal‐Based Thermoplastics Plasticized with Tri*

(ethylene glycol). Macromolecular Materials and Engineering, 2014. **299**(1): p. 85-95.

75.   Bier, J.M., C.J.R. Verbeek, and M.C. Lay, *Using synchrotron FTIR spectroscopy to determine secondary structure changes and distribution in thermoplastic protein.* Journal of Applied Polymer Science, 2013. **130**(1): p. 359-369.

76.   P.J, F., *Thermodynamics of high polymer solutions.* Journal of Chemical Physics, 1942. **10**: p. 51-61.

77.   Maurice, L.H., *Solutions of Long Chain Compounds.* The Journal of Chemical Physics, 1941. **9**(5): p. 440.

78.   Rigby, D., J. Lin, and R. Roe, *Compatibilizing effect of random or block copolymer added to binary mixture of homopolymers.* Macromolecules, 1985. **18**(11): p. 2269-2273.

79.   Zhong, Z. and X.S. Sun, *Properties of soy protein isolate/polycaprolactone blends compatibilized by methylene diphenyl diisocyanate.* Polymer, 2001. **42**(16): p. 6961-6969.

80.   John, J. and M. Bhattacharya, *Properties of reactively blended soy protein and modified polyesters.* Polymer International, 1999. **48**(11): p. 1165-1172.

81.   Calabria, L., et al., *Soy protein isolate/poly(lactic acid) injection-molded biodegradable blends for slow release of fertilizers.* Industrial Crops and Products, 2012. **36**(1): p. 41-46.

82.   Zhang, J., et al., *Morphology and Properties of Soy Protein and Polylactide Blends.* Biomacromolecules, 2006. **7**(5): p. 1551-1561.

83.   Xiong, X., et al., *Poly(lactic acid)/Soluble Eggshell Membrane Protein Blend Films: Preparation and Characterization.* Journal of Applied Polymer Science. **117**(4): p. 1955-1959.

84.   Utracki, L.A., *Compatibilization of polymer blends.* Canadian Journal of Chemical Engineering, 2002. **80**(6): p. 1008-1016.

85.   Dieteroch, D.G., E.; Hahn, W. , *Polyurethane Handbook.* 104.70 ed. 1985, New York: Hanser Publishers. 629.

86.   Wang, H., X. Sun, and P. Seib, *Strengthening blends of poly(lactic acid) and starch with methylenediphenyl diisocyanate.* Journal of Applied Polymer Science, 2001. **82**(7): p. 1761-1767.

87.   Hoogenboom, R., *Poly(2-oxazoline)s: A Polymer Class with Numerous Potential Applications.* Angewandte Chemie International Edition, 2009. **48**(43): p. 7978-7994.

88.   Bernard, A.M., *Molecular Modeling of Poly (2-ethyl-2-oxazoline).* 2008: ProQuest. 1-133.

89.   Liu, B., et al., *Synergetic Effect of Dual Compatibilizers on in Situ Formed Poly(Lactic Acid)/Soy Protein Composites.* Industrial & Engineering Chemistry Research, 2010. **49**(14): p. 6399-6406.

90.   Minoura, Y., et al., *The reaction of polypropylene with maleic anhydride.* Journal of Applied Polymer Science, 1969. **13**(8): p. 1625-1640.

91.   Shi, D., et al., *Functionalization of isotactic polypropylene with maleic anhydride by reactive extrusion: mechanism of melt grafting.* Polymer, 2001. **42**(13): p. 5549-5557.

92.   Gaylord, N.G. and M.K. Mishra, *Nondegradative reaction of maleic anhydride and molten polypropylene in the presence of peroxides.* Journal of Polymer Science: Polymer Letters Edition, 1983. **21**(1): p. 23-30.

93.   Li, Y., X.-M. Xie, and B.-H. Guo, *Study on styrene-assisted melt free-radical grafting of maleic anhydride onto polypropylene.* Polymer, 2001. **42**(8): p. 3419-3425.

94.   Sathe, S.N., G. Rao, and S. Devi, *Grafting of maleic anhydride onto polypropylene: Synthesis and characterization.* Journal of applied polymer science, 1994. **53**(2): p. 239-245.

95.   White, J.L. and A. Sasaki, *Free Radical Graft Polymerization.* Polymer-Plastics Technology and Engineering, 2003. **42**(5): p. 711-735.

96.   Sailaja, R.R.N. and M. Chanda, *Use of maleic anhydride–grafted polyethylene as compatibilizer for HDPE–tapioca starch blends: Effects on mechanical properties.* Journal of Applied Polymer Science, 2001. **80**(6): p. 863-872.

97. Cha, J. and J.L. White, *Maleic anhydride modification of polyolefin in an internal mixer and a twin-screw extruder: Experiment and kinetic model.* Polymer Engineering & Science, 2001. **41**(7): p. 1227-1237.

98. Cha, J. and J.L. White, *Methyl methacrylate modification of polyolefin in a batch mixer and a twin-screw extruder experiment and kinetic model.* Polymer Engineering & Science, 2003. **43**(12): p. 1830-1840.

99. Carlson, D., et al., *Maleation of polylactide (PLA) by reactive extrusion.* Journal of Applied Polymer Science, 1999. **72**(4): p. 477-485.

100. Zhu, R., *Preparation of Maleic Anhydride Grafted Poly (lactid acid)(PLA)*. Vol. Master of Science in Material Science. 2011, Doctoral Dissertation Washington State University.

101. Vaidya, U.R. and M. Bhattacharya, *Properties of blends of starch and synthetic polymers containing anhydride groups.* Journal of Applied Polymer Science, 1994. **52**(5): p. 617-628.

102. Bhattacharya, M., et al., *Properties of blends of starch and synthetic polymers containing anhydride groups. II. Effect of amylopectin to amylose ratio in starch.* Journal of Applied Polymer Science, 1995. **57**(5): p. 539-554.

103. Orozco, V.H., et al. *Preparation and Characterization of Poly (Lactic Acid)‐g‐Maleic Anhydride+ Starch Blends*. in *Macromolecular Symposia*. 2009. Wiley Online Library.

104. Zhu, R., H.Z. Liu, and J.W. Zhang, *Compatibilizing Effects of Maleated Poly(lactic acid) (PLA) on Properties of PLA/Soy Protein Composites.* Industrial & Engineering Chemistry Research, 2012. **51**(22): p. 7786-7792.

105. Utracki, L.A., *Commercial Polymer Blends*. 1998, London SE1 8HN, UK: Chapman & Hall.

106. Ajji, A. and L. Utracki, *Interphase and compatibilization of polymer blends.* Polymer Engineering & Science, 1996. **36**(12): p. 1574-1585.

107. Dedecker, K. and G. Groeninckx, *Reactively compatibilized polymer blends: Interfacial chemical reactions during melt-extrusion.* Pure and Applied Chemistry, 1998. **70**(6): p. 1289-1293.

108. Raquez, J.-M., et al., *Biodegradable materials by reactive extrusion: from catalyzed polymerization to functionalization and blend compatibilization.* Comptes Rendus Chimie, 2006. **9**(11): p. 1370-1379.

109. Zhang, Y., et al., *Promoting crystallization of polylactide by the formation of crosslinking bundles.* Materials Letters, 2014. **117**: p. 171-174.

110. Nyambo, C., A.K. Mohanty, and M. Misra, *Effect of Maleated Compatibilizer on Performance of PLA/Wheat Straw€ Based Green Composites.* Macromolecular Materials and Engineering, 2011. **296**(8): p. 710-718.

111. Zhang, J.-F. and X. Sun, *Mechanical properties of poly (lactic acid)/starch composites compatibilized by maleic anhydride.* Biomacromolecules, 2004. **5**(4): p. 1446-1451.

112. Roy, R.K., *Design of Experiments Using The Taguchi Approach: 16 Steps to Product and Process Improvement.* 2001: John Wiley & Sons.

113. Rajan, K.P., et al., *OPTIMIZATION OF PROCESSING PARAMETERS FOR A POLYMER BLEND USING TAGUCHI METHOD.* Yanbu Journal of Engineering and Science, 2010. **1**(1): p. 59-67.

114. Murali M. Reddy, A.K.M., Manjusri Misra, *Optimization of tensile properties thermoplastics blends from soy and biodegradable polyesters: Taguchi design of experiments approach.* J Mater Sci Springer, 2011. **47**: p. 2591-2599.

115. John, J., et al., *Synthesis and characterization of anhydride-functional polycaprolactone.* Journal of Polymer Science Part a-Polymer Chemistry, 1997. **35**(6): p. 1139-1148.

116. Mani, R., J. Currier, and M. Bhattacharya, *Polymerization of ϵ-caprolactone with maleic anhydride: Synthesis and characterization.* Journal of Applied Polymer Science, 2000. **77**(14): p. 3189-3194.

117. Sung, H.-W., C.-S. Hsu, and Y.-S. Lee, *Physical properties of a porcine internal thoracic artery fixed with an epoxy compound.* Biomaterials, 1996. **17**(24): p. 2357-2365.

118. Sung, H.W., et al., *Crosslinking characteristics of an epoxy‐fixed porcine tendon: Effects of pH, temperature, and fixative concentration.* Journal of biomedical materials research, 1996. **31**(4): p. 511-518.

119. Kurniawan, L., G.G. Qiao, and X. Zhang, *Formation of Wheat‐Protein‐Based Biomaterials through Polymer Grafting and Crosslinking Reactions to Introduce New Functional Properties.* Macromolecular bioscience, 2009. **9**(1): p. 93-101.

120. Chen, F. and J. Zhang, *In-situ poly (butylene adipate-co-terephthalate)/soy protein concentrate composites: Effects of compatibilization and composition on properties.* Polymer, 2010. **51**(8): p. 1812-1819.

121. Li, Y.-D., et al., *Structure and Properties of Soy Protein/Poly(butylene succinate) Blends with Improved Compatibility.* Biomacromolecules, 2008. **9**(11): p. 3157-3164.

122. Fang, K., et al., *Properties and morphology of poly(lactic acid)/soy protein isolate blends.* Journal of Applied Polymer Science, 2009. **114**(2): p. 754-759.

123. Ehrenstein, G.W., *Polymeric Materials: Structure, Properties, Applications.* 2001: Hanser Publishers.

124. Li, Y.-D., et al., *Rheology, Crystallization, and Biodegradability of Blends Based on Soy Protein and Chemically Modified Poly(butylene succinate).* Industrial & Engineering Chemistry Research, 2009. **48**(10): p. 4817-4825.

125. Mungara, P., et al., *Processing and Physical Properties of Plastics Made from Soy Protein Polyester Blends.* Journal of Polymers and the Environment, 2002. **10**(1-2): p. 31-37.

126. Park, J.W., et al., *Biodegradable polymer blends of poly(L-lactic acid) and gelatinized starch.* Polymer Engineering & Science, 2000. **40**(12): p. 2539-2550.

127. Li, H. and U. Sundararaj, *Morphology Development of Polymer Blends in Extruder: The Effects of Compatibilization and Rotation Rate.* Macromolecular Chemistry and Physics, 2009. **210**(10): p. 852-863.

128.   Sundararaj, U. and C.W. Macosko, *Drop Breakup and Coalescence in Polymer Blends - The Effects of Concentration and Compatibilization.* Macromolecules, 1995. **28**(8): p. 2647-2657.

129.   Utracki, L.A. and Z.H. Shi, *Development of Polymer Blend Morphology during Compounding in a Twin-Screw Extruder .1. Droplet Dispersion and Coalescence -A Review.* Polymer Engineering and Science, 1992. **32**(24): p. 1824-1833.

130.   Chen, X., J. Xu, and B.H. Guo, *Development of dispersed phase size and its dependence on processing parameters.* Journal of applied polymer science, 2006. **102**(4): p. 3201-3211.

131.   Deyrail, Y., R. Fulchiron, and P. Cassagnau, *Morphology development in immiscible polymer blends during crystallization of the dispersed phase under shear flow.* Polymer, 2002. **43**(11): p. 3311-3321.

132.   Graiver, D., et al., *Biodegradable soy protein-polyester blends by reactive extrusion process.* Journal of Applied Polymer Science, 2004. **92**(5): p. 3231-3239.

133.   Chen, F. and J. Zhang, *A new approach for morphology control of poly(butylene adipate-co-terephthalate) and soy protein blends.* Polymer, 2009. **50**(15): p. 3770-3777.

134.   Pötschke, P. and D. Paul, *Formation of co-continuous structures in melt-mixed immiscible polymer blends.* Journal of Macromolecular Science, Part C: Polymer Reviews, 2003. **43**(1): p. 87-141.

135.   Willemse, R.C., et al., *Tensile moduli of co-continuous polymer blends.* Polymer, 1999. **40**(24): p. 6645-6650.

Chapter 3

Properties of Bloodmeal/Linear Low Density Polyethylene Blends

Compatibilized with Maleic Anhydride Grafted Polyethylene

A paper

published in

Journal of Applied Polymer Science

by

K.I Ku Marsilla[1] and C.J.R. Verbeek

---

[1]As first author of this paper, I prepared the initial draft manuscript, which was refined and edited with consultation with my supervisor, who has been credited as co-author.

Properties of Bloodmeal/Linear Low-Density Polyethylene Blends Compatibilized with Maleic Anhydride Grafted Polyethylene

K. I. Ku Marsilla, C. J. R. Verbeek

Department of Engineering, University of Waikato, Hamilton 3240, New Zealand
Correspondence to: C. J. R. Verbeek (E-mail: jverbeek@waikato.ac.nz).

ABSTRACT: Novatein thermoplastics from bloodmeal (NTP) were blended with linear low-density polyethylene (LLDPE) using maleic anhydride grafted polyethylene (PE-*g*-MAH) as compatibilizer. The compatibilizing effect on mechanical, morphology, thermal properties, and water absorption were studied and compared with blends without compatibilizer. The amount of polyethylene added was varied between 20 and 70% in NTP with addition of 10% compatibilizer. An improvement in compatibility between NTP and LLDPE was observed across the entire composition range and the difference were more pronounced at higher NTP contents where the tensile strength of blends was maintained and never dropped below that of pure NTP. Theoretical models were compared to the results to describe mechanical properties. A finely dispersed small particles of NTP in compatibilized blends were observed using SEM. Improved compatibility has restricted chain movement resulting in slightly elevated T_g revealed by DMA. On the other hand, water absorption of the hydrophilic NTP has been decreased when blending with hydrophobic LLDPE. © 2013 Wiley Periodicals, Inc. J. Appl. Polym. Sci. 130: 1890–1897, 2013

INTRODUCTION

Meat is New Zealand's second-largest food export and is worth $5.14 billion.[1] One of the by-products from meat processing is bloodmeal, an insoluble powder of dried blood containing at least 86 wt % protein and <10% moisture. It is one of the highest non-synthetic sources of nitrogen coming from meat processing. Natural proteins are linear, unbranched and have a precise length with a molecular diversity consisting of up to different 20 amino acids as monomers. An understanding of the chemical reactivity of the amino acid functional groups is important because they provide many reaction sites for potential crosslinking or chemical grafting. Beef blood meal contains more lysine, threonine, valine, leucine, tyrosine, and phenylalanine while pork blood meal contains more histidine, arginine, proline,glycine, and isoleucine.[2] Of these, cysteine and lysine are the most reactive amino acids.

Utilization of bloodmeal as a bioplastic is an alternative to synthetic polymers and may offer a sustainable option over raw materials competing with food sources. It has been shown that bloodmeal can be converted into a Novatein thermoplastic (NTP) by using an appropriate combination of additives, followed by extrusion.[3–5] However, the material is very brittle and water sensitive which may limit its potential applications.

In general, developing blended materials with a full set of desired properties is much more effective and cheaper compared to synthesizing new polymers.[6,7] Linear low-density polyethylene (LLDPE) is among the most popular polyethylene products with significant numbers of short branches, commonly made by copolymerization of ethylene with longer-chain olefins. LLDPE is not biodegradable, however some believe that by blending it with biodegradable thermoplastics, the inert components will slowly decompose and disappear as long as the particle size of the thermoplastic resin is fine enough.[8,9] Blending LLDPE with natural polymers such as soy protein,[10–12] and starch[13–22] has become an important research interest in degradable plastics. However, most blends involving natural and synthetic polymer are immiscible due to the absence of specific interactions, thus requiring a compatibilizer to achieve miscibility.

Maleic anhydride is one of the popular choices used as monomer to graft onto polypropylene, polyethylene, and various other polymers.[23–25] PE-*g*-MAH has hydrophilic and hydrophobic end tail that can react with protein or starch and compatibilize of PE and polyolefin. The mechanical properties of LDPE and starch were reduced by increasing starch content despite the fact that the dispersion of starch particles improved after the addition of PE-*g*-MAH.[21,26] Research found that improved compatibility between rice starch and LDPE from PE-*g*-MAH was

69

attributed to the chemical reaction between hydroxyl groups in starch and anhydride groups in PE-*g*-MAH as well as the physical interaction between PE chains in PE-*g*-MAH and bulk LDPE.[13] A finely dispersed morphology of starch particles of about 5–10 μm was observed between LLDPE and thermoplastic starch, indicating good interfacial adhesion.[15] Anhydride groups were also found effective to improve the compatibility between immiscible blends of soy protein and thermoplastic polyesters.[27] It was found that the glass transition temperature and thermal properties of the protein and polymer remained unchanged even after blending. In a different study, reactive compatibilizers for starch–polycaprolactone (PCL) blends were synthesized and was found that PCL-*g*-diethyl maleate (PCL-*g*-DEM) was a more efficient compatibilizer than PCL-*g*-glycidyl methacrylate (PCL-*g*-GMA).[28]

Modeling Mechanical Properties

The behavior of polymer blends in this work was modeled using known relationships that have been used to predict properties of polymer blends and composites. These models were developed for spherical particles distributed in the matrix. For NTP, it is assumed as near-spherical particles therefore Kerner and Hashin equation was used. Kerner and Hashin considered the dispersed polymer phase as spheroidal in shape and modeled the blend's modulus using equation:[29]

$$E = E_1 \frac{\frac{\phi_2 E_2}{(7 - 5\nu_1)E_1 + (8 - 10\nu_1)E_2} + \frac{\phi_1}{15(1 - \nu_1)}}{\frac{\phi_2 E_1}{(7 - 5\nu_1)E_1 + (8 - 10\nu_1)E_2} + \frac{\phi_1}{15(1 - \nu_1)}} \quad (1)$$

where E, E_1, and E_2 are the modulus for the binary blend, the matrix and the dispersed phase respectively; ϕ_1 and ϕ_2 are the volume fractions of the matrix and the dispersed phase, respectively; ν_1 is the Poisson's ratio for the matrix.

In eq. (1), perfect adhesion is assumed between the two polymer phases; however, this is often not the case. In the absence of adhesion, the Kerner equation is simplified by assuming E_2 to be zero

$$E = E_1 \frac{(7 - 5\nu_1)\phi_1}{15(1 - \nu_1)\phi_2 + (7 - 5\nu_1)\phi_1} \quad (2)$$

The elongation at break for polymer and composites can be evaluated using Nielsen model. Typically, a decrease in elongation at break is observed with increase in filler content, and assuming a spherical dispersed polymer phase, the Nielsen model can be used.[30] For good adhesion between phases, the following Nielson equation is approximately correct:

$$\varepsilon_c = \varepsilon_0 \left(1 - \phi^{1/3}\right) \quad (3)$$

where ε_c is the elongation at break of the blends and ε_0 is the elongation at break of polymer constituting the matrix. The tensile strength is expected to decrease with an increase of dispersed particle (or dispersed polymer phase) content. The theoretical values of tensile strength have been modeled by Nicolais and Narkis[31] assuming no adhesion between phases and

failure is at the filler–matrix interface. In eq. (4), σ_c is the composite's tensile strength and σ_m is the polymer matrix's tensile strength:

$$\sigma_c = \sigma_m \left(1 - 1.21\phi^{2/3}\right) \quad (4)$$

In this study, NTP was blended with low linear density polyethylene (LLDPE) in different proportions containing PE-*g*-MAH as compatibilizer. The effect of PE-*g*-MAH on the materials water absorption and mechanical properties were analyzed in light of the resultant blend's morphology. Modeling of mechanical properties were also performed and correlated to observed values.

MATERIALS AND METHODOLOGY

Materials

Bloodmeal was supplied by Wallace Corporation (New Zealand) and sieved to an average particle size of 700 μm and is mostly bovine with some chicken blood. Technical grade sodium dodecyl sulfate (SDS) and analytical grade sodium sulfite were purchased from Biolab Nz and BDH Lab Supplies. Agricultural grade urea was obtained from Balance Agri-nutrients (NZ). LLDPE, Cotene 3901 was purchased from J.R. Courtenay (N.Z.). Polyethylene-*graft*-maleic anhydride (PE-*g*-MAH) and triethyl was purchased from Sigma Aldrich (NZ). Triethylene glycol was purchased from Merck (NZ).

Preparation of Novatein Thermoplastic Protein (NTP)

Samples were prepared by dissolving urea (20 g), sodium dodecyl sulfate (6 g) and sodium sulfate (6 g) in water (80g). The solution was heated until the temperature reached 50–60°C followed by blending with bloodmeal powder (200 g) in a high-speed mixture for 5 min. Triethylene glycol (40 g) was added to the mixture and blended for another 3–4 min. The mixtures were stored for at least 24 h prior to extrusion. NTP, LLDPE and PE-*g*-MAH were mixed in a plastic zip-lock bag prior to extrusion.

Extrusion

Extrusion was performed using a Thermo Prism TSE-16-TC twin screw extruder at a screw speed of 150 rpm and temperature settings of 70, 100, 100, 100, 120°C from feed to exit die. The screw diameter was 16 mm at *L/D* ratio of 25 and was fitted with a single 10-mm circular die. A relative torque of 50–60% was maintained, by adjusting the mass flow rate of the feed. The extrudate was granulated using a triblade granulator from Castin Machinery, New Zealand.

Injection Molding

Standard tensile bars (ASTM D638) were prepared using a BOY 35A injection molder with a temperature profile of 100, 115, 130, 135, and 140°C from feed to exit die.

Mechanical Testing

Tensile specimens were tested on an Instron model 4204 according to ASTM D638-86. For each experiment five specimens were conditioned at 23°C and 50% relative humidity, equilibrating to ∼10% moisture content and tested at a crosshead speed of 1 mm min^{-1} using 5-kN load cell. Tensile strength,

Table I. Formulations of NTP/LLDPE Blends and Control Samples

Sample name	NTP (wt %)	LLDPE (wt %)	PE-g-MAH (wt %)
0 NTP	0	100	0
20 NTP	20	70	10
30 NTP	30	60	10
40 NTP	40	50	10
50 NTP	50	40	10
60 NTP	60	30	10
70 NTP	70	20	10
100 NTP	100	0	0

elongation at break and Young's modulus were analyzed for conditioned samples.

Morphology

The microstructure of NTP/LLDPE was assessed using a field emission scanning electron microscope (SEM) Hitachi S-4700. Samples were immersed in liquid nitrogen and the fracture surfaces were sputter-coated with platinum before scanning. An accelerating voltage of 5 kV was applied.

Water Absorption

All samples were oven dried at 80°C until constant weight. Dried samples were immersed in water at room temperature for total of 9 days. Samples were removed from water, blotted with tissue paper to remove excess water and then weighed. The water absorption was calculated on a dry sample weight basis.

Simultaneous DSC-TGA (SDT)

Thermogravimetric analysis of pure LLDPE and blended samples were measured using a TA instrument SDT 2960. The samples were sealed in aluminum pan and tested from 50 to 800°C at a heating rate 10°C min^{-1} using air.

Dynamic Mechanical Analysis (DMA)

Dynamic mechanical properties of NTP/LLDPE were studied using a Perkin Elmer DMA 8000 fitted with a high temperature furnace and controlled with DMA software version 14306. DMA specimens (30 × 6.5 × 3 mm^3) were cut from injection molded samples and tested using a single cantilever fixture at 1-Hz vibration frequency in temperature range of −80–120°C.

Formulations

Table I lists the formulations of all samples studied in this work. NTP was extruded and injection molded with LLDPE using the same profile as above. NTP was produced first, followed by blending with the required LLDPE and compatibilizer after which it was extruded again.

RESULTS AND DISCUSSION

Mechanical Properties

Figure 1(a) shows the tensile strength of NTP/LLDPE blends with and without compatibilizer. LLDPE had a tensile strength of 14 MPa while that of NTP is only 6.2 MPa. It would therefore be expected that the blend's tensile strength would be some intermediate value of these. However, the specific value would

depend on the phase morphology as well as adhesion between phases.

The tensile strength of blends without compatibilizer decreased with increasing NTP contents. Above 50 wt % it dropped to values less than pure NTP, most likely due to lack of compatibility between NTP and LLDPE. This observation is in agreement with the fact that blending synthetic and natural polymers are challenging because of their dissimilar nature. NTP is hydrophilic while LLDPE is hydrophobic and the difference resulted in separation of two phases. In polymer blends it is often observed that either one of the two polymers will be the dispersed phase or the other is a continuous phase. Which polymer forms the specific phase is dependent on the amount
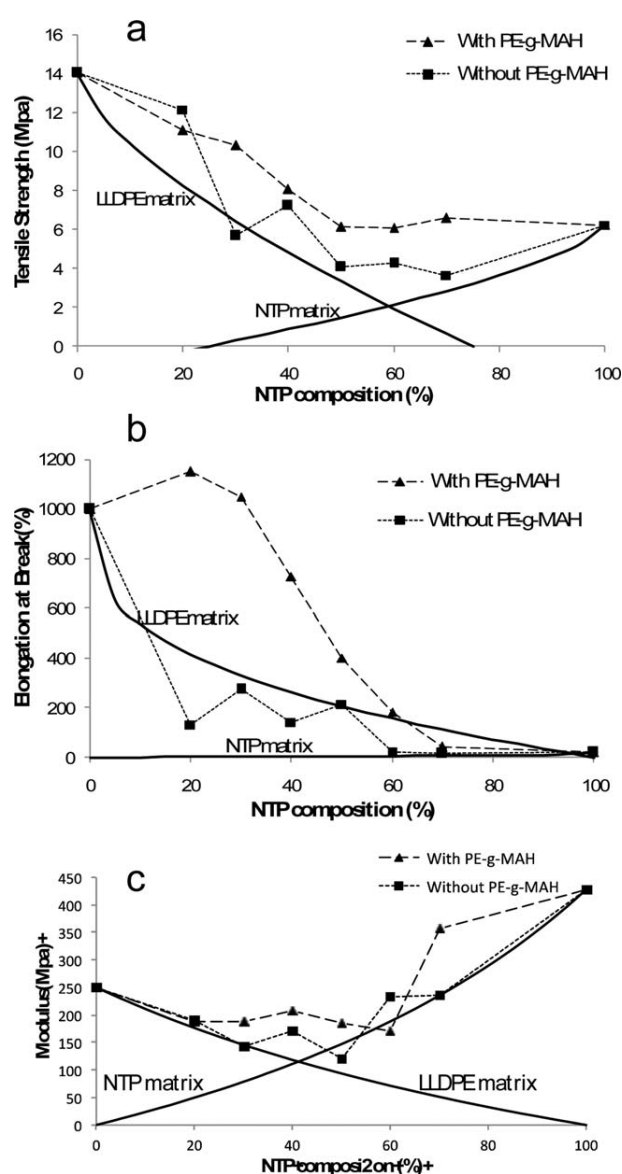

Figure 1. Mechanical properties of NTP/LLDPE blend with and without PE-g-MAH. (a) Tensile strength, (b) Elongation at break, and (c) Young's modulus. Relevant models also included using either NTP or LLDPE as matrix.
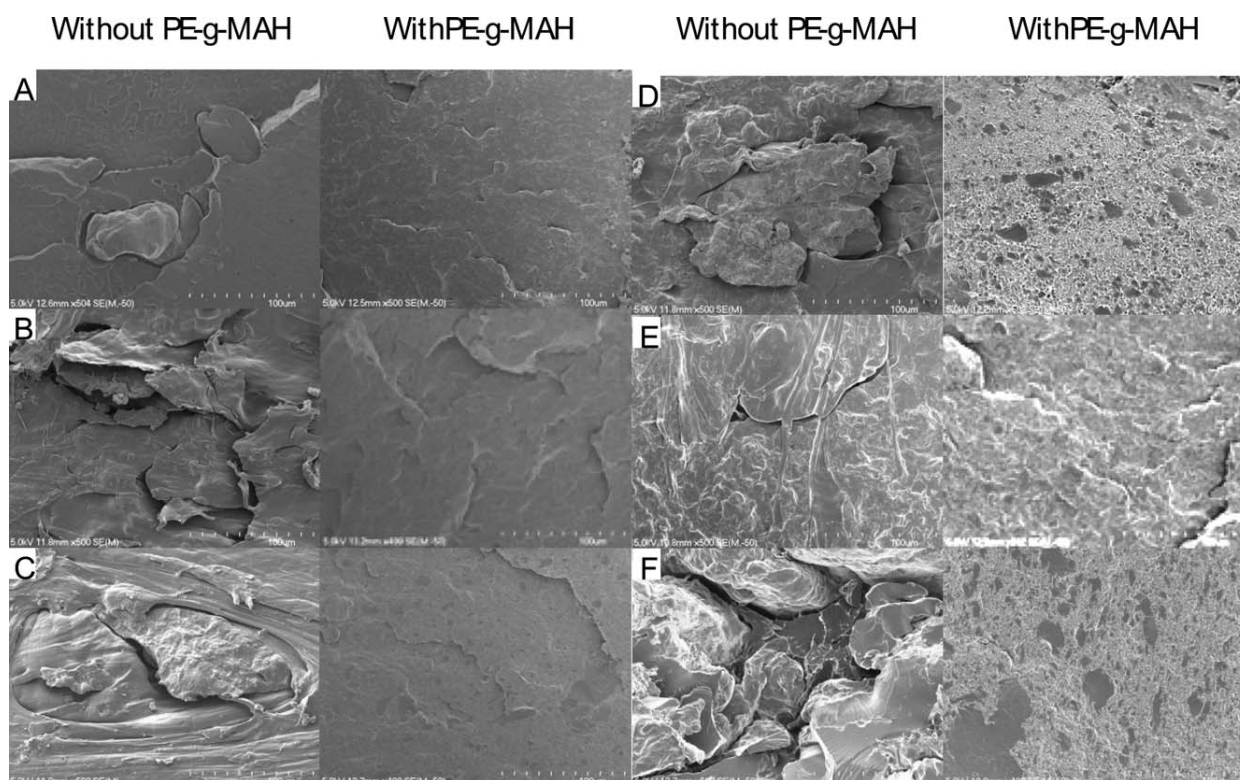
71

Figure 2. SEM morphology of NTP/LLDPE blends without PE-*g*-MAH and with PE-*g*-MAH (a: 20 NTP, b: 30 NTP, c: 40 NTP, d: 50 NTP, e: 60 NTP, f: 70 NTP).

present. Results would suggest that NTP formed a dispersed phase at low NTP content and LLDPE forming the dispersed phase a high NTP content, with significant lack of phase compatibility leading to the low tensile strength of the blends.

A similar decrease in tensile strength was observed for blends containing PE-*g*-MAH, however, the tensile strength leveled off at about 50 wt % NTP, never dropping below that of pure NTP. It was thought that increased interfacial adhesion lead to this behavior leading to blends with increased tensile strength over those without PE-*g*-MAH. As concentration increased, some phase inversion may have occurred leading to a region where neither polymer was the dispersed phase. It was thought that at almost equal proportions, a cocontinuous phases-morphology could have lead to the observed increase in strength and was further explored using SEM.

Elongation at break for blends without PE-*g*-MAH showed a very sharp drop at low NTP content. Considering that NTP is much more brittle than LLDPE (20% vs. 1100%), the result is not surprising and is similar to what is expected of particulate composites with poor interfacial adhesion or the addition of second immiscible phase to a ductile material.[32] Relevant models also included using either NTP or LLDPE as matrix.

In the case of compatibilized blends the situation was completely different. After an initial increase, the elongation at break dropped gradually from that of LLDPE. The synergistic effect at 20–30% of NTP was consistent with findings by Walia et al.[33] using PHEE and starch with different moisture contents.

Despite the decrease over that of pure LLDPE, elongation was always higher to blends without a compatibilizer. It was concluded that the phase morphology must be the determining factor governing changes in the observed mechanical properties. At low NTP content, sufficient interfacial adhesion leads to high elongation to break values, despite the inclusion of a more brittle NTP phase. As the proportion NTP increased, the elongation did decrease as the blend's behavior approached that of pure NTP. Based on the tensile strength at high NTP content, it was concluded that NTP must form a continuous phase under these conditions. This would be consistent to previous observation, which suggested that as the volume fraction of minor
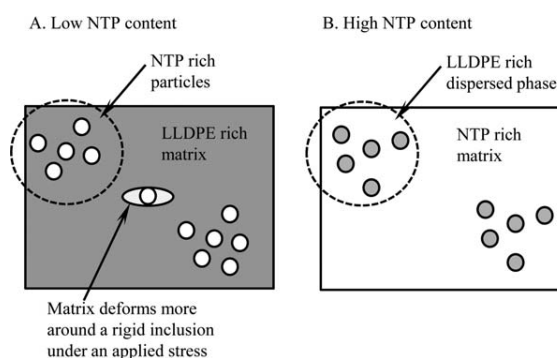

Figure 3. Schematic illustration of NTP/LLDPE blends when LLDPE as the matrix (a) and NTP as the matrix (b).
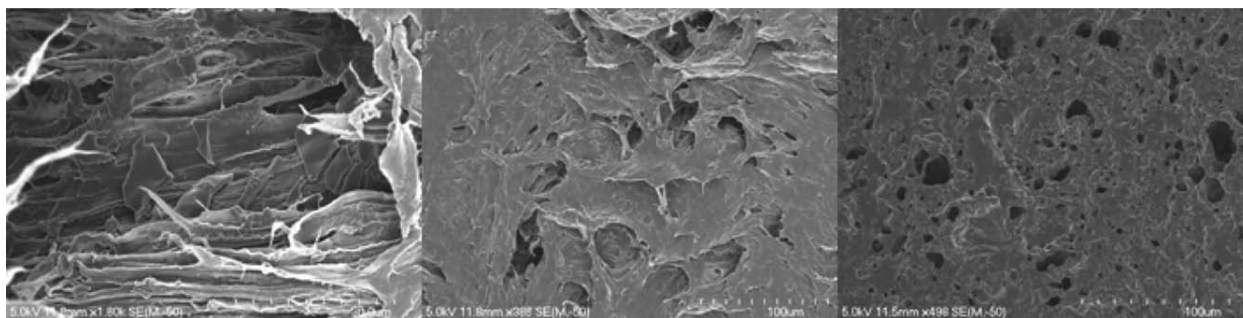
Figure 4. SEM of compatibilized blends containing 50, 60, and 70 wt % NTP after digestion in nitric acid.

components increases, the morphology would change from a dispersed phase to the continuous phase.[34]

The Young's modulus for blends with and without PE-g-MAH showed very similar trends. A sharp drop in modulus was observed with the inclusion of NTP, but increased with increasing NTP content above 50 wt % NTP in the absence of PE-g-MAH or 70 wt % with PE-g-MAH. NTP has a higher modulus than LLDPE and the results would be consistent to what is expected of including rigid particles in a ductile matrix. At low filler content, the disruption of chain interaction could lead to a reduction in modulus, but when as filler content is increased chain mobility is restricted leading to an increase in modulus. However, tensile strength and elongation at break values suggested that NTP formed the continuous phase at high NTP content. All the blends tested had a modulus lower of either of the polymers, suggesting that either dispersed phase disrupted chain interaction, as explained earlier.

In this study, theoretical models were used as interpretation of the mechanical property results. The Poisson's ratio for NTP was assumed to be 0.3 and for LLDPE is 0.5. To estimate the volume fractions, a density of 1.2 and 0.9 g cm^{-3} were used for NTP and LLDPE, respectively.

In the Kerner model, poor interfacial adhesion is assumed and most successfully described Young's Modulus using NTP as matrix in the absence of PE-g-MAH. The assumption of LLDPE being the dispersed phase would appear to be reasonable in light of these results.

The theoretical values of tensile strength have been calculated using the Nicolais–Narkis model, which assumes no adhesion between NTP and LLDPE. Experimental values with and without compatibilizer was significantly higher than theoretical values, but compatibilized blends suggested that there is strong adhesion between NTP and LLDPE when PE-g-MAH was added. This result is in agreement with the starch-LDPE with PE-g-MA blends properties that have been reported by others.[13,26,35]

Elongation at break calculated from the Nielsen model is plotted in Figure 1(b). The most obvious indication of good adhesion between NTP and LLDPE when PE-g-MAH was added to the blends were seen from elongation at break values. The Nielson model did not show agreement with experimental values,

except at high NTP content for blends without PE-g-MAH. For compatibilized blends, the model underestimated the behavior, but at about 50 wt % NTP the Nielson model was unable to predict elongation at break, using either polymer as matrix.

Morphology

Fracture surfaces of blends with and without PE-g-MAH are shown in Figure 2. Samples without compatibilizer showed two distinct phases at all compositions. It was clear that at low NTP content, NTP formed the dispersed phase with relatively large particles. The incompatibility between the two polymers was suspected to lead to large domains of NTP-rich particles suspended in a weak matrix of mostly LLDPE. This result was supported by mechanical properties where at NTP content between 20 and 30% the tensile strength dropped rapidly indicating that the dispersion of NTP has disrupted the LLDPE matrix. Veenstra et al.[36] suggested that when a stiff component (NTP-rich phase) is the minor phase, the weak matrix (LLDPE rich) will deform most at the interface between the stiff droplets and the weak matrix, as illustrated in Figure 3(a). The elongation properties obtained at low NTP is mainly contributed by LLDPE polymer matrix and quickly diminishes with increasing NTP content.

In the case of NTP contents >50%, the influence of a dispersed phase (LLDPE rich) will be limited as the continuous phase will contain mostly NTP, further decreasing the elongation at break.
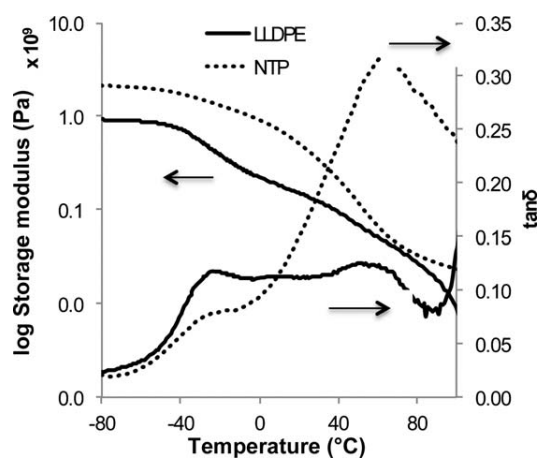

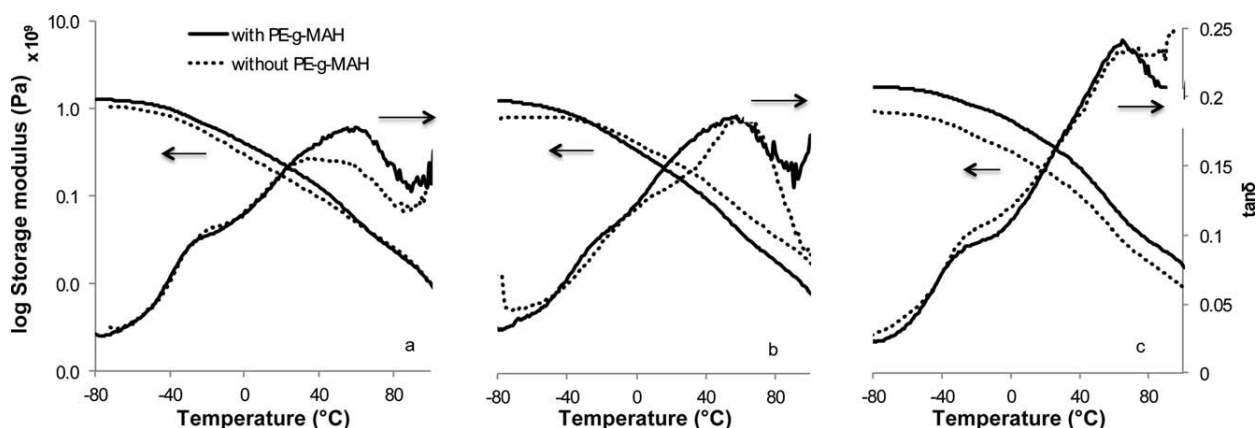**Figure 5.** DMA thermograms of LLDPE and NTP.

73

Figure 6. DMA thermograms of blends of (a) 40 wt % NTP, (b) 50 wt % NTP, and (c) 60 wt % NTP with and without compatibilizer.

In all cases where a dispersed phase was observed, a very rough fracture surface was evident with a clear separation between the phases. Poor interfacial adhesion would therefore account for the observed low strength and elongation at break.

During dispersive mixing, the size of minor cohesive component is reduced while distributive mixing is the process of dispersing the minor component throughout the matrix.[37] Including PE-g-MAH as compatibilizer, a large improvement in dispersion was observed. It was difficult to distinguish between different phases and the fracture surfaces appeared smooth suggesting fine dispersion between the phases.[38] Some interfacial boundaries were observed as ridges, as indicated in Figure 2(a). At 40% NTP, a second finely dispersed phase appeared and was thought to an NTP-rich phase. There was no clear separation between these phases, suggesting good interfacial adhesion. This was supported by earlier observations regarding improved mechanical properties. It is known that at the point of phase inversion, cocontinuous morphologies are mainly formed. Above 50% NTP a clear LLDPE rich phase was evident from ductile fracture regions. NTP appeared to have formed a co-continuous phase with LLDPE, but in addition, larger NTP rich particles were also observed at higher NTP levels (70%).

The interesting phase morphology in the compatibilized blends above 50 wt % NTP was further explored by digesting the protein phase using nitric acid. LLDPE is not digested using this acid, which would reveal the morphology of the LLDPE phase in the blends. In Figure 4, SEM images of compatibilized blends after digestion are shown. Considering NTP was the major constituent, only a small amount of material has been removed after digestion. This would suggest the presence of a finely dispersed NTP phase as well as a LLDPE-rich phase which prevented NTP removal during digestion. This would be consistent to the observed ductile fracture regions observed in the compatibilized blends (Figure 2).

It was concluded that 10% PE-g-MAH was sufficient to compatibilize NTP and LLDPE. The addition of compatibilizer has reduced the interfacial tension between the phases, increased the surface area of the dispersed phase, improves adhesion and

stabilized the phase morphology, consistent with other research.[15] The mechanism of compatibilizing was thought to be through ester bond formation of anhydride groups in PE-g-MAH and amine groups on protein chains, and chain entanglement between PE-g-MAH and LLDPE.

DMA Analysis

The DMA thermograms for NTP and LLDPE are shown in Figure 5. NTP had a glass transition (T_g) at ~60°C as well as a β-transition at about -20°C, consistent with earlier findings.[39] LLDPE had a T_g at about -20°C as well as a transition associated with amorphous regions trapped within crystalline regions at just under 60°C.[40,41]

Thermograms for blends containing 40, 50, and 60 wt % NTP are shown in Figure 6. It can be seen that all samples exhibited two glass transition temperatures between that of NTP and LLDPE. Including PE-g-MAH raised the T_g associated with the NTP rich phase and the storage modulus was also slightly higher in these blends. It was thought that the addition of PE-g-MAH improved compatibility, thereby restricting chain
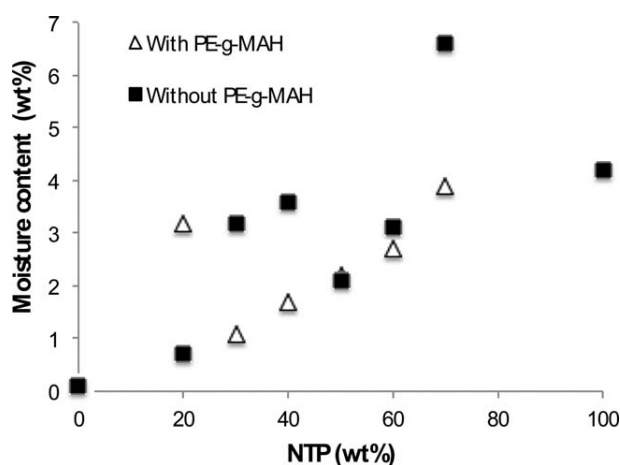

Figure 7. Equilibrium moisture content determined as mass loss percentage at 120°C.
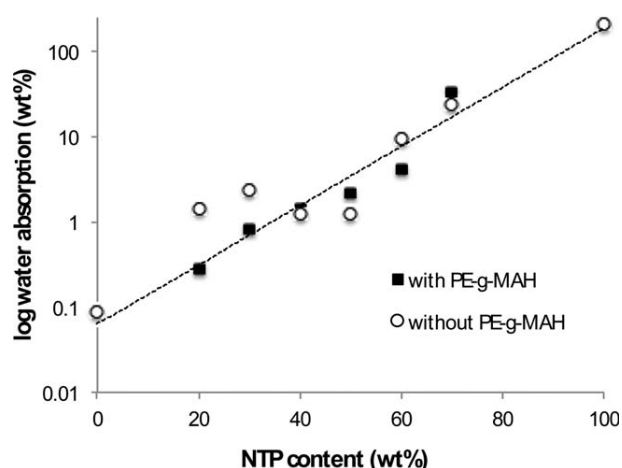
Figure 8. Effect of PE-*g*-MAH on water absorption (%) of NTP/LLDPE blends after 24 h.

movement resulting in a slightly higher T_g, but only when the NTP fraction was low.

Water Absorption

One of the largest challenges with protein-based plastics are their water sensitivity, attributed to their hydrophilic nature. Blending with a hydrophobic polymer, such as LLDPE, could greatly improve water resistance. From Figure 7, it can be seen that the equilibrium moisture content increased with increasing NTP content. In most cases, compatibilization further reduced the moisture content. Moisture content was taken as the percentage mass loss at 120°C using thermogravimetric analysis.

Samples were also immersed in water for a period of 9 days. Absorption occurred rapidly within a day regardless the amount of LLDPE added. Figure 8 shows the results for water absorption after a period of 1 day. NTP absorbed the most (214 wt %) as a consequence of hydrophilic nature, compared to hydrophobic LLDPE, which absorbed only 0.09 wt %. Blending these two polymers was expected to decrease the water absorption of NTP. From Figure 8, it can be seen that water absorption decreased with decreasing NTP.

Including PE-*g*-MAH lead to a slight decrease in water absorption, probably because PE-*g*-MAH improved dispersion of NTP in the LLDPE matrix at low NTP content. Virtually no difference between blends with or without compatibilizer was observed at high NTP content.

CONCLUSION

NTP/LLDPE blends with addition of 10% of PE-*g*-MAH were shown to be more compatible as evident from a more homogenous distribution of the dispersed phase as well as a finer dispersion of each phase. The morphology of compatibilized blends suggested a cocontinuous phase at NTP >50 wt %. It was concluded that a 50 wt % NTP without PE-*g*-MAH, a phase inversion must have occurred as evident from a significant increase in tensile properties. Using PE-*g*-MAH also prevented the blends mechanical properties to be less than that of pure NTP, at any level of LLDPE. PE-*g*-MAH could be

considered as a suitable candidate to toughen NTP/LLDPE blends as evident from the change to more ductile fracture surfaces of blended samples. LLDPE has significantly reduced the water absorption of NTP, but improved phase morphology did not further improve this at high NTP content.

REFERENCES

1. New Zealand Trade and Enterprise, Available at: http://cache.business.newzealand.com/vAmseKA/media/103386/meat_industry_fact_sheet.pdf(accessed August 3, **2011**).

2. Kramer, S. L.; Waibel, P. E.; Behrends, B. R.; El Kandelgy, S. M. *J. Agric. Food Chem.* **1978**, *26*, 979.

3. Verbeek, C. J. R.; van den Berg, L. E. *J. Polym. Environ.* **2010**, *19*, 1.

4. Verbeek, C. J. R.; van den Berg, L. E. *Macromol. Mater. Eng.* **2010**, *295*, 10.

5. Verbeek, C. J. R.; van den Berg, L. E. *Macromol. Mater. Eng.* **2011**, *296*, 524.

6. Paul, D. R.; Newman, S. Polymer Blends; Academic Press: New York, **1978**.

7. Rudin, A. *J. Macromol. Sci. C Polym. Rev.* **1980**, *19*, 267.

8. Janssen, L. Leszek Mościcki, *Thermoplastic Starch: A Green Material for Various Industries*; Wiley-VCH Verlag GmbH & Co. KGaA, **2010**, p 119–148.

9. Utracki, L. A. *Commercial Polymer Blends*; Chapman & Hall, London SE1 8HN, UK, **1998**.

10. Kaur, I.; Bhalla, T. C.; Deepika, N.; Gautam, N. *J. Appl. Polym. Sci.* **2009**, *111*, 2460.

11. Sam, S. T.; Ismail, H.; Ahmad, Z. *J. Vinyl Addit. Technol.* **2009**, *15*, 252.

12. Ting, S. S.; Ismail, H.; Ahmad, Z. *J. Vinyl Addit. Technol.* **2012**, *18*, 57.

13. Wang, Y. J.; Liu, W.; Sun, Z. *J. Appl. Polym. Sci.* **2004**, *92*, 344.

14. Liu, H.; Wu, Q.; Zhang, Q. *Bioresour. Technol.* **2009**, *100*, 6088.

15. Wang, S.; Yu, J.; Yu, J. *J. Appl. Polym. Sci.* **2004**, *93*, 686.

16. Vieyra Ruiz, H.; Martínez, E. S. M.; Méndez, M. Á. A. *Starch—Stärke* **2010**, *63*, 42.

17. Vaidya, U. R.; Bhattacharya, M.; Zhang, D. *Polymer* **1995**, *36*, 1179.

18. Vaidya, U. R.; Bhattacharya, M. *J. Appl. Polym. Sci.* **1994**, *52*, 617.

19. St-Pierre, N.; Favis, B. D.; Ramsay, B. A.; Ramsay, J. A.; Verhoogt, H. *Polymer* **1997**, *38*, 647.

20. Sailaja, R. R. N.; Chanda, M. *J. Appl. Polym. Sci.* **2001**, *80*, 863.

21. Sabetzadeh, M.; Bagheri, R.; Masoomi, M. *J. Appl. Polym. Sci.* **2012**, *126*, E63–E69.

22. Ratanakamnuan, U.; Aht-Ong, D. *J. Appl. Polym. Sci.* **2006**, *100*, 2717.

23. Sathe, S. N.; Rao, G. S. S.; Devi, S. *J. Appl. Polym. Sci.* **1994**, *53*, 239.

24. Vermeesch, I.; Groeninckx, G. *J. Appl. Polym. Sci.* **1994**, *53*, 1365.

25. Gaylord, N. G.; Mehta, M. *J. Polym. Sci. Polym. Lett. Ed.* **1982**, *20*, 481.

26. Liu, W.; Wang, Y. J.; Sun, Z. *J. Appl. Polym. Sci.* **2003**, *88*, 2904.

27. John, J.; Bhattacharya, M. *Polym. Int.* **1999**, *48*, 1165.

28. Sugih, A. K.; Drijfhout, J. P.; Picchioni, F.; Janssen, L. P. B. M.; Heeres, H. J. *J. Appl. Polym. Sci.* **2009**, *114*, 2315.

29. Kerner, E. H. *Proc Phys Soc* **1956**, *69B*, 808.

30. Nielsen, L. E. *Mechanical Properties of Polymers and Composites.* Marcel Dekker: New York, **1974**.

31. Nicolais, L. N. M. *Polym. Eng. Sci.* **1971**, *1*, 194.

32. Pedroso, A. G.; Rosa, D. S. *Carbohydr. Polym.* **2005**, *59*, 1.

33. Walia, P. S.; Lawton, J. W.; Shogren, R. L. *J. Appl. Polym. Sci.* **2002**, *84*, 121.

34. Willemse, R. C.; de Boer, A. P.; van Dam, J.; Gotsis, A. D. *Polymer* **1998**, *39*, 5879.

35. Bikiaris, D.; Panayiotou, C. *J. Appl. Polym. Sci.* **1998**, *70*, 1503.

36. Veenstra, H.; Verkooijen, P. C. J.; van Lent, B. J. J.; van Dam, J.; de Boer, A. P.; Nijhof, A. P. H. *J. Polymer* **2000**, *41*, 1817.

37. Manas-Zloczower, I. *Rheol. Bull.* **1997**, *66*, 5.

38. Shin, B. Y.; Jang, S. H.; Kim, B. S. *Polym. Eng. Sci.* **2011**, *51*, 826.

39. Bier, J. M.; Verbeek, C. J. R.; Lay, M. C. *J. Ther. Anal. Calorimetry* **2012**, 1–13.

40. Khonakdar, H. A.; Wagenknecht, U.; Jafari, S. H.; Hässler, R.; Eslami, H. *Adv. Polym. Technol.* **2004**, *23*, 307.

41. Popli, R.; Glotin, M.; Mandelkern, L.; Benson, R. S. *J. Polym. Sci. Polym. Phys. Ed.* **1984**, *22*, 407.

76

Chapter 4

Mechanical Properties of Thermoplastic Protein From Bloodmeal and Polyester Blends

A paper

published in

*Macromolecular Materials and Engineering*

by

K.I Ku Marsilla[1] and C.J.R. Verbeek

[1]As first author of this paper, I prepared the initial draft manuscript, which was refined and edited with consultation with my supervisor, who has been credited as co-author.

Mechanical Properties of Thermoplastic Protein From Bloodmeal and Polyester Blends

K. I. Ku Marsilla, Casparus J. R. Verbeek*

Blends of bloodmeal-based thermoplastic (NTP) and polybutylene succinate (PBS) were prepared to study the effect of compatibilization on mechanical properties. The Taguchi method was used for experimental design and the results were analysed in terms of signal-to-noise (S/N) ratios using analysis of variance (ANOVA). Between 5 and 10 wt.-% of either poly-2-ethyl-2-oxazoline (PEOX) and poly [(phenyl isocyanate)-co-formaldehyde] (pMDI) were used as compatibilizers in blends of 20–100% NTP. The tensile strength of the blends depended on the type of compatibilizer used while for elongation at break and modulus, NTP content had the largest influence. Compatibilizing efficiency was more pronounced at higher NTP content. The blend's morphology showed a smaller particle size for blends at optimal tensile properties while plastic deformation was observed for samples where elongation at break was optimal.
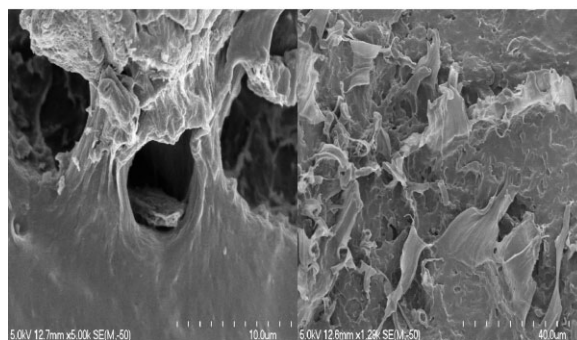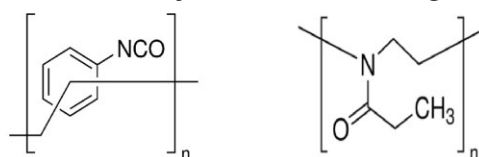
1. Introduction

Bloodmeal is dried blood resulting from slaughterhouse operations and contains about 85% protein, with haemoglobin accounting for 75% of the protein content and plasma protein the other 25% with less than 10% moisture. Recently, biodegradable plastics have been manufactured using starting materials[1] such as soy protein,[2–4] starch[5,6] and gluten.[7,8] As a material from non-food source, research on the utilisation of bloodmeal is on

going.[9–13] Natural proteins are linear, unbranched and have a precise length with a molecular diversity consisting of up to different 20 amino acids as monomers. Without disrupting strong intra- and intermolecular interactions in proteins, processing using conventional equipment such as extruders or injection moulders present a challenge. Sufficient amounts of water and plasticisers are required to ensure processability. In previous work, a mixture of bloodmeal with sodium dodecyl sulphate, sodium sulphite, urea, tri-ethylene glycol and water has successfully been developed into a biodegradable plastic. This material is known as Novatein Thermoplastic Protein (NTP).[14] NTP is best suited for agricultural and horticultural applications such as seedling trays, biodegradable plant pots, vine clips, containers and pegs.

K. I. Ku Marsilla, C. J. R. Verbeek
School of Engineering, Faculty of Science and Engineering
University of Waikato, Hamilton, 3240, New Zealand
E-mail: jverbeek@waikato.ac.nz

Although NTP shows significant potential as a thermoplastic, its hydrophilic nature and brittleness could be disadvantageous. These can be improved by blending NTP with other polymers to increase its processability and mechanical properties. Blending is a cheaper and more convenient method compared to synthesising a novel material.

In blending, miscibility is often defined as miscibility on a molecular scale. In practice, polymer blends are said to be compatible when two phases, on a macroscopic level, have sufficient interactions to provide useful functional or mechanical properties. Compatibility in polymer blends is often explained in terms of its property–composition relationship.[15] Compatibility could be implied when no gross symptoms of phase separation is present. In other words, a blend's properties may be significantly different depending on the volume fraction of a each polymer, as the system may not be compatible over the entire composition range.[16]

Another factor that affects compatibilization and properties of polymer blends is the compatibilizer itself. Strategies for compatibilization include addition of a third component that is miscible with both phases or addition of copolymers that is miscible with either phase.[15–18] The copolymer layer promotes a strong mechanical interface by forming entanglements with the homopolymer bulk phase.[19] Polymers modified for this purpose typically have nucleophilic end-groups such as carboxylic acids, anhydride, amine or hydroxyl groups. These groups then form covalent bonds with suitable electrophilic functional groups, such as epoxide, oxazoline, isocyanate, or carboiimide.[20]

Liu et al.[21] reported a synergetic effect of dual compatibilizers by using both poly(2-ethyl-2-oxazoline) (PEOX) and polymeric methylene diphenyl diisocyanate (pMDI) in blends of polylactic acid (PLA) and soy protein concentrate (SPC). Hydrogen bonding between carbonyl groups in PEOX and hydroxyl and carboxylic end groups (PLA) reduced SPC inclusion size and increased interfacial bonding between PLA and SPC. The addition of pMDI later strengthened the interactions, thereby reducing stress concentration and promoting stress transfer at the interface leading to increased tensile strength.[21] An investigation by Takasu et al.[22] found a single glass transition temperature over the entire composition range of blends between polyvinyl alcohol (PVA) and chitin-g-poly (2-ethyl-2oxazoline). Solubility of the chitin-g-poly (2-ethyl-2oxazoline) was improved, indicating that the crystal structure of chitin has been destructed during grafting which later improved interaction with PVA.

Using PEOX to compatiblize PLA with soy protein isolate (SPI) and SPC increased the tensile strength, reduced particle size and reduced water absorption.[23] pMDI is highly reactive with hydroxyl functional groups to form urethane linkages[24] and the residues of untreated MDI are not expected in blends due to high reactivity of the isocyanate groups.[25]

Generally, the amount of fillers (or second polymer phase) in polymer blends will affect mechanical properties and processability. Injection moulding difficulties were encountered when using more than 65% protein in polyesters blends.[26] 45% starch and 0.5 wt.-% MDI was an optimum combination in PLA/starch blends and it was suggested that each starch level had an optimum MDI content.[27] A far more effective method to optimise processing parameters or mechanical properties of blends is by using a design of experiments (DOE) approach.

NTP has been blended with low linear density polyethylene (LLDPE) using maleic anhydride grafted polyethylene (PE-g-MAH).[30] Without PE-g-MAH, blends had very poor mechanical properties. Furthermore, blend morphology was highly dependent on composition as well as the presence of a compatibilizer. The main disadvantage of these blends was that the material's overall biodegradability was compromised by the presence of LLDPE. Li et al.[31] used urethane functional groups and toluene-2,4-diisocyanate (TDI) to pre-treat polybutylene succinate (PBS) before blending it with SPI. The modulus and tensile strength of the blends were improved due to improved compatibility and a finer dispersion of the polyester in the protein matrix.

The Taguchi method has considerable popularity among researchers by limiting the number of experiments involved. This approach has been used in biodegradable blends of soy protein to study the effect of denaturant, plasticiser and polyester type on tensile properties of the blends.[28] Experimental values at optimal tensile strength and elongation at break were very close to the predicted mean value calculated using the Taguchi approach. Processing parameters were also successfully optimised using Taguchi method in thermoplastic polyurethane (TPU) and poly dimethyl siloxane rubber (PDMS) blends.[29]

In this study, blends of a succinic acid-based aliphatic polyester (PBS) and NTP were prepared using different amounts of NTP, two different compatibilizers and various levels of compatibilizers. PBS, also known as Bionolle, is a polyester synthesised by condensation polymerisation of succinic acid with 1,4-butanediol and ethylene glycol. The advantages of PBS are excellent biodegradability, thermoplastic processability and balanced mechanical properties. Despite its good performance, many efforts have been made to modify PBS-based materials to reduce the cost. In this study, PBS was chosen because its melting point is similar to the processing temperature of NTP. An L9 Taguchi array was used allowing 4 three-level factors.

www.MaterialsViews.com

79

2. Methodology

2.1. Materials

Bloodmeal was supplied by Wallace Corporation (New Zealand) and sieved to an average particle size of 700 μm and was mostly bovine with some chicken blood. Technical grade sodium dodecyl sulphate (SDS) and analytical grade sodium sulphite were purchased from BiolabNZ and BDH Lab Supplies. Agricultural grade urea was obtained from Balance Agri-nutrients (NZ). Poly-2-ethyl-2-oxazoline (PEOX) and poly (phenyl isocyanate)-co-formaldehyde (pMDI) were obtained from Sigma–Aldrich and were used as received. PBS was purchased from Showa High Polymer, injection moulding grade #3020.

2.2. Preparation of Novatein Thermoplastic Protein (NTP)

Samples were prepared by dissolving urea (20 g), sodium dodecyl sulphate (6 g), and sodium sulphate (6 g) in water (80 g). The solution was heated until the temperature reached 50–60 °C followed by blending with bloodmeal powder (200 g) in a high-speed mixer for 5 min. The mixtures were stored for at least 24 h prior to extrusion. Extrusion was performed using a ThermoPrism TSE-16-TC twin screw extruder at a screw speed of 150 rpm and temperature settings of 70, 100, 100, 100 and 120 °C from feed to exit die. The screw diameter was 16 mm at L/D ratio of 25 and was fitted with a single 10 mm circular die. A relative torque of 50–60% was maintained by adjusting the mass flow rate of the feed. The extruded NTP was granulated using a tri-blade granulator from Castin Machinery Manufacturer Ltd., China.

2.3. Preparation of Blends

PBS was mixed with NTP granules followed by extruding at the same conditions as for NTP alone. Compatibilizer was added and was extruded again. In the case of dual compatibilizer, the second compatibilizer, pMDI, was added to the granulated blend just before injection moulding. The pMDI content was maintained at 2%, while the amount of PEOX was changed. The specimens were conditioned at 23 °C and 50% relative humidity to approximately 10%

moisture. Standard tensile bars (ASTM D638) were prepared using a BOY 35A injection moulding machine with a temperature profile of 110, 115, 120, 120 and 120 °C from feed to die zone.

2.4. Design of Experiments

2.4.1. Taguchi Method

The Taguchi method involves reducing the variation in a process through a robust design of experiments in order to produce high-quality but low-cost product.[32] It was used to study the effects of multiple variables by identifying the performance trends for each factor and determines the combination that yields optimum conditions. The Taguchi method is described by the following steps: identification of the factors and their levels; selection of a suitable orthogonal array (OA) and assignment of the factors and levels to the OA; conducting experiments; determination of the optimum levels; verification of the optimum design factors through experiment.

After the experiments, results are analysed using signal to noise (S/N) ratios. The (S/N) ratio was calculated for each experiment to determine the effect of each variable and parameter level that maximised the performance. The S/N ratio can be divided into three categories depending on the desired output performance: nominal, smaller-the-better and larger-the-better, according to Equations 1, 2, and 3.

$$\frac{S}{N} = -10 \log \frac{\sum_{i=1}^{n} (Y_i - M)^2}{n} \tag{1}$$

$$\frac{S}{N} = -10 \log \frac{\sum_{i=1}^{n} Y_i^2}{n} \tag{2}$$

$$\frac{S}{N} = -10 \log \frac{\sum_{i=1}^{n} \left(\frac{1}{Y_i^2}\right)}{n} \tag{3}$$

In these equations, M is the average of the observed data, n is the number of observations, and Y is the observed data. A higher S/N ratio is generally considered the better result.

The selection of factors and their levels is shown in Table 1. Three factors and three levels for each factor were selected. These were chosen after some initial

Table 1. Selected factors and their respective levels.

Factors	Symbol	Level 1	Level 2	Level 3
Compatibilizer	A	PEOX	pMDI	PEOX/pMDI
NTP composition	B	20	50	70
% compatibilizer	C	5	7	10

80

Table 2. Taguchi L9 orthogonal array of designed experiments based on the coded levels.

Experiment trials	Compatibilizer	NTP[%]	% compatibilizer
R1	PEOX	20	5
R2	PEOX	50	7
R3	PEOX	70	10
R4	pMDI	20	7
R5	pMDI	50	10
R6	pMDI	70	5
R7	PEOX-pMDI	20	10 (2 pMDI + 8 PEOX)
R8	PEOX-pMDI	50	5 (2 pMDI + 3 PEOX)
R9	PEOX-pMDI	70	7 (2 pMDI + 5 PEOX)

experimentation to determine a feasible range for blend preparation. Table 2 shows a standard L9 orthogonal array and is based on the coded levels in Table 1. This configuration does not allow for the determination of interactions between factors.

The objective of this work was to study the effect of various NTP compositions, type and amount of compatibilizer on mechanical properties and morphology. As a comparison, blends of NTP/PBS without compatibilizer in the range of 0–100% NTP were prepared as a control.

2.4.2. Data Evaluation and Analysis

A larger-is-better response (Equation 3) was chosen for tensile strength, elongation at break and secant modulus. The relative effect of factors that affecting the response can be calculated by analysis of variance (ANOVA). ANOVA is used to determine statistically significant factors and to explore the percentage contribution of each factor and level to the total variation using Statistica version 10.0 MRI.

Regression analysis was used for estimating the relationship among a selected dependent variable, y, and several independent variables, x_i. A general formula for a multiple variable linear model is as follows:

$$y = b_o + b_1 x_1 + b_2 x_2 + \cdots + b_p x_p \tag{4}$$

Following ANOVA, regression analysis was used to determine the optimal set of parameters b (b_0, b_1, b_2,...., b_p) in the model by minimising the error of sum of squares (SS) between the actual and predicted values for each observed value. A correlation was established between the factors and by using Statistica software. The predicted optimum conditions were then verified using Statistica.

3. Mechanical Testing

After conditioning, tensile properties were determined using an Instron model 33R4204 according to ASTM 638–86.

An extension rate of $5 \, \text{mm} \cdot \text{min}^{-1}$ and an extensometer gauge length of 50 mm were used for testing. Samples were tested in replicas of five after conditioning for 15 d at 23 °C and 50% relative humidity before tensile testing. The secant modulus was calculated between a strain of 0.0005 and 0.0025 and the toughness was calculated as the area under the stress–strain graph and is more accurately referred to as energy-to-break.

3.1. Modelling Mechanical Properties

The behaviour of polymer blends in this work was modelled using known relationships that have been used to predict properties of polymer blends and composites. The theoretical values of tensile strength have been modelled by Nicolais and Narkis[33] and assumes no adhesion between phases and failure is at the filler–matrix interface. In Equation 4, σ_c is the composite's tensile strength, σ_m is the polymer matrix's tensile strength and Ø is the volume fraction:

$$\sigma_c = \sigma_m (1 - 1.21 \emptyset^{\frac{2}{3}}) \tag{4}$$

The elongation at break for polymers and composites can be evaluated using the Nielsen model.[34] Typically, a decrease in elongation at break is observed with increase in filler content, and assuming a spherical dispersed polymer phase, the Nielsen model can be used. For good adhesion between phases, the following equation can be used:

$$\varepsilon_c = \varepsilon_0 (1 - \emptyset^{\frac{1}{3}}) \tag{5}$$

The modulus of polymer blends generally in range between an upper bound, E_u, given by the parallel model (Equation 6) and a lower bound, E_L, given by the series model (Equation 7):

$$E_u = \emptyset_1 E_1 + \emptyset_2 E_2 \tag{6}$$

www.MaterialsViews.com

$$\frac{1}{E_{\mathrm{L}}} = \frac{\varnothing_1}{E_1} + \frac{\varnothing_2}{E_2} \qquad (7)$$

in which E_i and $\varnothing_i$ are the modulus and volume fraction of phase i. These models are frequently used as limiting models regardless of morphology.

4. Morphology

The microstructures of NTP/PBS were fractured after immersion in liquid nitrogen and sputter-coated with platinum before scanning using scanning electron microscopy (SEM) Hitachi S-4700. An accelerating voltage of 5 kV was used.

5. Results and Discussion

5.1. Mechanical Properties

Figure 1 presents the tensile strength, elongation at break, secant modulus and toughness of NTP/PBS blends consisting of 0–100% NTP for blends without compatibilizers. For tensile strength, it was apparent that the tensile strength generally decreased with increasing NTP content. At 60 NTP/40 PBS, the tensile strength dropped to about 70% lower than pure PBS. In general, the tensile strength of the blends was below that of pure NTP, suggesting that adhesion between the two phases was very poor. This was also supported by the Nicolais–Narkis model, which assume that there is no adhesion between the spherical fillers with matrix if the fracture goes through the filler–matrix interface.

The addition of NTP decreased the elongation at break of blends without compatibilizer. At 70% NTP, the elongation at break dropped below the elongation at break of pure NTP. Considering that NTP is much more brittle than PBS (5% vs. 43%), the result is not surprising and is similar to what is expected of particulate composites. Poor interfacial adhesion or introduction of a dispersed phase into a matrix typically causes a dramatic decrease in elongation at break. Despite the poor adhesion, PBS can still elongate significantly at lower NTP content. However PBS gets constrained by NTP at higher NTP content, resulting in a significantly lower elongation at break comparable to that of NTP.

The modulus of uncompatibilized blends increased with increased NTP content. NTP has a higher modulus than PBS and the trend appeared similar to what would be expected using the mixing rule of series and parallel model for polymer blends. These results would be consistent to what is expected when including rigid particles into a soft PBS matrix. The increase in modulus was mostly unaffected by poor adhesion, contrary to what was observed for tensile strength.
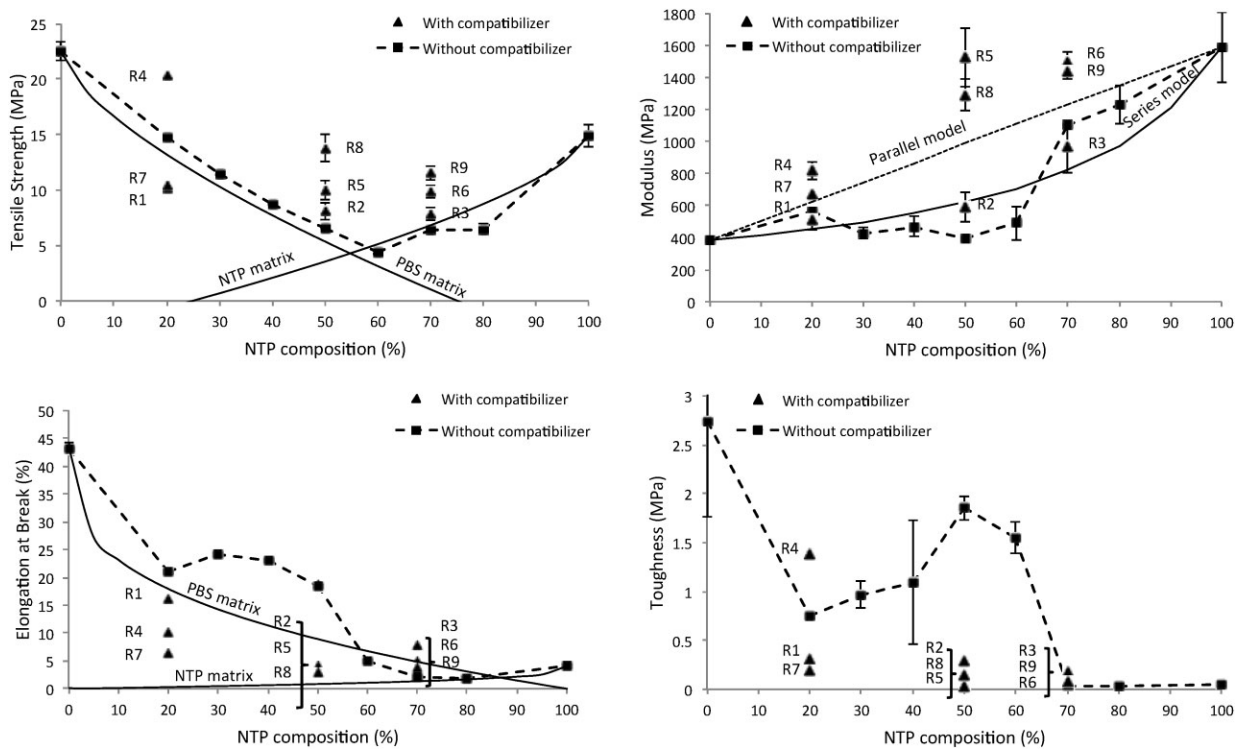

Figure 1. Tensile strength, elongation at break, secant modulus and toughness of NTP/PBS blends without compatibilizer and those from Taguchi array.

To achieve a high toughness, a good combination of strength and ductility is required. The toughness of PBS was much higher (2.7 MPa) compared to NTP (0.06 MPa). At low NTP content, toughness decreased drastically, but increased again between 40 and 60% NTP; reaching an optimal value at 50% NTP (1.9 MPa). Above 70% NTP, the toughness was very poor, similar to that of pure NTP. The results would suggest that at about 50% NTP the morphology of the blends must be such that it allows PBS chains to extend under load, without significant interference from NTP. This probably suggests a co-continuous or finely dispersed morphology, similar to that observed in NTP/LLDPE blends.[35]

In the case of blends with compatibilizer, the tensile strength generally improved over equivalent samples without compatibilizer. According to literature, isocyanate (NCO) groups in pMDI have the capability to react with amines, carboxylic acids or hydroxyl containing polymers meanwhile for PEOX, oxazoline functional groups can react with either amines or carboxylic acid end groups or acid end-groups of polyesters.[36] It may therefore react with amine and carboxylic end groups of NTP and hydroxyl end group of PBS.

At 20% NTP (R4), the tensile strength nearly approached the tensile strength of pure PBS, suggesting that the addition of 7% pMDI led to effective interaction between NTP and PBS phases. This was contrary to the research by Mohamed et al.[8] that found that the addition of pMDI had no significant impact on tensile strength of PCL-MDI-gluten as the addition only provided reinforcement in the interface between PCL and fillers. When using either PEOX (R1) or PEOX and pMDI in combination (R7), the tensile properties were below the uncompatibilized blends, indicating that these compatibilizers did not lead to sufficient interactions.

Using two compatibilizers, at 50 and 70% NTP, showed the highest tensile strength (R8 and R9). At near equal proportion NTP and PBS, morphology such as either a co-continuous phase or that of a finer dispersed phase is likely, especially when using compatibilizers. Research on PLA/soy protein blends using two compatibilizers (PEOX and pMDI) showed a reduction in SPC inclusion size and increased tensile strength to higher than that of pure PLA.[21] In this study, using only pMDI (R5 and R6) showed the second highest tensile strength although the values were slightly lower than pure NTP, while using PEOX (R2 and R3) showed the lowest tensile strength of compatibilized blends. According to literature, PEOX has the capability to reduce particle size that results in finer morphology, although significant improvement in tensile strength was not observed.[21,23] This is in agreement with our results where blends of PEOX showed unsatisfactory results. The changes in morphology for samples using PEOX will be discussed later. The biggest improvement in strength was observed when using two compatibilizers (R8 and R9). It would appear that introducing pMDI just

before injection moulding allowed the greatest interaction between phases, probably because the functional groups were not hydrolysed during extrusion as a result of the high water content of NTP.

Elongation at break generally decreased with the increase in NTP content when a compatibilizer was included. This is most likely due to improved compatibility (and a change in morphology away from dispersed phase, as used by the Nielsen model) thereby restricting chain movement and decreasing the elongation at break. However, R1, R2, and R3 showed the highest elongation at break values for blends containing a compatibilizer (PEOX). Considering these blends also had the lowest tensile strength of the compatibilized blends, it can be concluded that PEOX was not an effective compatibilizer and may simply stiffen the NTP matrix. In the absence of strong interactions, PBS can likely elongate independently from NTP leading to higher elongation at break values, especially at lower NTP content and only using PEOX. This further supported by changes in morphology, as discussed later.

The secant modulus of compatibilized NTP/PBS blends was generally higher than uncompatibilized blends. Filling a flexible matrix with rigid bodies would normally stiffen the matrix such that given sufficient interfacial adhesion. The results presented here would support the conclusion that interfacial adhesion was weak in the absence of compatibilizers. At 50% NTP and above, improved adhesion and possible changes in morphology led to significant stiffening of the flexible PBS matrix. The secant modulus became even higher when using compatibilizer, suggesting some interfacial modification promoting chain stiffening.

Toughness of all the compatibilized blends was lower than uncompatibilized blends (except R4). The combination of high stiffness and low elongation at break produced blends with very low toughness. Improved adhesion between a dispersed phase and the matrix often leads to a reduction in toughness, unless the dispersed phase is rubbery material.[37]

5.2. Optimal Properties

Table 3 lists the average mechanical properties obtained from repeated measures. The highest tensile strength and elongation at break corresponded to R4. Using ANOVA of the calculated S/N ratios, optimal performance can be estimated and may not correspond to the highest value observed from the orthogonal array.

The calculated S/N ratio for each parameter and level (Table 4) allows ranking the relative importance of each factor influencing a measured property. For tensile strength, the order of importance was type of compatibilizer, NTP content and percentage compatibilizer. The optimum level was at 7% pMDI and 20% NTP, which was in agreement with the experimental results (R4).

83

Table 3. Average data of tensile strength and elongation at break of compatibilized NTP/PBS blends.

Experimental trials	Tensile strength [MPa]	Elongation at break [%]	Secant Modulus [MPa]
R1	10.23	16.35	515.42
R2	8.06	9.99	589.14
R3	7.84	6.32	970.35
R4	20.23	18.68	818.43
R5	9.92	4.25	1524.76
R6	9.84	2.99	1503.07
R7	10.37	7.87	670.33
R8	13.80	4.91	1289.64
R9	11.57	3.78	1435.54

In the case of elongation at break, the ranking order was NTP content, type of compatibilizer and the percentage of compatibilizer. Optimal results would correspond to 20% NTP, using 7% PEOX as compatibilizer.

The results would suggest that to have a ductile polymer, NTP content was the most influencing factor. NTP is brittle and it was expected that a lower NTP content would give higher elongation at break properties. The percentage compatibilizer had a greater impact on elongation at break as this follows a complex mechanism requiring some interfacial adhesion. Perfect adhesion between rigid inclusions and a ductile matrix would again lower the toughness of the material.

It appears that the ranking of secant modulus is similar with the ranking order of tensile strength but the optimal result was at different factors level. 5% pMDI in 70% NTP was the optimal condition for modulus, which corresponded to R6.

ANOVA (Table 5) was done at a 95% level of confidence and all the factors were found to be statistically significant. The type of compatibilizer used contributed the most to tensile strength (41%) while %NTP and % compatibilizer had comparable influences (30.4 and 28.2%, respectively).

For elongation at break, %NTP had the highest percentage contribution (68.3%) followed by the type of compatibilizer (18%) and percentage compatibilizer (13.7%). These were in agreement with the experimental results. At 20% of NTP and PEOX as a compatibilizer, the best elongation at break value was observed. NTP itself was brittle and to increase ductility, such an amount of compatibilizer was needed to modify the interfacial adhesion. However, from previous analysis using the *S/N* ratio, the optimum condition suggested was 7% PEOX in 20% of NTP/PBS blends. A confirmatory test was needed to prove the optimum condition suggested by the Taguchi method. In the case of modulus, NTP content (51.9%) and type of compatibilizer (45.1%) showed the highest influence. The percentage compatibilizer (3.0%) had little contribution to modulus.

Table 4. S/N ratios values of tensile strength, elongation at break and secant modulus of compatibilized blends.

Test	Factors	Level 1	Level 2	Level 3	Δ[a]	Rank
Tensile strength	A	12.44	**15.75**	14.86	3.31	1
	B	**15.89**	13.71	13.45	2.43	2
	C	14.58	**15.37**	13.10	2.27	3
Elongation at break	A	**17.69**	15.56	14.09	3.60	3
	B	**22.05**	14.81	10.49	11.57	1
	C	15.39	**18.63**	13.33	5.30	2
Secant Modulus	A	48.62	**55.40**	54.18	6.79	1
	B	49.88	53.39	**54.93**	5.06	2
	C	**53.33**	52.03	52.84	1.29	3

[a]Δ = difference between highest and lowest *S/N* values. Bold letters indicate optimal levels.

Materials
Views
www.MaterialsViews.com

Macromol. Mater. Eng. **2014,** *299,* 885–895
© 2014 WILEY-VCH Verlag GmbH & Co. KGaA, Weinheim

Macromolecular
Journals

891

84

Table 5. Analysis of variance (ANOVA) of tensile strength, elongation at break and secant modulus.

	Factors	SS	Df	MS	F	% contribution
Tensile strength	A	168.1	2	84.06	13.38	41.4
	B	123.6	2	61.81	9.84	30.4
	C	114.7	2	57.35	9.13	28.2
	Total	406.4	6			
Elongation at break	A	218.1	2	109.1	9.97	18.0
	B	827.2	2	413.6	37.81	68.3
	C	165.2	2	82.6	7.55	13.7
	Total	1210.5	6			
Secant Modulus	A	2.82E + 06	2	1.41E + 06	31.49	45.1
	B	3.25E + 06	2	1.62E + 06	36.18	51.9
	C	1.89E + 05	2	9.46E + 04	2.11	3.0
	Total	6.26E + 06	6			

6. Optimum Conditions

Once all the control factors were optimised, confirmatory tests were performed at the optimum level of each factor. Table 6 presents the performance at optimum level for tensile strength (20 NTP/7% pMDI), elongation at break (20 NTP/7% PEOX) and secant modulus (70 NTP/5%pMDI). The average values, experimental values as well as the predicted values (calculated using regression) are shown in Table 6. Results from regression analysis (Statistica) are shown in Equations 6, 7 and 8:

$$\text{Tensile strength}: y = 15.14 + 0.345A - 0.43B - 0.25C \tag{6}$$

$$\text{Elongation at break}: y = 26.75 - 0.36A - 0.7B - 0.16C \tag{7}$$

$$\text{Secant Modulus}: y = 35.46 + 0.427A - 0.631B - 0.03C \tag{8}$$

where A is compatibilizer type, B is NTP composition (%) and C is percentage of compatibilizer.

Table 6. Performance at optimum level for tensile strength, elongation at break and secant modulus.

	Experimental values at optimal	Values predicted by regression
Tensile Strength (MPa)	20.2	13.6
Elongation at Break (%)	13.3	16.6
Secant Modulus (MPa)	1503.1	1350.6

The experimental value of tensile strength was 35% higher than the predicted value while for elongation at break, the experimental value was 18.8% lower than the predicted value. About 10% difference in secant modulus was obtained between experimental and predicted values. For tensile strength, the optimum condition calculated by Taguchi was effective to obtain a high tensile strength. However, for elongation at break and secant modulus, there was a slight decrease compared to the predicted value and average value. It was expected that morphology could be the determining factor to explain this behaviour.

The largest discrepancy between predicted and experimental optimal conditions was for tensile strength. This would imply that other factors, not considered in the Taguchi array, or large variations in experimental values are causing the difference. Factors such as processing conditions may also influence tensile strength, although care was taken to keep these constant. For modulus and elongation at break, it would appear that factors other than the ones selected did not have a significant influence on the experimental results.

6.1. Morphology

Figure 2 presents the morphology of NTP/PBS blends without compatibilizer (C1–C3) at different NTP content. The fracture surface at 20% NTP showed large dispersed particles of NTP in a PBS matrix. At 50% NTP, the fracture surface was smooth, but contained a substantial void fracture indicating poor consolidation. This could be attributed to lack of adhesion, which explained the decrease in mechanical properties. Meanwhile at 70% NTP, an agglomerated NTP rich phase was formed. At low NTP
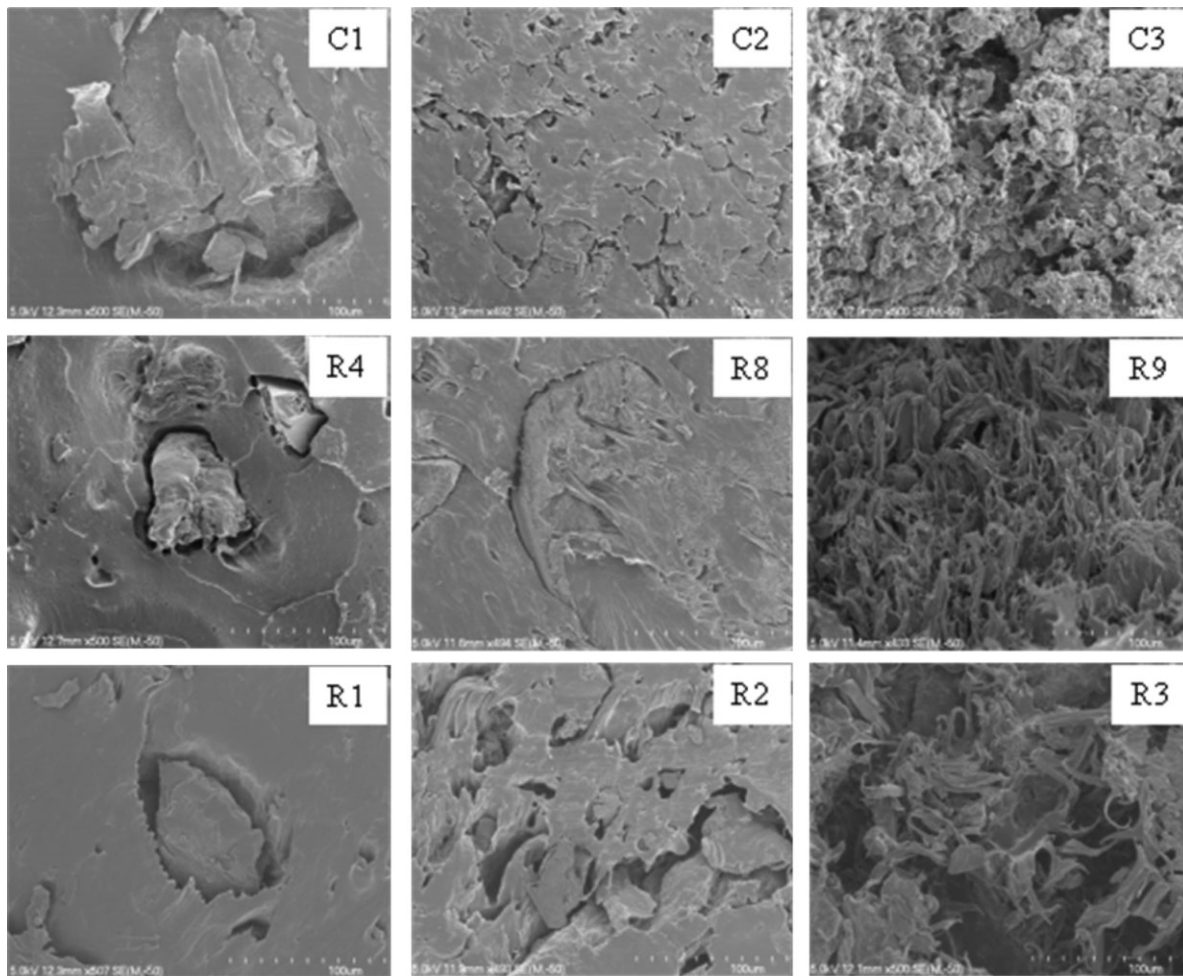
Figure 2. Morphology of NTP/PBS blends without compatibilizer at 20% NTP (C1), 50% NTP (C2), 70% NTP (C3) and those from the Taguchi array.
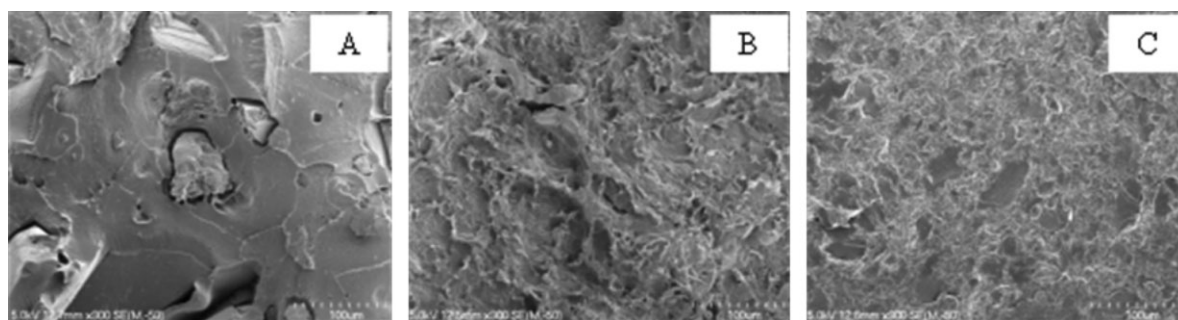
content NTP was the dispersed phases, while at high NTP content, PBS was the dispersed phase.

An interesting morphology was observed when compatibilizer was added in NTP/PBS blends. R4, R8 and R9 illustrate the morphology of the highest tensile strength blends at different NTP content, while R1, R2 and R3 present the morphology of the highest elongation at break blends. At 20% NTP/7% pMDI (R4), it is clear that NTP formed a dispersed phase with a mixture of large and small particles in the matrix. Partial adhesion was also observed between NTP particles and the PBS matrix, which is in agreement with the tensile strength results. It can also be noted that at 50% NTP/5% PEOX-pMDI, adhesion was more apparent between the NTP particles and PBS matrix (R8). In the case of higher NTP content, particles are less evident from the fracture surface. It would appear that the addition of 7% PEOX-pMDI enabled PBS to elongate independently without interference from the NTP phase, evident for the necking observed on the fracture surface. This was consistent with elongation at break results in mechanical properties section.

The morphology of R1 and R2 shows that the addition of compatibilizer had little effect on the morphology compared with blends without compatibilizer. This was in agreement with elongation at break results, which indicated that the addition of compatibilizer reduced the elongation at break properties of the blends. On the other hand, the fracture surface of R3 had fewer particles evident at the surface. A ductile fracture is evident from the elongated protrusions from the surface. This supports the earlier observations that PEOX was effective at producing a more ductile blend, however, interfacial adhesion appears to be better than what the tensile results would suggest.

Figure 3 shows the morphology of NTP/PBS blends at the optimum formulation for tensile strength (A), elongation at break (B) and secant modulus (C). Sample A was R4 for which the morphology has been discussed above. When 7%

www.MaterialsViews.com

Macromol. Mater. Eng. **2014,** *299*, 885–895
© 2014 WILEY-VCH Verlag GmbH & Co. KGaA, Weinheim

Macromolecular
Journals

893

86

■ *Figure 3.* Morphology of NTP/PBS blends at optimum conditions of tensile strength (A), elongation at break (B) and secant modulus (C).

of PEOX was added in 20% NTP (B), clear plastic deformation was observed. From the elongation at break results, R1 had an elongation at break value of 16%, which is similar to the experimental value at optimum conditions, but contained 5% compatibilizer as apposed to 7%. When 5% PEOX was added to the blend (R1), it reduced the size of NTP particles. However, when 7% of PEOX was used, the morphology changed from brittle to ductile. This highlights the importance of the amount of compatibilizer to optimise elongation at break. In the case of secant modulus, at 70% NTP/5%pMDI, the morphology showed a co-continuous phase, which similar finding was obtained for NTP/LLDPE blends.[35] This indicated that the type of compatibilizer played an important role in stabilizing the blend morphology to improve the adhesion.

7. Conclusion

The Taguchi approach was used to optimise the formulation of NTP/PBS blends using PEOX, pMDI or PEOX-pMDI as compatibilizer at 20, 50 and 70% NTP. 20% NTP/7%pMDI was the optimal combination to obtain high tensile strength, while for elongation at break, 20% NTP/7%PEOX was effective to have a ductile blend. In the case of secant modulus, 5% of pMDI was optimal in 70% NTP/PBS blends. ANOVA analysis showed that the type of compatibilizer had the largest contribution to the tensile strength, while NTP content had the largest contribution to elongation at break and secant modulus. The experimental results of tensile strength were found to be much higher than predicted, while experimental results of elongation at break were found to be lower than predicted. Although the elongation at break value for experimental was lower than predicted, the morphology showed that the sample change from brittle to a ductile under these conditions.

[1] J. Svenson, A. Walallavita, C. Verbeek, *Waste Biomass Valor* **2013**, *4*, 147.
[2] H. J. Sue, S. Wang, J. L. Jane, *Polymer* **1997**, *38*, 5035.
[3] M. M. Reddy, A. K. Mohanty, M. Misra, *Macromol. Mater. Eng.* **2011**, *297*, 455.
[4] A. K. Mohanty, P. Tummala, W. Liu, M. Misra, P. V. Mulukutla, L. T. Drzal, *J. Polym. Environ.* **2005**, *13*, 279.
[5] U. R. Vaidya, M. Bhattacharya, *J. Appl. Polym. Sci.* **1994**, *52*, 617.
[6] B. Y. Shin, S. H. Jang, B. S. Kim, *Polym. Eng. Sci.* **2011**, *51*, 826.
[7] A. A. Mohamed, S. H. Gordon, C. J. Carriere, S. Kim, *J. Food Qual.* **2006**, *29*, 266.
[8] A. Mohamed, V. L. Finkenstadt, S. H. Gordon, D. E. Palmquist, *J. Appl. Polym. Sci.* **2010**, *118*, 2778.
[9] C. J. R. Verbeek, L. E. van den Berg, *Macromol. Mater. Eng.* **2011**, *296*, 524.
[10] C. J. R. Verbeek, L. E. van den Berg, *Macromol. Mater. Eng.* **2010**, *295*, 10.
[11] C. J. R. Verbeek, L. E. van den Berg, *J. Polym. Environ.* **2010**, *19*, 1.
[12] J. M. Bier, C. J. R. Verbeek, M. C. Lay, *Int. J. Life Cycle Assess.* **2012**, *17*, 208.
[13] J. M. Bier, C. J. R. Verbeek, M. C. Lay, *Int. J. Life Cycle Assess.* **2012**, *17*, 314.
[14] United States. **2010**, NOVATEIN LIMITED (Hamilton, NZ), inv. K.L.H. Pickering, NZ), Verbeek, Casparus Johannes Reinhard (Hamilton, NZ), Viljoen, Carmen (Howick, NZ), Van Den, Berg Lisa Eunice (Hamilton, NZ).
[15] R. Fayt, R. Jerome, P. Teyssie, *Makromol. Chem. -Macromol. Chem. Phys.* **1986**, *187*, 837.
[16] L. A. Utracki, *Overview-Polymer Alloys and Blends*, March 1990 edition, Oxford University Press, USA, March **1990**.
[17] L. A. Utracki, ''Polyblends '93 Preprints, Montreal,'' in: *Encyclopedia Dictionary of Commercial Polymer Blends* (Ed: L. A. Utracki), ChemTec Publishing, Toronto **1994**.
[18] L. A. Utracki, *Encyclopedic Dictionary of Commercial Polymer Blends*, ChemTec, Toronto **1994**.
[19] C. Yeung, K. A. Herrmann, *Macromolecules* **2003**, *36*, 229.
[20] L. A. Utracki, *Commercial Polymer Blends*, Chapman & Hall, London, UK **1998**.
[21] B. Liu, L. Jiang, H. Liu, J. Zhang, *Ind. Eng. Chem. Res.* **2010**, *49*, 6399.
[22] K. Aoi, A. Takasu, M. Tsuchiya, M. Okada, *Macromol. Chem. Phys.* **1998**, *199*, 2805.
[23] J. Zhang, L. Jiang, L. Zhu, J.-L. Jane, P. Mungara, *Biomacromolecules* **2006**, *7*, 1551.
[24] D. Dieteroch, E. Grigat, W. Hahn, *Polyurethane Handbook*, 104.70 edition, Hanser Publishers, New York **1985**, p. 629.
[25] H. Wang, X. Sun, P. Seib, *J. Appl. Polym. Sci.* **2001**, *82*, 1761.

87

[26] J. John, M. Bhattacharya, *Polym. Int.* **1999**, *48*, 1165.

[27] H. Wang, X. Sun, P. Seib, *J. Appl. Polym. Sci.* **2002**, *84*, 1257.

[28] A. K. M. Murali, M. Reddy, M. Misra, *J. Mater. Sci. Springer* **2011**, *47*, 2591.

[29] K. P. Rajan, N. Veena, P. Singh, G. Nando, *Yanbu J. Eng. Sci.* **2010**, *1*, 59.

[30] K. I. K. Marsilla, C. J. R. Verbeek, *J. Appl. Polym. Sci.* **2013**, *130*, 1890.

[31] Y.-D. Li, J.-B. Zeng, X.-L. Wang, K.-K. Yang, Y.-Z. Wang, *Biomacro-molecules* **2008**, *9*, 3157.

[32] R. K. Roy, *Design of Experiments Using the Taguchi Approch: 16 Steps to Product and Process Improvement*, John Wiley & Sons, New York **2001**.

[33] L. N. Nicolais, *Mater. Polym. Eng. Sci.* **1971**, *1*, 194.

[34] R. F. Landel, L. E. Nielsen, *Mechanical Properties of Polymers and Composites*, 2nd edition, Taylor & Francis, **1993**.

[35] K. I. K. Marsilla, C. J. R. Verbeek, *J. Appl. Polym. Sci.* **2013**, n/a.

[36] L. M. Robeson, *Polymer Blends: A Comprehensive Review*, Hanser Munich, Cincinnati **2007**.

[37] W. G. Perkins, *Polym. Eng. Sci.* **1999**, *39*, 2445.

Chapter 5

Compatibilization of Protein Thermoplastics and Polybutylene

Succinate Blends

A paper

published in

*Macromolecular Materials and Engineering*

by

K.I Ku Marsilla[1] and C.J.R. Verbeek

[1]As first author of this paper, I prepared the initial draft manuscript, which was refined and edited with consultation with my supervisor, who has been credited as co-author.

Compatibilization of Protein Thermoplastics and Polybutylene Succinate Blends

K. I. Ku-marsilla, C. J. R Verbeek*

Reactive extrusion was used to prepare blends of Novatein thermoplastic protein (NTP) and poly(butylene succinate) (PBS) compatibilized with poly-2-ethyl-2-oxazoline (PEOX) and polymeric methylene diphenyl diisocyanate (pMDI). PEOX improved the dispersion of NTP in PBS and in conjunction with pMDI led to improved water resistance and a tensile strength exceeding that of NTP and PBS. The secant modulus, elongation as well as energy to break were also improved. The glass transition temperature (T_g) of compatibilized blends remained unchanged, however, the melting enthalpy and temperature decreased. This suggested that the crystalline structure of PBS has been disrupted by NTP as a result of compatibilization.
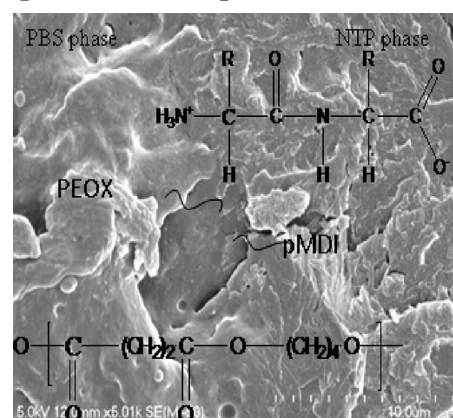
1. Introduction

Raw materials for new biodegradable plastics such as soy protein,[1–3] starch,[4,5] and gluten[6,7] have received increased attention due to their economic benefits. Novatein thermoplastic protein (NTP) is a newly developed material using bloodmeal as starting material.[8] NTP is best suited for agricultural and horticultural applications such as seedling trays, biodegradable plant pots, vine clips, containers, and pegs. NTP consists of complex macromolecules containing 20 different amino acids with strong intra- and intermolecular interactions. The mobility and flexibility of protein chains are required to enable flow and consolidation during extrusion. Plasticizers are widely used to reduce intermolecular interactions and reducing the T_g. However, depending on the amount of plasticizer used, it will affect mechanical properties, equilibrium moisture content[9] as well as leading to phase separation.[10] Previous research showed that extrusion and injection moulding were successfully used to produce NTP with good

mechanical properties.[11–13] However, water evaporates during processing and storage, which leads to embrittlement and loss of functionality. Blending NTP with other polymers may offer a solution to these problems, otherwise not possible by using pure NTP.

The properties of polymer blends are determined by four factors; component properties, composition, structure, and interactions. The compatibility in polymer blends is often explained in terms of property–composition relationships. Typically, thermodynamic incompatibility and poor interfacial adhesion between two components decrease the blend's mechanical properties. These could be improved by incorporating compatibilizers. Their interactions in the blend are usually characterized in terms of the distribution and concentration of inter- and intra-molecular forces such as hydrogen bonding, van der Waals forces, hydrophobic interactions, and ionic bonding.[14,15] However, to achieve such interactions, the polymer composition, type of compatibilizer, amount of compatibilizer, and processing techniques are very important parameters.

Polybutylene succinate (PBS) is a succinic acid-based biodegradable aliphatic polyester, which is synthesized by condensation polymerization of succinic acid with 1,4-butanediol and ethylene glycol. It is a semicrystalline polymer with excellent biodegradability, good processability, and

K. I. Ku-marsilla, C. J. R. Verbeek
School of Engineering, University of Waikato, Hamilton 3240, New Zealand
E-mail: jverbeek@waikato.ac.nz

mechanical properties similar to those of polyethylene. It is predicted that by 2020, 50% of packaging will be coming from PBS and 15% from agriculture use.[16] PBS also has been listed as promising material concerning bone and cartilage repair. It present better processability than poly (lactic acid) (PLA) and has higher mechanical properties than polyethylene (PE) and polypropylene (PP).[17,18] Despite its good performance, significant research effort is directed at modifying PBS-based materials to reduce cost.[7] Soy protein has been blended with PBS and the tensile strength was the highest compared to blends with polycaprolactone (PCL) or soy protein/PCL/PBS, although the elongation at break showed an opposite trend.[19] PBS was pretreated with urethane and isocyanate groups before blending with soy protein and the blend has reduced the glass transition of the soy protein, improved the morphology to a fine phase structure and increased the mechanical properties.[20]

Other than modification of PBS, melting behavior of PBS itself has attracted significant interest.[21,22] The interpretation of multiple melting endotherms can be ambiguous; sometimes interpreted as a result of the measurement technique or characteristic of the original polymer. Several researchers suggested that the behavior corresponded to the presence of melting, re-crystallization, and re-melting phenomenon.[21–23] The first step of the process is melting and re-crystallization of the low melting crystallite with lower thermal stability and followed by melting of crystallites with higher thermal stability formed through the re-crystallization of lower melting fractions. This was confirmed by observation of only one crystal structure suggesting that PBS have the same crystal structure even at different crystallization temperatures.[21,22] However, this melt and crystallization phenomenon during differential scanning calorimeter (DSC) depends on the rate of crystallization during heating and the heating rate.[21] Therefore, when blending PBS with proteins, complex crystallization may be observed as a result of protein and PBS interactions.

Recently, we have reported on the mechanical properties and morphology of NTP and PBS blends (20–100% NTP) compatibilized using poly (2-ethyl-2-oxazoline)(PEOX) and polymeric methylene diphenyl diisocyanate (pMDI) (5–10%). NTP content had the largest contribution to elongation at break and secant modulus while type of compatibilizer had the largest contribution to the tensile strength in NTP/PBS blends.[24] NTP has very low energy to break (0.06 MPa) and blends without any compatibilizer showed an optimal value of 1.9 MPa at 50% NTP. Mechanical properties and morphology varied greatly when using different amounts and type of compatibilizers. PEOX led to a significant change in morphology, however, adhesion between phases was not strong enough to improve the mechanical properties. On the other hand, pMDI increased the tensile strength but decreased the elongation at break.

Also for blends with LLDPE, an improvement in compatibility was observed across the entire composition range when using maleic anhydride grafted polyethylene as a compatibilizer.[25]

The present study further investigates this system at 50 wt.-% NTP, but using different methods to incorporate the compatibilizers. It was postulated that the sequence in which the compatibilizers are added could further change the morphology of the blend, leading to additional improvement in mechanical properties.

2. Methodology

2.1. Materials

Bloodmeal was supplied by Wallace Corporation (New Zealand) and sieved to an average particle size of 700 μm and was mostly bovine with some chicken blood. Technical grade sodium dodecyl sulfate (SDS) and analytical grade sodium sulfite (SS) were purchased from BiolabNZ and BDH Lab Supplies. Agricultural grade urea was obtained from Balance Agri-nutrients (NZ). Poly-2-ethyl-2-oxazoline (PEOX) and poly (phenyl isocyanate)-co-formaldehyde (pMDI) were obtained from Sigma–Aldrich and were used as received. PBS was purchased from Showa High Polymer, injection moulding grade #3020.

2.2. Preparation of Novatein Thermoplastics Protein (NTP)

NTP was prepared by dissolving urea (20 g), SDS (6 g), and sodium sulphate (6 g) in water (80 g). The solution was heated until the temperature reached 50–60 °C followed by blending with bloodmeal powder (200 g) in a high-speed mixer for 5 min. The mixtures were stored at <5 °C for at least 24 h prior to extrusion. Extrusion was performed using a ThermoPrism TSE-16-TC twin screw extruder at a screw speed of 150 rpm and temperature settings of 70, 100, 100, 100, and 120 °C from feed to exit die (Figure 1). The screw diameter was 16 mm at L/D ratio of 24:1 and was fitted with
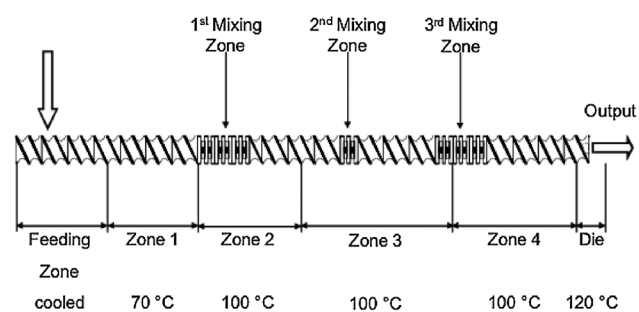

Figure 1. Extruder screw configuration with temperature profile.

www.MaterialsViews.com

91

a single 10 mm circular die. A relative torque of 50–60% was maintained by adjusting the mass flow rate of the feed. The extruded NTP was granulated using tri-blade granulator from Castin Machinery Manufacturer Ltd., China.

2.3. Preparation of NTP/PBS Blends

PBS was extruded with pre-prepared NTP and granulated according to the formulations listed in Table 1. Standard tensile bars (ASTM D638), were prepared using a BOY 35A injection moulding machine with a temperature profile of 110, 115, 120, 120, 120 °C from feed to exit die zone.

Compatibilizers were added after PBS and NTP were extruded except in the case of using two compatibilizers, where the second compatibilizer (pMDI) was added to the granulated blend just before injection moulding (NTP$_{7/3}$). However, for sample NTP$_{7/3^*}$, PEOX was dissolved in other additives during NTP production, but pMDI was still added before injection moulding. These procedures were followed to prevent excessive pMDI hydrolysis. Initially, both compatibilizers were added during extrusion, however, mechanical properties were very poor. This was believed to be due to the reactions of PEOX occurring mostly with NTP, and preventing reactions with PBS. To overcome this, NTP and PBS were extruded first, followed by addition of PEOX, followed by pMDI just before injection moulding.

2.4. Analysis

Injection moulded specimens were fractured after immersion in liquid nitrogen and fracture surfaces were observed using a field emission scanning electron microscope (SEM) Hitachi S-4700. Samples were sputter coated with platinum before scanning using an accelerating voltage of 5 kV.

After conditioning, tensile properties were measured using an Instron model 33R4204 according to ASTM D638-86. An extension rate of 5 mm · min^{-1} and an extensometer gauge length of 50 mm were used for testing. Samples were tested in replicas of five directly after removal from the humidity chamber. Samples were conditioned for up to 15 d at 23 °C and 50% relative humidity before tensile testing. The secant modulus was calculated between a strain of 0.0005 and 0.0025 and the toughness was calculated as the area under the stress-strain graph and is more accurately referred to as energy-to-break.

Dynamic mechanical properties of NTP/PBS blends were studied using a Perkin Elmer DMA 8000 fitted with a high temperature furnace and controlled with DMA software version 14306. DMA specimens (30 × 6.5 × 3 mm^3) were cut from injection moulded samples and tested using a free length of 12.5 mm using a single cantilever fixture at 1 Hz with displacement of 0.03 mm at temperature −80 to 100 °C.

Differential scanning calorimetry (DSC) was conducted on a DSC 8500 from Perkin Elmer. The specimens were crimp sealed in 30 µL aluminum pans and run under constant nitrogen purge gas. Specimens were heated from −80 to 120 °C at 10 °C · min^{-1}, held for 1 min at 120 °C, cooled to −80 °C (10 °C · min^{-1}) after which the cycle was repeated using the same method.

In order to fully characterize complex materials, it may be necessary to determine if there are any overlapping transitions. Rates of 50 and 250 °C · min^{-1} were used to observe the blend's T_g where higher scan rates may separate any overlapping peaks; for these, data was collected between −80 and 100 °C.

All samples were oven dried at 80 °C until constant weight. Dried samples were immersed in water at room temperature for 5 d. Samples were removed from water, blotted with a tissue paper to remove excess water and then weighed. The water absorption was calculated on a dry sample basis.

3. Results and Discussions

3.1. Morphology

Blending two immiscible polymers at near equal proportions often leads to a co-continuous morphology.[26] Usually, a compatibilizer is used to reduce the interfacial tension, stabilizing the morphology, leading to a co-continuous structure. Blends with low interfacial tension tend to form co-continuous morphologies over a wider composition range than those with high interfacial tension.[27] An inversion point is observed when two immiscible phases are fully co-continuous such that the matrix is hardly distinguishable from the dispersed phase. However, the fundamentals behind the formation of inversion point is not well understood.[28]

The morphology of blends without compatibilizer Figure 2A and B revealed NTP particles evenly distributed

Table 1. Formulations of NTP/PBS blends.

Sample Name	NTP [wt.-%]	PBS [wt.-%]	pMDI [wt.-%]	PEOX [wt.-%]
PBS	0	100	0	0
NP$_{0/0}$	50	50	0	0
NP$_{7/0}$	50	43	7	0
NP$_{7/3}$	50	40	7	3
NP$_{7/3^*}$	50	40	7	3
NTP	100	0	0	0

*PEOX added as part of additive content used in NTP preparation.

that the blend formed two phases, a NTP rich and a PBS rich phase.

Using two compatibilizers did not drastically change the morphology (Figure 2E and F). NTP-rich phases were encapsulated in PBS rich phases with much less voids. At higher magnification, NTP-rich phases were somewhat separated from PBS-rich phases, but with improved adhesion compared to using pMDI only. Zhang et al.[29] found that addition of 3 phr PEOX in soy protein concentrate (SPC) and PLA blends showed a co-continuous phase at SPC to PLA ratios ranging from 30:70 to 70:30. Liu et al.[30] reported that the addition of PEOX in SPC/PLA blends increased the tensile strength of the blends which was attributed to the morphology of SPC particles changing from circular shape to thread-like structures due to shearing during mixing. For compatibilized NTP/PBS blends, it is proposed that the polymers form two co-continuous phases, one rich in NTP and the other PBS, with moderate adhesion between phases.

PEOX is water soluble and it was thought that its efficiency to compatibilize NTP and PBS would be improved by dissolving it into water during the production of NTP. The morphology of blends using this method showed virtually no phase separation. Only at high magnification (Figure 2H), a slight variation in surface topography was observed. This suggests that this resulted in a truly compatible blend, which was further explored using thermal analysis and mechanical properties.

Pure NTP does not have a very even morphology either (Figure 3A). It appears to have large number of particulate matter distributed throughout the bulk material. By dissolving PEOX in the water used to prepare NTP, the morphology of NTP

Figure 2. SEM morphology of NTP/PBS blends [A:NP$_{o/o}$; C:NP$_{7/o}$; E:NP$_{7/3}$; G:NP$_{7/3°}$]. Left pictures and right pictures show magnification of 500 and 5.01 K.

in the PBS matrix. At higher magnification, clear separation between NTP and PBS was observed, indicative of poor interfacial adhesion.

The blend containing pMDI only (Figure 2C and D) revealed fewer agglomerated NTP particles. However, clear phase separation was still visible (Figure 2D), but better than blends without a compatibilizer. The fracture surface also revealed bridging between NTP and PBS rich phases, evident from elongated strands of polymer. It was thought

changed and particles were much smaller and more evenly dispersed (Figure 3B). Using this method of incorporating PEOX not only changed the morphology, but also the mechanical properties of NTP that will be discuss later.

3.2. Mechanical Properties

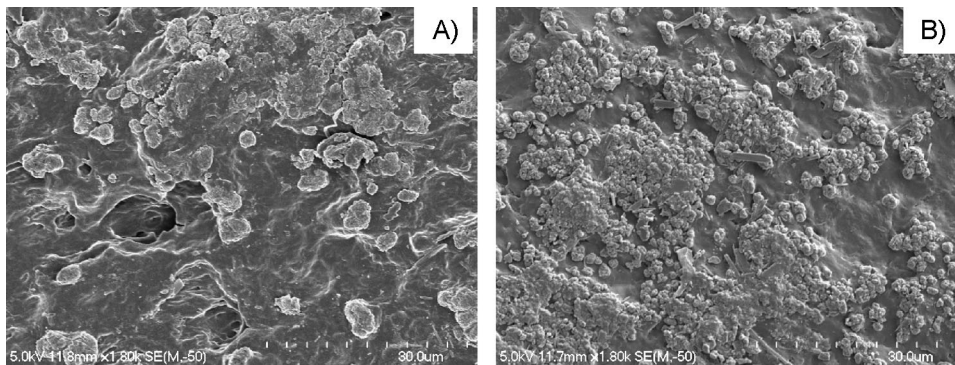The tensile strength of PBS and NTP were 22 and 14 MPa, respectively (Figure 4A). In equal proportions, without

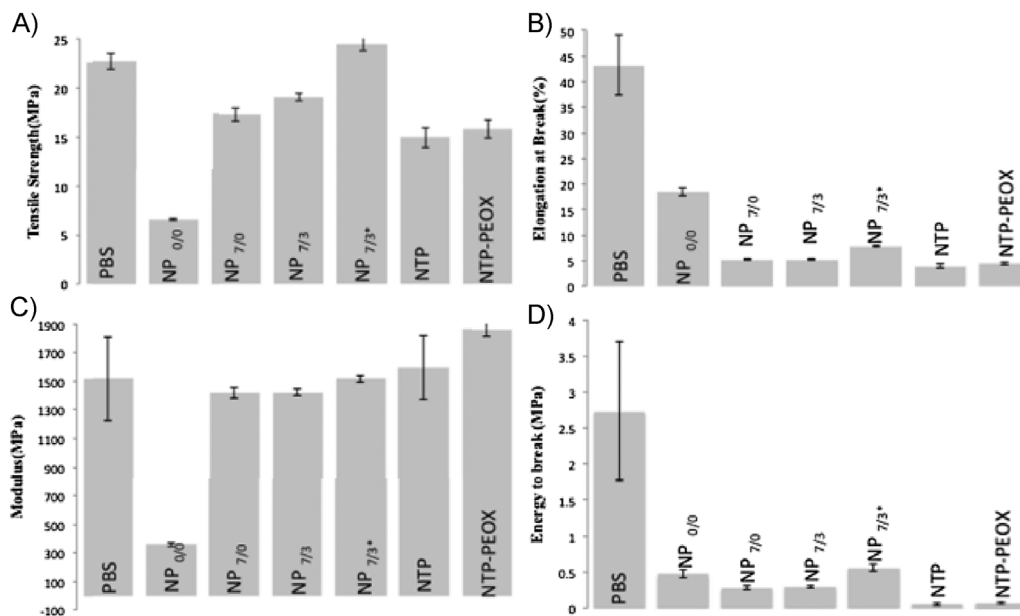**Figure 3.** Morphology of NTP and NTP with PEOX (ii).

Figure 4. Tensile strength (A), percent elongation (B), secant moodulus (C) and toughness (D) of NTP/PBS blends.

compatibilizer, the tensile strength reduced to the lowest compared to all other samples. This suggested that NTP and PBS are highly incompatible, with little adhesion between phases, these findings were also supported by the observed morphology.

When using pMDI as compatibilizer ($NP_{7/0}$), the tensile strength more than doubled over that of blends without any compatibilizer. Using two compatibilizers ($NP_{7/3}$ and $NP_{7/3^*}$) resulted in a further moderate increase. It appears that PEOX promoted adhesion between phases. PEOX has been shown to reduce particle sizes of the dispersed phase, resulting in finer structure, although not leading to great improvement in tensile strength.[29–31] However, PLA/soy protein blends using PEOX and pMDI as compatibilizers showed a significant increase in tensile strength, higher than pure PLA.[30] Dissolving PEOX in water prior to

extrusion led to a higher tensile strength than that of pure PBS ($NP_{7/3^*}$). This was supported by earlier morphological observations. This suggested that the blending technique played an important role establishing the required interactions to form a compatible blend. The results suggested that the microstructure was a result of the improved interfacial adhesion between NTP and PBS after the addition of pMDI. When adding just PEOX to NTP, the tensile strength increased slightly, suggesting good compatibility between PEOX and NTP, the first requirement for compatibility to be effective.

NTP is much more brittle than PBS, which is already very brittle, having an elongation at break of only 42%. Blending NTP and PBS led to a reduction in elongation compared to PBS. PBS chains are constrained by the inclusion of NTP, which is present as a dispersed phase similar to particulate

K. I. Ku-marsilla, C. J. R Verbeek

reinforced composites. However, when using compatibilizers, the strength of interactions and entanglements between NTP and PBS have been improved, further restricting movement of polymer chains, thereby decreasing the elongation at break further. Incorporating a compatibilizer may lead to changes in the properties of the dispersed phase as well as the matrix. In addition, interactions between dispersed phase and the matrix may also have caused a reduction in elongation. Blends with compatibilizers showed a slight increase compared to pure NTP, while a considerable increase in elongation at break was observed for $NP_{7/3^*}$, exceeding that of pure NTP. It was thought that this improvement was due to the truly compatible nature of this formulation.

NTP and PBS have a very similar secant modulus. Blends without a compatibilizer showed the lowest modulus (Figure 4C). Including compatibilizers, the modulus increased to about the same as the virgin materials. The secant modulus of $NP_{7/3^*}$ was slightly higher compared to the other blends, but not as high NTP-PEOX. It was clear, that in the absence of compatibility, interfacial adhesion was not sufficient to maintain the stiffness of each component, however, the degree of interfacial adhesion was not dominant.

The energy to break of PBS was 2.7 MPa while that of NTP was very low (0.06 MPa) and this behavior was also observed for blends with compatibilizers (Figure 4D). Energy to break of blends with compatibilizers ($NP_{7/0}$ and $NP_{7/3}$) decreased compared to samples without compatibilizers. However, energy to break for $NP_{7/3^*}$ showed a considerable increase suggesting that the sample could absorb energy before rupturing mostly due to its ability to deform more before fracture.

3.3. Reaction Mechanism

PEOX can be considered as a broadly compatible polymeric solvent or compatibilizing agent for various polymers.[32] PEOX is highly water soluble because of its polar hydrophilic groups. The possibility of partial organization of the PEOX-water system is through specific hydrogen bonding interactions between the carbonyl oxygen on the PEOX side chain and water molecules in solution.[33] This behavior was also found to occur in peptides.[34] The peptide backbone of NTP is relatively hydrophilic where their complex folded structures are stabilized by hydrogen bonding. It is believed that mutual hydrogen bonded networks between NTP, water, and PEOX contributed to better dispersion in NTP leading to

improved mechanical properties. Furthermore, PEOX is slightly basic due to its tertiary amide structure while NTP is slightly acidic. This suggested that an acid–base interaction between PEOX and NTP could also contribute to compatibilization. These were consistent with our morphology results that showed better dispersion of NTP when PEOX was dissolved first.

Isocyanate (NCO) is highly reactive with hydroxyl and carboxyl groups to form urethane linkages.[35] NCO groups can react with NH_2 groups in NTP and OH groups in PBS. Li et al.[20] reported that NCO groups prefer to react with NH_2 groups in soy protein isolate (SPI) rather than OH groups, therefore PBS was first reacted with isocyanate before blending with SPI. This was done to avoid the occurrence of an extreme situation where the isocyanate only reacted with SPI. This was supported by other research, which reported that the mechanical properties of PCL and gluten was strengthened mostly by interactions of pMDI with the gluten rather than interactions with PCL.[7] Others have shown that there is also the possibility that pMDI could be interacting predominantly with the hydroxyl groups of water rather than starch.[7] It was also shown that covalent bonds were formed at the PLA/starch interface by pMDI, and such adhesion might not cause severe restriction of elongation by forming proper chain entanglement.[36]

One possible mechanism of interaction is shown in Figure 5. From our observations, without PEOX, the tensile strength was the lowest of all compatibilized blends ($NP_{7/0}$). When PEOX was included, the tensile strength increased, suggesting that PEOX interacted with NTP through the organization of hydrogen bonded water molecules adjacent to the polymer and the addition of pMDI during injection moulding have further strengthened the interactions between PBS and NTP. Although the structure may not entirely describe most of the interactions such as pMDI
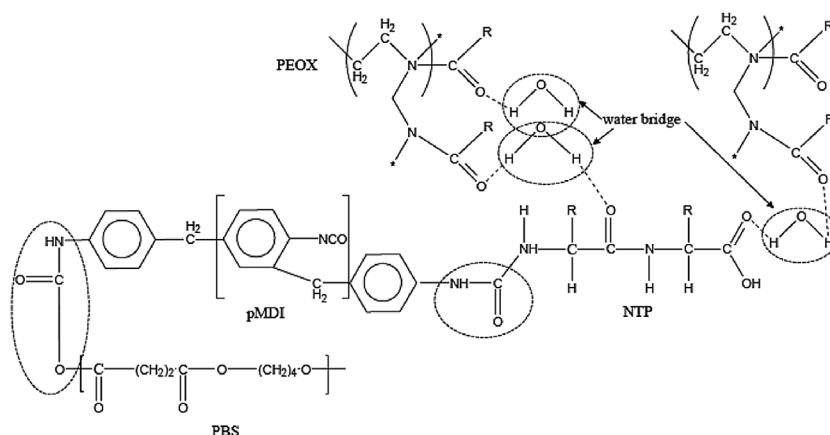

Figure 5. Possible reactions between water, PEOX and pMDI with hydroxyl groups of PBS and amine end group of protein.

95

reacting with itself, pMDI interacting with water, hydrogen bonding, hydrophobic interactions or ionic bonding, this was considered as the main possible interactions between the polymers.

3.4. DMA Analysis

In multicomponent blends, the degree of miscibility between each component could be observed in shifting and broadening of the T_g peaks toward each other. The glass transition of polymer blends is usually situated between the T_g's of the parent materials in proportion to the amount of each phase present in the blend. The change in T_g of two polymers, frequently moving toward each other, is usually evaluated as compatibility and good interaction between two phases.[7,20,37]

Figure 6 shows the storage modulus, loss modulus, and tan δ as a function of temperature for NTP and PBS. PBS showed a T_g at −35 °C while NTP showed a T_g at around 70 °C as well as β-transition at about −20 °C.[38] The blends with compatibilizers showed the highest storage modulus over the entire temperature range indicating stronger intermolecular interaction between NTP and PBS. At low temperature (between −80 and −40 °C), the blends were in a glassy state, however, the compatibilizers did not significantly affect the T_g observed. At high temperature, blends with compatibilizer showed a second T_g, consistent with that of pure NTP.
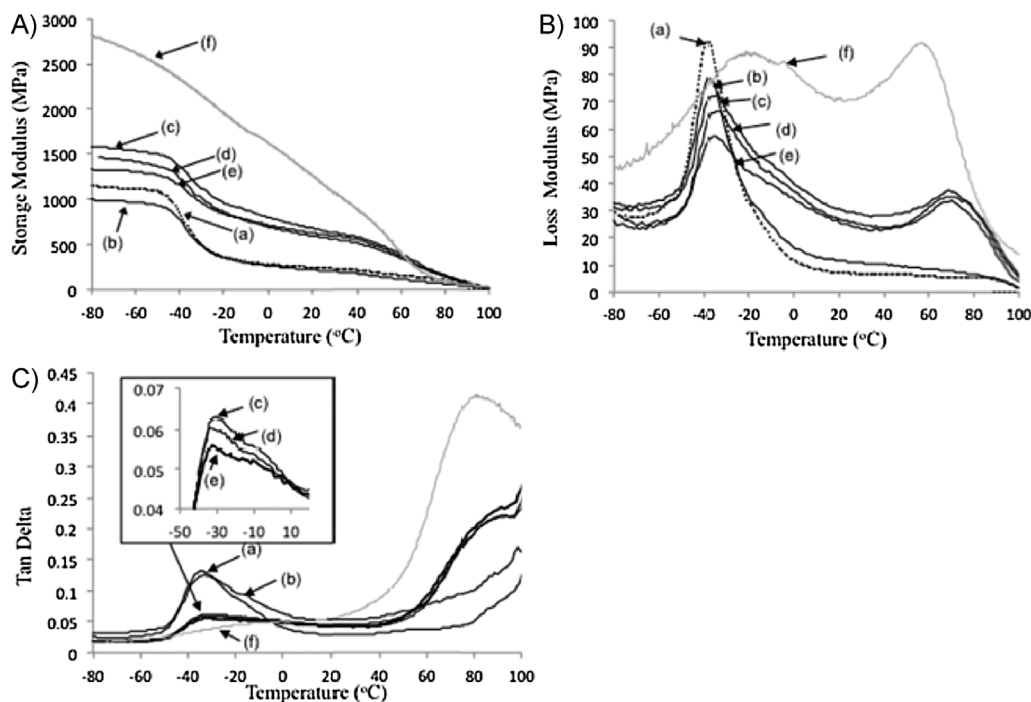
The effects of compatibilizers are clearly seen from the loss modulus (Figure 6b). A clear T_g was observed at −35 °C, consistent with the PBS phase. In blends without compatibilizer, no T_g was observed at high temperature as NTP was the dispersed phase. When PBS melts, the material lost its integrity and only melting will be observed. When compatibilizers were added, a clear T_g was observed at about 65 °C, and the low temperature T_g increased slightly.

Peaks in tan δ peaks (−35 °C) for compatibilized blends broadened and decreased in intensity. The blend with the strongest expected chain interactions ($NP_{7/3^*}$) showed the broadest peak compared to other compatibilized blends. Furthermore, the damping peak at 70 °C shifted to a slightly higher temperature. It was concluded that without a compatibilizer, NTP and PBS forms a completely immiscible blend and that improved compatibility increased the PBS-rich phase's T_g, but only to a small extent.
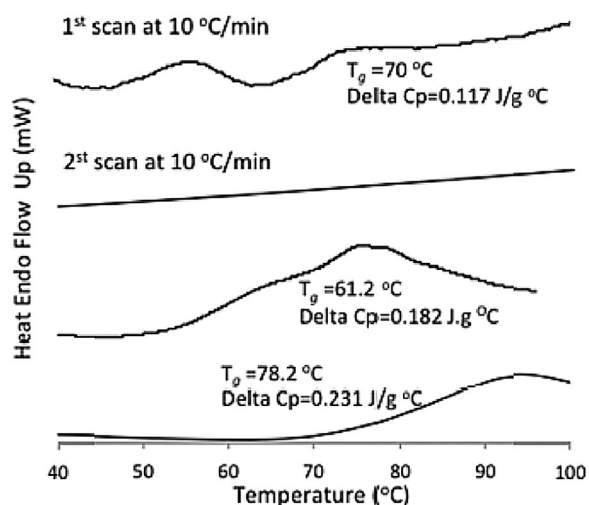
3.5. DSC Analysis

3.5.1. Glass Transition Temperature

Figure 7 shows the T_g of NTP at different heating rates. Determination of T_g by DSC is difficult as the signal of heat flow is usually weaker than that of conventional polymers. Theoretically, a higher heating rate is beneficial in detecting T_g and both the temperature and breadth of the glass transition are affected by increased heating rates.[39,40]

Figure 6. A: Storage modulus, B: Loss modulus and C: tan δ of PBS (a), $NP_{o/o}$ (b), $NP_{7/o}$ (c), $NP_{7/3}$ (d), $NP_{7/3}{}^*$(e) and NTP (f).

www.MaterialsViews.com

Macromol. Mater. Eng. **2015**, 300, 161–171
© 2014 WILEY-VCH Verlag GmbH & Co. KGaA, Weinheim

Macromolecular
Journals

167

■ *Figure 7.* Glass transition (T_g) of NTP.

NTP has a T_g above room temperature; at $10\,°C \cdot min^{-1}$, the first heating scan detected a endotherm, closely followed by a T_g, but was not present in second heating scan. The endotherm was thought to be relaxation behavior related to a tightly pocket chain structure where cooperative molecular motion is required for internal readjustments while the second step change is corresponded to the T_g. This T_g was confirmed by observations at higher higher heating rate, at which the heating is too fast to observe endothermic peak.

The T_g of PBS, at a heating rate of 10 and $50\,°C \cdot min^{-1}$ are shown in Figure 8 (taken from the second scan). The T_g of PBS and the blends were about $10\,°C$ different between the two scan ratios, as expected. Results at 10 and $50\,°C \cdot min^{-1}$ for the blends were consistent to that
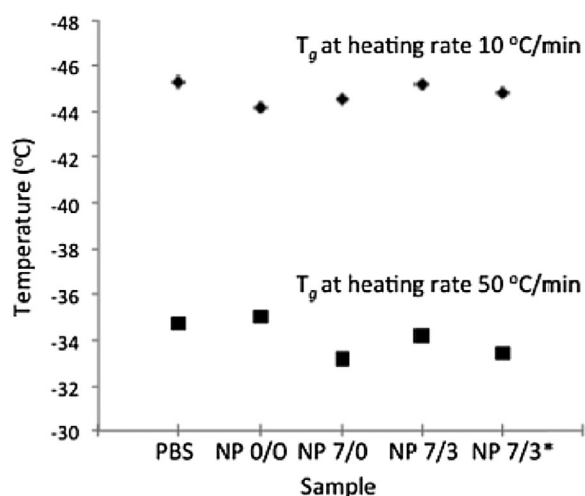
■ *Figure 8.* T_g of PBS and NTP/PBS blends at different heating rates.

observed in DMA. The T_g close to that of PBS, increased only slightly, with no obvious trend between the various compatibilized blends.

3.5.2. Melting Behavior of NTP/PBS Blends

The DSC thermograms of PBS and NTP/PBS blends for the first and second scan ($10\,°C \cdot min^{-1}$) are presented in Figure 9 in conjunction with data normalized to the amount of PBS in Table 2. During the first heating cycle (Figure 9a), two small peaks were observed for PBS at low temperature ($35–60\,°C$) while a prominent peak was observed at $95.2\,°C$. It was suggested that the low temperature endotherms corresponded to the melting of original crystallites followed by melting of recrystallized PBS.[22] To avoid the effect of thermal history, melting behavior during a second heating cycle was also considered. The two small endotherm peaks during the first scan disappeared, replaced by a single endothermic peak at $80.6\,°C$ before the melting endotherm ($95.2\,°C$).

The blends without compatibilizer ($NP_{0/0}$) had the same multiple endotherms as PBS at lower temperature. A smaller peak, similar to what was observed for PBS during second scan, was also observed at the same temperature. A small step change corresponding to a T_g of NTP ($68.8\,°C$) was observed in first scan, but was not clear in the second scan. This T_g was not observed in DMA for blends without compatibilizer but was clear for blends with compatibilizer. The enthalphy of melting did not change between the first and second scan suggesting that thermal history did not affect the blend's properties however, the enthalphy of melting during first scan for PBS was much lower compared to uncompatibilized blend. This would imply that either NTP influenced the crystallization process or more PBS crystallizes during cooling after production.

In the case of blends with compatibilizers (first scan), the first smaller melting endotherm has merged with the main melting endotherm and appeared like a shoulder in those peaks. The melting has a slightly broader melting peak with lower peak temperature reduced by about $5\,°C$. For blends with two compatibilizers ($NP_{7/3}$ and $NP_{7/3^*}$), the enthalphy value is similar with uncompatibilized blend and the melting temperature remained unchanged. Neither the shoulder peak nor the two smaller peaks were observed for $NP_{7/3^*}$.

During a $10\,°C \cdot min^{-1}$ cooling cycle, PBS crystallized at $62\,°C$ while blends without a compatibilizer crystallized almost $5\,°C$ lower (Figure 10, Table 2). Without compatibilizer, high interfacial tension between phases resulted in phase separation. NTP probably hindered the rate of PBS crystallization thereby reducing the crystallization temperature. The low crystallization rate also led to the appearance of small endotherms preceding the main
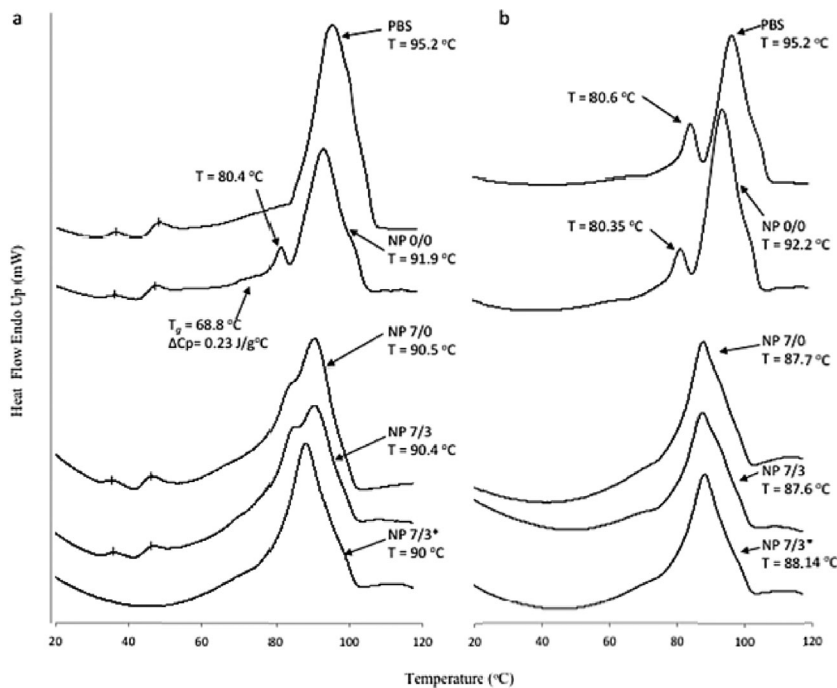
Figure 9. Melting thermograms of NTP/PBS blends of 1st heating scan at 10 °C · min⁻¹ (A), 2nd heating scan at 10 °C · min⁻¹ (B).

melting peak, even after the first heating cycle. NTP must have disrupted or prevented the growth of large PBS crystals resulting in a melting-recrystallization phenomenon.[21]. However, the ΔH_c of uncompatibilized blends almost tripled over that of pure PBS. This might be due to nucleation, where high interfacial tension usually induces nucleating at the interface.[41]

Including compatibilizers, the crystallization temperature increased significantly, exceeding that of pure PBS while ΔH_c dropped about 20% over that of the uncompatibilized blends. The presence of compatibilizers probably resulted in reduced interfacial tension as a result of interactions between phases such as hydrogen bonding. These interactions were also believed to

promote crystallization of PBS. The ΔH_c observed was still far greater than pure PBS suggesting that NTP may have nucleated crystallization in the PBS rich phase. Similar results have been observed in soy-protein and chemically modified PBS.[42] These serve a good starting point in the future to better explaining the crystallization behavior of complex chain system in protein blends.

3.6. Water Absorption

PBS is a hydrophobic polymer and is resistant toward water absorption, while NTP can absorb water because of its hydrophilic nature. One of the major challenges using natural polymers is to increase its water resistance. Water absorption of pure NTP, PBS, and their blends is presented in Figure 11. Water absorption occurred rapidly within 1 d; NTP absorbed about 228% water, while PBS only absorbed 1%. Without any compatibilizer, water absorption decreased to about 22%. When compatibilizers were added, a further reduction to 12% was observed, probably due to the absence of a distinct NTP phase. NP$_{7/0}$ exhibited the lowest water absorption compared to blends containing PEOX probably because PEOX is hydrophilic. This improvement widens their applications especially in agriculture and packaging applications. For example, because of their

Table 2. Summary of DSC data during first melting (T_{m1}), second melting (T_{m2}) and cooling (T_c).

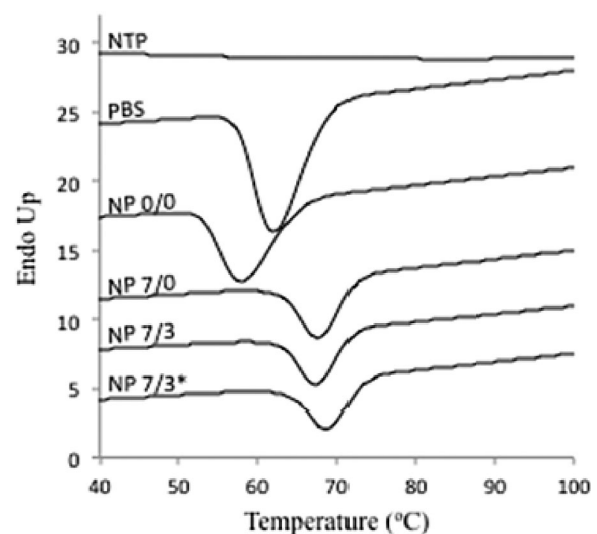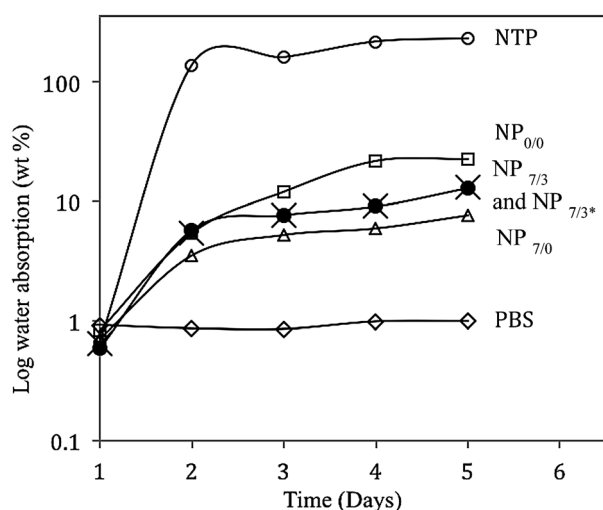| Sample	T_{m1}	ΔH_{m1}	T_{m2} (°C)	ΔH_{m2} [J · g⁻¹]	T_c [°C]	ΔH_c [J · g⁻¹]
PBS	95.2	40.02	95.2	39.69	62.1	−44.4
NP 0/0	91.9	77.28	92.2	75.9	58.1	−114.4
NP 7/0	90.5	72.00	87.7	79.09	67.7	−89.53
NP 7/3	90.4	77.25	87.6	75.0	68.3	−76.75
NP 7/3*	90.0	77.6	88.14	80.23	68.3	−79

Figure 10. Crystallization of NTP/PBS blends during cooling.

98

Figure 11. Water absorption of NTP/PBS blends over 5 d.

extend shelf life, it can be used in compostable seedling trays.

4. Conclusion

Blends contain 50% NTP were successfully produced through reactive extrusion. Adding PEOX during NTP production greatly increased tensile strength and energy to break. This was attributed to PEOX, improving dispersion of NTP, while pMDI strengthened the adhesion between PBS and NTP. Compatibilization did not affect the T_g of the blends but shifted the melting peaks to a lower temperature. The crystallization temperature of compatibilized blends occurred at higher temperature indicative at reduced chain mobility. The water resistance of the NTP was improved significantly due to incorporation of PBS. However, the compatibilized blends containing PEOX showed slightly less water resistance due to the hydrophilic nature of the compatibilizer.

[1] H. J. Sue, S. Wang, J. L. Jane, *Polymer* **1997**, *38*, 5035.
[2] M. M. Reddy, A. K. Mohanty, M. Misra, *Macromol. Mater. Eng.* **2011**, *297*, 455.
[3] A. K. Mohanty, P. Tummala, W. Liu, M. Misra, P. V. Mulukutla, L. T. Drzal, *J. Polym. Environ.* **2005**, *13*, 279.
[4] U. R. Vaidya, M. Bhattacharya, *J. Appl. Polym. Sci.* **1994**, *52*, 617.

[5] B. Y. Shin, S. H. Jang, B. S. Kim, *Polym. Eng. Sci.* **2011**, *51*, 826.
[6] A. A. Mohamed, S. H. Gordon, C. J. Carriere, S. Kim, *J. Food Quality* **2006**, *29*, 266.
[7] A. Mohamed, V. L. Finkenstadt, S. H. Gordon, D. E. Palmquist, *J. Appl. Polym. Sci.* **2010**, *118*, 2778.
[8] United States. (2010), NOVATEIN LIMITED (Hamilton, NZ), inv. K. L. H. Pickering, NZ), Verbeek, Casparus Johannes Reinhard (Hamilton, NZ), Viljoen, Carmen (Howick, NZ), Van Den, Berg Lisa Eunice (Hamilton, NZ).
[9] C. J. Verbeek, N. J. Koppel, *J. Mater. Sci.* **2012**, *47*, 1187.
[10] J. M. Bier, C. J. R. Verbeek, M. C. Lay, *J. Appl. Polym. Sci.* **2013**, n/a.
[11] C. J. R. Verbeek, L. E. van den Berg, *J. Polym. Environ.* **2010**, *19*, 1.
[12] C. J. R. Verbeek, L. E. van den Berg, *Macromol. Mater. Eng.* **2010**, *295*, 10.
[13] C. J. R. Verbeek, L. E. van den Berg, *Macromol. Mater. Eng.* **2011**, *296*, 524.
[14] V. Hernandez-Izquierdo, J. Krochta, *J. of Food Sci.* **2008**, *73*, R30.
[15] Y. Zhang, J. Han, *J. Food Sci.* **2008**, *73*, E313.
[16] P. Sarnacke, S. Wildes, ''Global Market for Biodegradable Polymers,'' in *Bioplastics Magazine*, 1st edition, OMNI Tech International, Ltd, Michigan, USA **2008**.
[17] D. Puppi, F. Chiellini, A. M. Piras, E. Chiellini, *Prog. Polym. Sci.* **2010**, *35*, 403.
[18] H. Wang, J. Ji, W. Zhang, Y. Zhang, J. Jiang, Z. Wu, S. Pu, P. K. Chu, *Acta Biomater.* **2009**, *5*, 279.
[19] M. M. Reddy, A. K. Mohanty, M. Misra, *Macromol. Mater. Eng.* **2012**, *297*, 455.
[20] Y.-D. Li, J.-B. Zeng, X.-L. Wang, K.-K. Yang, Y.-Z. Wang, *Biomacromolecules* **2008**, *9*, 3157.
[21] E. S. Yoo, S. S. Im, *J. Polym. Sci. Part B: Polym. Phys.* **1999**, *37*, 1357.
[22] X. Wang, J. Zhou, L. Li, *Eur. Polym. J.* **2007**, *43*, 3163.
[23] S. S. Ray, J. Bandyopadhyay, M. Bousmina, *Polym. Degrad. Stab.* **2007**, *92*, 802.
[24] K. I. Ku Marsilla, C. J. R. Verbeek, *Macromol. Mater. Eng.* **2014**, *299*, 885.
[25] K. I. K. Marsilla, C. J. R. Verbeek, *J. Appl. Polym. Sci.* **2013**, *130*, 1890.
[26] L. A. Utracki, ''Overview-Polymer Alloys and Blends,'' March edition, Oxford University Press, USA **1990**.
[27] H. Veenstra, J. Van Dam, A. Posthuma de Boer, *Polymer* **2000**, *41*, 3037.
[28] F. Prochazka, C. Carrot, M. Castro, C. Celle, J. Majesté, ''Phase Inversion and Cocontinuity in Immiscible Polymer Blends,'' in *Conference in Polymer Processing Society*, **2002**.
[29] J. Zhang, L. Jiang, L. Zhu, J-l. Jane, P. Mungara, *Biomacromolecules* **2006**, *7*, 1551.
[30] B. Liu, L. Jiang, H. Liu, J. Zhang, *Ind. Eng. Chem. Res.* **2010**, *49*, 6399.
[31] B. Liu, L. Jiang, H. Liu, L. Sun, J. Zhang, *Macromol. Mater. Eng.* **2010**, *295*, 123.
[32] K. Aoi, M. Okada, *Prog. Polym. Sci.* **1996**, *21*, 151.
[33] N. Adams, U. S. Schubert, *Adv. Drug Deliv. Rev.* **2007**, *59*, 1504.
[34] A. M. Bernard, ''*Molecular Modeling of Poly (2-ethyl-2-oxazoline),*'' ProQuest, **2008**.
[35] D. Dieteroch, E. Grigat, W. Hahn, ''*Polyurethane Handbook,*'', 104.70 edition, Hanser Publishers, New York **1985**, p. 629.
[36] H. Wang, X. Sun, P. Seib, *J. Appl. Polym. Sci.* **2001**, *82*, 1761.

[37] K. Aoi, A. Takasu, M. Tsuchiya, M. Okada, *Macromol. Chem. Phys.* **1998**, *199*, 2805.

[38] J. M. Bier, C. J. R. Verbeek, M. C. Lay, *J. Therm. Anal. Calorim.* **2012**, 1.

[39] J. Foreman, S. Sauerbrunn, C. Marcozzi, *"Thermal Analysis & Rheology,"* Kyoritsu Chem. & Co., Ltd, Kisarazu, Japan **2013**.

[40] P. Liu, L. Yu, H. Liu, L. Chen, L. Li, *Carbohydr. polym.* **2009**, *77*, 250.

[41] A. Kumar, R. K. Gupta, *"Fundamentals of Polymers,"* McGraw-Hill, New York **1998**.

[42] Y.-D. Li, J.-B. Zeng, W.-D. Li, K.-K. Yang, X.-L. Wang, Y.-Z. Wang, *Ind. Eng. Chem. Res.* **2009**, *48*, 4817.

www.MaterialsViews.com

Macromol. Mater. Eng. **2015,** *300*, 161–171
© 2014 WILEY-VCH Verlag GmbH & Co. KGaA, Weinheim

Macromolecular
Journals

171

100

Chapter 6

Modification of poly (lactic acid) using itaconic anhydride by

reactive extrusion

A paper

published in

European Polymer Journal

by

K.I Ku Marsilla[1] and C.J.R. Verbeek

[1]As first author of this paper, I prepared the initial draft manuscript, which was refined and edited with consultation with my supervisor, who has been credited as co-author.

Contents lists available at ScienceDirect

European Polymer Journal

Modification of poly(lactic acid) using itaconic anhydride by reactive extrusion

K.I. Ku Marsilla, C.J.R. Verbeek *

Department of Engineering, School of Science and Engineering, University of Waikato, Hamilton 3204, New Zealand

A B S T R A C T

Itaconic anhydride (IA) was grafted onto poly(lactic acid) (PLA) using dicumyl peroxide (DCP) as radical initiator using free-radical grafting. Different concentrations of monomer (2–6 wt.%) and initiator (0.5–0.75 wt.%) at 180 and 200 °C were used for chemical modification. Grafting was confirmed using titration and the highest degree of grafting was 0.75%. The degree of grafting increased gradually with increasing IA and DCP concentration, with minimal chain scission. Reaction kinetics showed that the initial rate of reaction was between 0.024 and 0.03 $(l/mol\ s)^{1/2}$, depending on temperature. Grafted PLA showed a significant change in enthalpy of crystallization, enthalpy of fusion as well as increased tensile strength and elongation at break accompanied by a reduction in stiffness.

© 2015 Elsevier Ltd. All rights reserved.

1. Introduction

Poly(lactic acid) (PLA) is one of the most promising biodegradable thermoplastics and has received considerable attention because of its glossy optical appearance, high tensile strength and good barrier properties toward carbon dioxide, oxygen and water. PLA is used in compostable packaging materials such as bags, food packaging and disposable tableware, as well as in medical applications such as ligament reconstruction, suture, tissue engineering, and controlled release systems [1]. It is also used in blends with other polymers, but may require chemical modification to improve compatibility. However, PLA lacks reactive side-chain groups, which make surface and bulk modification challenging.

PLA can be modified using techniques such as plasticization, chemical modification or melt blending with flexible polymers. High molecular mass plasticizers such as, polyethylene glycol (PEG), poly(propylene glycol) (PPG), atactic poly(3-hydroxybutyrate (a-PHB), polyester diol (PED), poly(diethylene adipate) (PDEA), tributyl citrate-oligo-ester (DBM-oligoester) and oligoesteramide (DBM-oligoesteramide) have been reported to be miscible with PLA and are efficient plasticizers, while acetyl triethyl citrate and triethyl citrate were shown to be the most effective plasticizers [2,3]. Although plasticization is well known, the high amount required (10–20 wt.%) to reduce the T_g and improve ductility is not always cost effective [4].

Among chemical modification methods used, free radical grafting is probably the most successful and cost effective treatment for improving adhesion efficiency and preparing compatibilizers for polymer/polymer blends. It can be carried out either in solution or during a melt-compounding process. Maleic anhydride (MA) is by far the most commonly used monomer for grafting reactions due to its availability and low propencity for homopolymerization. Grafting MA onto polyolefins is an established technique, however, MA grafted onto PLA (PLA-g-MA) is not commercially available.

Carlson et al. and Mani et al. first reported grafting MA onto PLA using twin-screw extrusion, achieving a 0.5 wt.% degree of grafting [5,6]. However, the grafting efficiency

* Corresponding author. Tel.: +64 7 8384947; fax: +64 7 8384835.
E-mail addresses: marsyilla@yahoo.com (K.I. Ku Marsilla), jverbeek@waikato.ac.nz (C.J.R. Verbeek).

was low compared to other polyesters due to PLA's limited reactivity [7]. This is due to poor activity of MA toward macro-radicals resulting from a low-density electron around —CH═CH— bonds and PLA's structural symmetry [8]. The competition between monomer and initiator suggests that there is an optimum radical concentration that depends on the peroxide/monomer ratio to promote grafting efficiency before termination reactions and chain scission become predominant [6]. Zhu reported an improved grafting yield when using an electron-donating monomer styrene as a co-monomer [9]. Grafting decreased the T_g, crystallinity (X_c) and thermal stability of PLA. The physical properties of PLA were affected because of new regular structures forming after grafting.

The mechanical properties of grafted PLA were not changed significantly [10] but were improved when blended with other polymers. Improved interfacial adhesion was observed between granular starch and PLA using PLA-g-MA [5]. PLA-g-MA also improved tensile strength and elongation at break of soy protein/PLA composites and finer domain sizes of soy protein concentrate (SPC) were observed suggesting improved dispersion [11]. Addition of 3 parts per hundred (phr) and 5 phr PLA-g-MA to PLA/wheat straw-based composites resulted in a significant improvement in tensile strength (20%) and flexural strength (14%) of the composites [12].

Although MA grafted polymers have shown great importance as compatibilizers their reaction with proteins may result in unstable amide bonds that can easily be hydrolyzed. Itaconic anhydride (IA) is less harmful compared to MA and is extremely stable when reacted with proteins and can used also be used for acetylating lysine, tyrosine and cysteine [13]. IA is a very reactive monomer in free radical grafting as it can produce tertiary radicals [14]. Owing to its chemical similarity to MA, it can be an alternative to MA, but it has not been studied extensively. IA has been used as a renewable monomer for the synthesis of biobased (PLA)-graft copolymers via conventional copolymerization and has potential as bio-based polymer [15]. IA also has been successfully grafted onto polyethylene with a high degree of grafting [16].

Side reactions such as chain scission, branching and crosslinking are common and depend on the nature of the macro-radicals and the polymer backbone [5]. Excessive chain scission usually leads to lower molecular weight and poor performance of the polymer, while crosslinking may lead to formation of insoluble polymers [9]. For polyethylene (PE), crosslinking during grafting reactions reduced the melt flow index and elongation at break whilst improving the impact strength and creep resistance and not affecting the tensile strength [17]. Maleation of propylene (PP) with maleic anhydride (MA) led to degradation rather than crosslinking due to rapid peroxide decomposition [18].

In this study, free radical grafting of IA onto PLA was carried out using dicumyl peroxide (DCP) as initiator in a twin-screw extruder. The effect of grafting parameters on the degree of grafting, thermal and mechanical properties was studied. Grafted PLA can be used as compatibilizer in blends of thermoplastic proteins and PLA, resulting in a blend that could potentially be 100% bioderived.

2. Methodology

2.1. Materials

Poly(lactic acid) was purchased from NatureWorks Ltd in pellet form (3051D). Analytical grade itaconic anhydride (IA), dicumyl peroxide (DCP), chloroform, acetone, potassium hydroxide, hydrochloric acid and phenolphthalein were purchased from Sigma Aldrich and were used as received.

2.2. Sample preparation

2.2.1. Extrusion
PLA was dried at 80 °C for 4 h to remove moisture. Itaconic anhydride (IA) and dicumyl peroxide (DCP) were dissolved in 20 mL dehydrated acetone and mixed with 300 g dried PLA according to the specifications in Table 1. After the acetone evaporated completely, the mixtures were reactively compounded using a LTE-20-44 twin-screw co-rotating extruder with a L/D of 44:1 and a screw diameter of 20 mm. The extruder barrel temperature was set to 145, 145, 165, 165, 180, 180, 180, 180, 160, 160, 155 °C (feed to die) and the screw speed was maintained at 100 rpm. A vacuum pump was connected to the vent at the 7th heating zone on the barrel to remove vapor generated during extrusion. The extrudate was collected in a water bath and pelletized. Pellets were dried in a convection oven at 80 °C for 12 h before further analysis.

2.2.2. Compounder mixer
To determine reaction kinetics, samples were prepared using a twin blade compounder mixer equiped with a torque sensor (Kistler) and motor unit (Flex 4 M). The mixing chamber diameter was 40 mm. The temperature was set to selected temperatures (180 and 200 °C) with a rotor speed of 100 rpm. PLA was first melted until the torque was constant (around 3 min) before DCP and IA were added. Samples were collected at different time intervals between 10 and 320 s.

2.3. Sample purification

2.5 g grafted PLA was dissolved in 40 mL chloroform and 0.75 mL, 1 M hydrochloric acid solution were added to hydrolyze the anhydride functional groups into carboxylic acids at room temperature. The solution was stirred vigorously for 30 min. The grafted sample was further purified by drop-wise precipitating into cold

Table 1
Formulations used in grafting reactions.

IA (%)	DCP (%)			
	0	0.5	0.75	1
0	PLA	–	–	–
2	–	PLA1	PLA6	PLA11
3	–	PLA2	PLA7	PLA12
4	–	PLA3	PLA8	PLA13
5	–	PLA4	PLA9	PLA14
6	–	PLA5	PLA10	PLA15

methanol (200 mL) to remove any homo- and copolymers of IA. A white sponge of filtered precipitate was collected and washed by methanol and distilled water several times and dried in vacuum oven for 24 h. Each sample was purified and analyzed in triplicate.

2.4. Intrinsic viscosity

The intrinsic viscosity of PLA and grafted PLA were determined by dissolving the polymer in chloroform to concentrations between 0.88 and 8.28 g/dL at a constant temperature of 20 °C. A Ubbelohde viscometer was used partially submerged in a temperature controlled water bath. The elution time of the solvent was determined and used to calculate the relative viscosity of each sample for each concentration. The intrinsic viscosity was obtained by extrapolating a plot of concentration vs. relative viscosity to zero concentration.

2.5. Degree of grafting

Purified PLA-g-IA (0.4 g) was dissolved in 20 mL chloroform and the solution was titrated to a phenolphthalein end-point using potassium hydroxide in methanol (0.04 M). Grafted samples were completely soluble and did not precipitate during titration. The degree of grafting was calculated using Eq. (1). Each sample was tested in triplicate and average values are reported.

$$\% \text{ IA} = \frac{N_{KOH} V_{KOH}}{2W_{sample}} \times 130.099 \frac{g}{mol} \times 100 \tag{1}$$

where N_{KOH} is the normality (moles per equivalent) of the KOH solution V_{KOH} is the volume (l) and W_{sample} is the sample mass (g).

2.6. Differential scanning calorimetry

Differential scanning calorimetry (DSC) was conducted using a DSC 8500 from Perkin Elmer. Specimens were crimp sealed in 30 µL aluminum pans and run under constant nitrogen purge gas. Specimens were heated from 0 to 250 °C at 10 °C/min, held for 10 min at 250 °C, cooled to 0 °C (10 °C/min) after which the cycle was repeated using the same method. The absolute degree of crystallinity can be calculated using Eq. (2), from data obtained during the second scan to avoid thermal history effects.

$$\chi_c \text{ (\%)} = \frac{\Delta H_m(\text{PLA}) - \Delta H_c(\text{PLA})}{\Delta H_m^\infty(\text{PLA})} \times 100 \tag{2}$$

where ΔH_m is melting enthalphy of material, ΔH_c is enthalpy of crystallization and ΔH_m^∞ (PLA) is the melting enthalpy per gram of 100% crystalline PLA (93 J/g) [19]. During the first heating cycle, no exothermic peaks were observed between 180 and 250 °C, indicating that the grafting reaction was complete (data not presented). The difference between unpurified and purified PLA-g-IA was also considered, and it was found that the DSC curve of purified samples was similar to unpurified samples; therefore, data of unpurified samples were presented. In order

to avoid the effect of thermal history, data from the second heating cycle was used for analysis.

2.7. Simultaneous DTA–TGA

Thermogravimetric analysis of pure PLA and grafted PLA were measured using a TA instrument SDT 2960. The samples were sealed in aluminum pans and tested from 25 to 800 °C at a heating rate 10 °C/min in air.

2.8. Mechanical properties

Tensile properties of blends of 2% PLA-g-IA with PLA were measured using an Instron model 33R4204 according to ASTM D638-86. An extension rate of 5 mm/min and an extensometer gauge length of 50 mm were used for testing. Samples were tested in replicas of five directly after removal from the humidity chamber. Samples were conditioned for up to 15 days at 23 °C and 50% relative humidity before tensile testing. The secant modulus was calculated between a strain of 0.0005 and 0.0025 and the toughness was calculated as the area under the stress–strain graph and is more accurately referred to as energy-to-break.

3. Results and discussion

3.1. Intrinsic viscosity

The effect of DCP and IA concentration on intrinsic viscosity is shown in Fig. 1 while PLA's intrinsic viscosity was 0.63 dL/g. At 0.5 wt.% DCP, all grafted samples had a higher intrinsic viscosity. Generally, grafting functional groups onto PLA in the presence of peroxide initiators results in significant β-chain scission that is reflected in a reduction in intrinsic viscosity (i.e. a reduction in average molecular weight) [20]. However, in this situation, an increase in degree of grafting increased the intrinsic viscosity probably due to the bulky functional group of IA that altering chain mobility. This would increase the end-to-end distance of the dissolved molecule, leading to a higher intrinsic viscosity compared to unmodified PLA. The increase in intrinsic viscosity was unlikely due to crosslinking, as all samples dissolved completely.
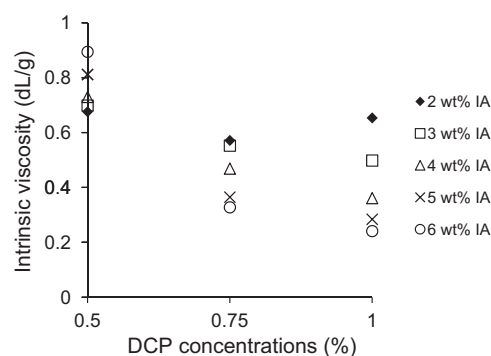

Fig. 1. Intrinsic viscosity of PLA and grafted PLA at different DCP and IA concentrations.

Increasing the DCP concentration lead to a significant reduction in intrinsic viscosity between 4 and 6 wt.% IA. At low IA concentration this reduction was less severe. This would suggest that chain scission did occur at higher peroxide concentration and was more severe at high monomer concentration.

3.2. Degree of grafting

In general, an increase in concentration of either of the reagents led to a higher degree of grafting (Fig. 2). Concentrations between 0.5 and 1 wt.% were used by considering the half-life of DCP (<1 min at 200 °C) [16]. Grafting always compete with side reactions and at lower concentrations and higher temperature peroxide decomposition will be too rapid a low degree of grafting. A higher amount of initiator (1 wt.%) affects the total free radical concentration that causes greater crosslinking [6].

The degree of grafting increased nearly linearly with increasing concentration. The highest grafting content was achieved at 6 wt.% IA for every initiator concentration used. At higher IA concentration the effect of DCP concentration was more pronounced. Between 2 and 4 wt.% IA, increasing DCP concentration had a much smaller effect on grafting, whereas above 5 wt.% IA, the degree of grafting drastically increased with increasing DCP.

Within the concentration range tested, the continuous increasing trend suggests that although chain scission occurred (decreased intrinsic viscosity), grafting was dominant. If chain scission was dominant, the degree of grafting would have decreased, as observed by some others [6,20,21]. For example, Mani et al. showed that chain scission become significant above 5% MA and 0.3% initiator [6].

As the concentration of DCP increased, it would be expected that a higher amount of macro-radicals be produced, but the degree of grafting would be limited by the slower reaction with IA. One would therefore require sufficient IA to react with the excess radicals that form when using higher DCP concentrations. However, this is not always linear; the degree of grafting of MA onto PLA was found to decrease above 1 wt.% initiator [6]. When using styrene as a co-monomer in grafting of MA onto PLA, 0.75 wt.% initiator was found to be optimal [9].
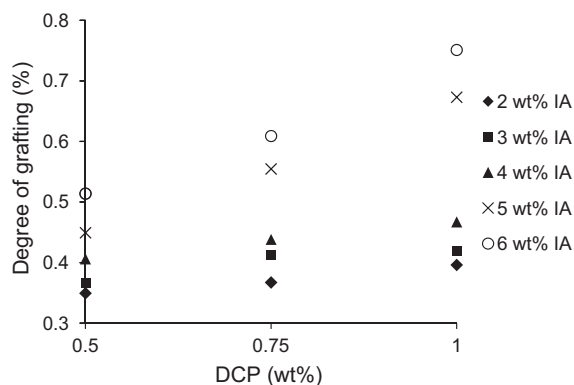
3.3. Temperature and residence time

Generally, higher temperatures lead to increased reaction rates, brought about by faster initiator decomposition. However, higher temperatures does not necessarily lead to a higher degree of grafting as most initiators have an optimum temperature for decomposition [22]. For reactive extrusion, the grafting reaction will also depend on residence time, where excessively long residence times may reduce the degree of grafting due to polymer degradation [23]. The half time of DCP is 60 s at 180 °C and 15 s at 200 °C while the residence time in the extruder, under the conditions for this study, is 160 s.

The degree of grafting increased only marginally at higher temperature (Fig. 3). This was similar to observations by Carlson et al. [5] who observed a slight difference in the degree of grafting at temperature between 180 and 200 °C. In other research, a significant increase was observed at 200 °C when using styrene as a co-monomer when grafting MA onto PLA [9]. However, at high temperature, although molecular motion increase, radical decay and homopolymerization of the monomer will also increase, thereby reducing the degree of grafting [24].

In the reaction of a polymeric system, the relationship between residence time and degradation plays a significant role. Prolonged reaction time in extruder is required for sufficient reaction, but it may also contribute to degradation. However, final process design usually needs a trade-off between higher degree of grafting and a shorter residence time. The effect of residence time at different temperatures is shown in Fig. 4. In these experiments, residence time was increased up to 320 s by performing the reaction in a compounder mixer instead of a twin-screw extruder. At 0.5 wt.% DCP (Fig. 4A), the degree of grafting increased and reached a plateau after about 60 s at 2 wt.% IA, and increased to about 160 s at 6 wt.% IA. At 180 °C, increasing DCP concentration to 1 wt.% shortened the time to reach a plateau to 60 s for all IA concentrations (Fig. 4B). However, a small decrease was observed over the maximum degree of grafting at higher IA concentrations, similar to what others have observed [6,20]. A lower degree of grating usually suggests either a lack of monomer or initiator. In this case, higher initiator concentrations (1 wt.% DCP) showed a higher degree of grafting with
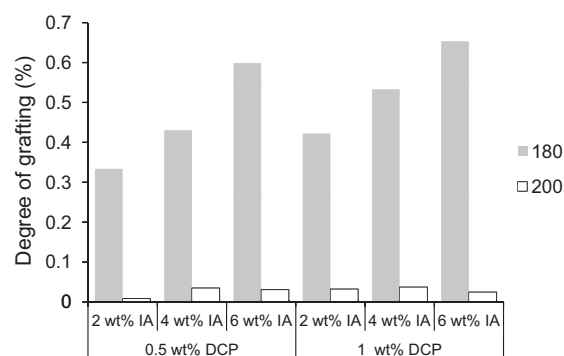
Fig. 2. Effect of monomer and initiator concentration on the degree of grafting.

Fig. 3. Effect of temperature on the degree of grafting for selected samples.
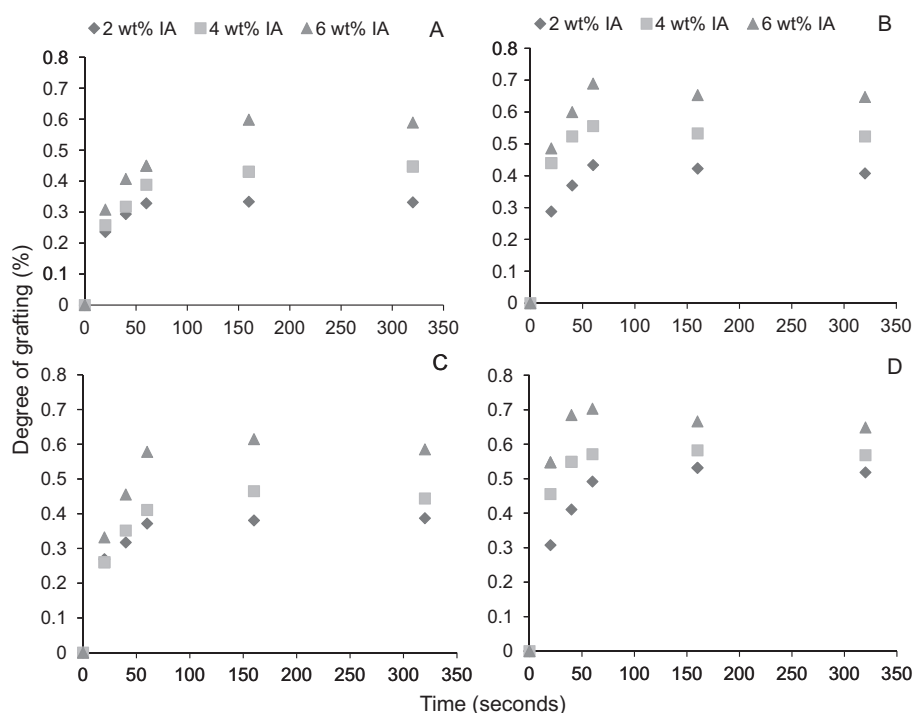
Fig. 4. Effect of prolonged residence time at different temperature on IA grafted PLA at various DCP and IA concentrations. At 180 °C, 0.5 wt.% DCP (A), 180 °C, 1 wt.% DCP (B), 200 °C, 0.5% DCP (C) and 200 °C, 1 wt.% DCP (D).

shorter reaction time compared to low initiator concentrations (0.5 wt.% DCP) and the prolonged residence time (up to 350 s) had no significant effect on grafting, suggesting none or a minimal degradation of the polymer.

At higher temperature, the maximum degree of grafting was reached after about 60 s, regardless of IA concentration (Fig. 4C). At 1 wt.% DCP, virtually no difference was observed between 180 and 200 °C (Fig. 4D). Although, DCP's half-life is shorter at higher temperature, no significant temperature effects were observed, other than a slight reduction in the time it takes to reach the maximum degree of grafting, which means higher temperatures could be beneficial for extrusion at higher rates where a shorter residence time is expected. The effect of temperature and consumption of initiator are further explained in light of the reaction kinetics.
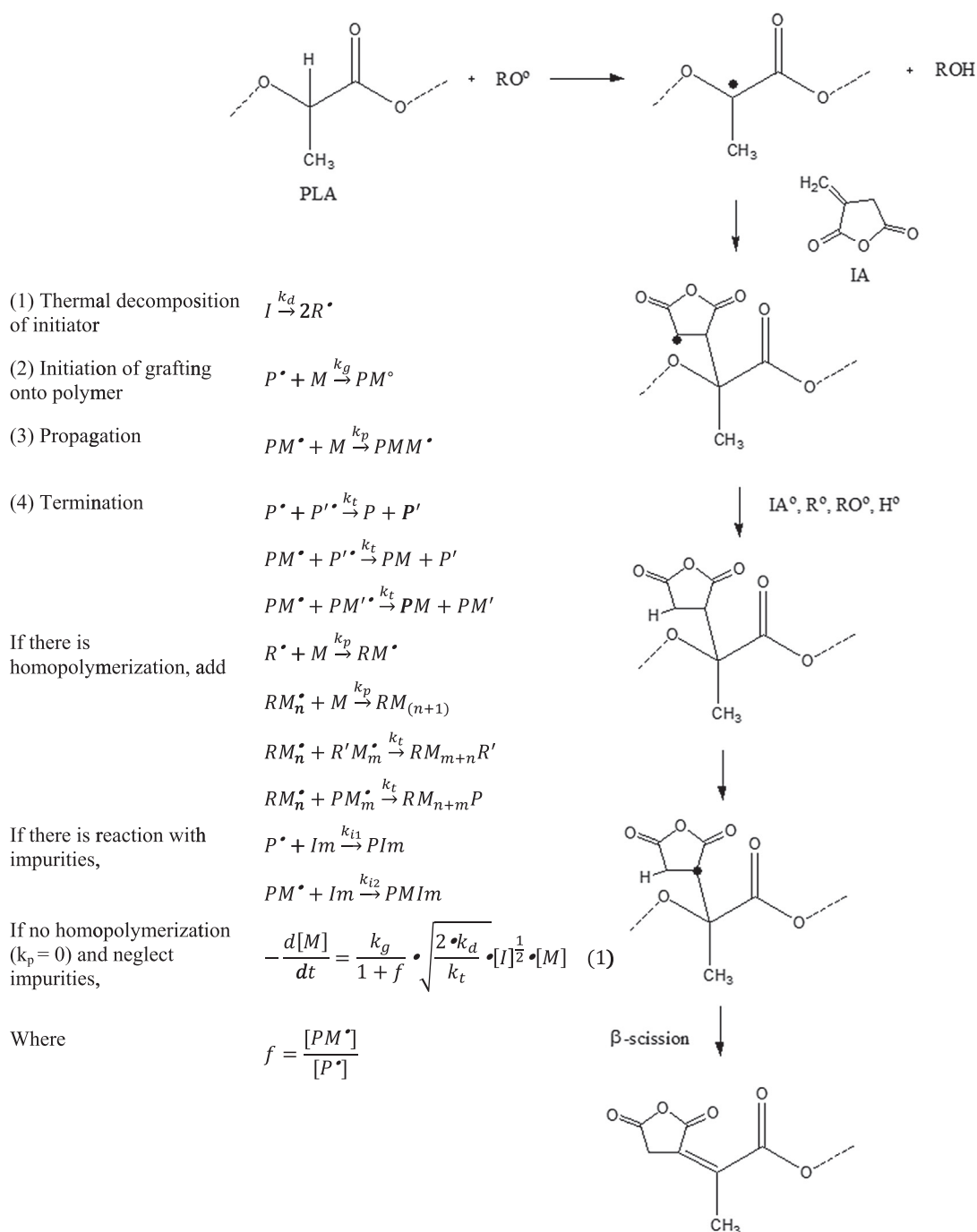
3.4. Reaction kinetics

A schematic of the potential reaction mechanism for grafting IA onto PLA is presented in Scheme 1. For the kinetics of grafting, the most important intermediates are free radicals. Free radicals generated by the decomposition of DCP (1) initiates grafting which involves removing a labile atom from PLA to regenerate a reactive center at a new location. This is followed by initiation reactions (2) that occur via hydrogen abstraction of an α-carbon relative to the carbonyl group in PLA when this radical reacts with the double bond on IA. During initiation, the polymer radicals have the ability to combine with another radicals such as IA, peroxide, polymer radicals or hydrogen (IA°, R°, RO°

or H°). Propagation (3) is the next step in generating a graft copolymer by a free radical polymer/monomer mechanism that depends on the concentration of polymer radicals. This reaction continues until either the initiator has been consumed or the radicals have been consumed by termination (β-scission). During the termination step (4), when no more radicals are generated, grafting slows and eventually stops. To obtain a high degree of grafting, it is essential that the macro-radicals react with the IA monomers before undergoing side reactions, such as homopolymerization, recombination and chain scission.

However, Kim and White [25] proposed more simplified kinetics of polypropylene maleation assuming that homopolymerization was absent because the temperature was above the ceiling temperature for homopolymerization of MA. By using the same assumption for IA, k_p is equal to 0 and by neglecting the role of impurities, the reaction can be further simplified to Eq. (1).

It is known that initially, at time zero, the initiator concentration is high, leading to a high initial reaction rate. Reaction rate increases with concentration and can be temperature dependent. The rate of initial rate (R_g) was calculated by changing the concentration of monomer at constant initiator and temperature. From a graph of degree of grafting vs. time (Fig. 4), a steep initial slope is observed, and an initial rate of reaction can be determined for these starting conditions.

Fig. 5 presents a plot of initial monomer concentration vs. R_g at different temperatures and initiator concentrations. The R_g was calculated from a slope between 0 and 20 s, obtained from Fig. 4. A linear correlation was

(1) Thermal decomposition of initiator

$$I \xrightarrow{k_d} 2R^{\bullet}$$

(2) Initiation of grafting onto polymer

$$P^{\bullet} + M \xrightarrow{k_g} PM^{\circ}$$

(3) Propagation

$$PM^{\bullet} + M \xrightarrow{k_p} PMM^{\bullet}$$

(4) Termination

$$P^{\bullet} + P'^{\bullet} \xrightarrow{k_t} P + P'$$

$$PM^{\bullet} + P'^{\bullet} \xrightarrow{k_t} PM + P'$$

$$PM^{\bullet} + PM'^{\bullet} \xrightarrow{k_t} PM + PM'$$

If there is homopolymerization, add

$$R^{\bullet} + M \xrightarrow{k_p} RM^{\bullet}$$

$$RM_n^{\bullet} + M \xrightarrow{k_p} RM_{(n+1)}$$

$$RM_n^{\bullet} + R'M_m^{\bullet} \xrightarrow{k_t} RM_{m+n}R'$$

$$RM_n^{\bullet} + PM_m^{\bullet} \xrightarrow{k_t} RM_{n+m}P$$

If there is reaction with impurities,

$$P^{\bullet} + Im \xrightarrow{k_{i1}} PIm$$

$$PM^{\bullet} + Im \xrightarrow{k_{i2}} PMIm$$

If no homopolymerization ($k_p = 0$) and neglect impurities,

$$-\frac{d[M]}{dt} = \frac{k_g}{1+f} \bullet \sqrt{\frac{2 \bullet k_d}{k_t}} \bullet [I]^{\frac{1}{2}} \bullet [M] \quad (1)$$

Where

$$f = \frac{[PM^{\bullet}]}{[P^{\bullet}]}$$

Scheme 1. Potential mechanism of IA grafting onto PLA.

observed for R_g vs. initial monomer concentration. At 0.5 wt.% DCP, the slope, which represent the order of reaction with respect of IA, are 0.01440 and 0.0153 at 180 and 200 °C, respectively. When the concentration of DCP increased (Fig. 5B), the slopes increased slightly, indicating that at higher amount of macro-radicals, the reaction with IA proceeded at higher rate. Very little difference was

observed between the initial rate of reaction at 180 and 200 °C, similar to the degree of grafting results.

To calculate the effective rate constant, $\frac{k_g}{(1+f)\sqrt{k_t}}$, Eq. (1) can be simplified to $\frac{k_g}{1+f\sqrt{k_t}} = \frac{\frac{dM}{dt}\left[\frac{1}{[M]}\right]}{\sqrt{2k_d[I]^{1/2}}}$, where dM/dt [M] is the slope of R_g vs. monomer concentration (Fig. 5). Using
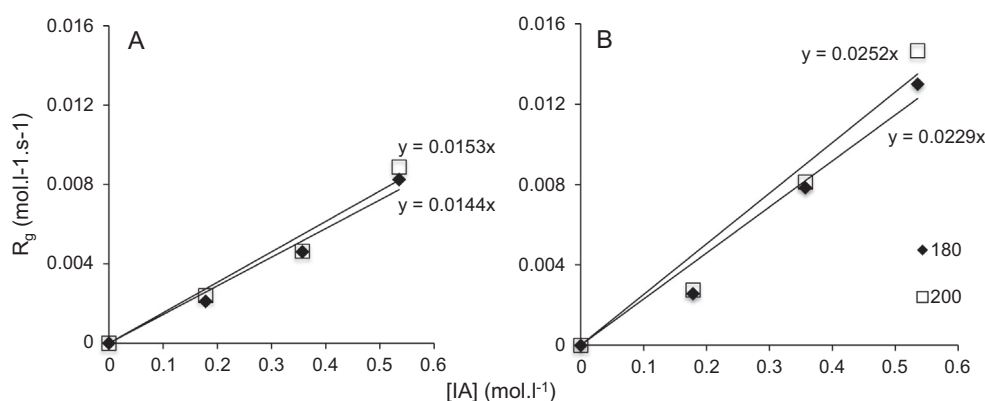
Fig. 5. Initial rate of reaction (R_g) at different temperatures, monomer concentration and initiator concentration; (A) 0.5 wt.% DCP and (B) 1 wt.% DCP.

$k_d = 194.8 \ s^{-1}$ for DCP, the effective rate constant at different initiator concentrations is listed in Table 2 and was consistent with other research [16,26]. The effective rate constant was slightly higher at higher initiator concentration and almost independent of temperature. Designing a reactive extrusion process for grafting IA should therefore account for the fact that using higher IA concentration should be balanced by an increase in DCP, but the effect is not large. Also, using temperatures much higher than the melting point of PLA will not be required for efficient grafting.

3.5. Thermal properties

3.5.1. Glass transition temperature

The glass transition temperature (T_g) strongly depends on chain mobility and grafting a bulky functional group could alter this by either increasing chain stiffness or creating free volume. Without any grafting, pure PLA had a T_g of 42 °C but increased to about 48 °C, depending on the percentage grafting. The DSC thermograms are shown in Fig. 6. Increasing the DCP concentration decreased the T_g, falling below that of pure PLA at 1 wt.% DCP (Fig. 7A). When the degree of grafting is low, the higher T_g is probably as a result of decreased chain mobility due to steric hindrance by the bulky IA molecule. However, at high IA and DCP concentrations, the reduction in T_g could be the result of chain scission as evident from intrinsic viscosity results (Section 3.1). Jang et al. [27] suggested that MA could also function as a plasticizer after confirming the absence of chain scission in PLA/starch blends.

3.5.2. Crystallization temperature

PLA showed an exothermic crystallization peak (T_c) around 100–120 °C (Fig. 6) as a result of rapid cooling from

the melt after the first heating cycle. This would imply that cooling was rapid enough to prevent crystallization during cooling. PLA had a T_c around 106 °C. Theoretically, a higher T_g suggests reduced chain mobility and crystallization should also occur slower, i.e. a higher T_c (Fig. 7B). At higher IA and DCP, the reduction in T_c is probably due to steric effects from IA that possibly reduce the growth of crystals, similar to grafting MA on PLA [8,28].

3.5.3. Melting temperature (T_m)

PLA showed a double endothermic melting peak (T_m) around 140–150 °C (Fig. 6). This behavior is typically observed for crystalline polymers due to melt–recrystallization behavior [29,30]. It has been explained that this behavior arises from α and α' forms of PLA whereby α' is due to the fusion of crystals with lower thermal stability corresponding to melting of initial lamellae, while α is due to the melting of thicker and more perfect lamellae after structural reorganization.

The melting temperature of grafted PLA shifted to slightly lower temperatures when using 0.5–0.75% DCP and was unaffected by IA concentration (Fig. 7C). At higher IA concentrations, the melting peaks decreased more drastically with increasing DCP. It is expected that grafting would decrease the melting point as crystal structures would be disrupted. PLA would probably form less perfect crystals, which melt at lower temperatures.

3.5.4. Crystallinity

The crystallinity of grafted PLA was higher than PLA (0.5%), and generally increased with increasing wt.% DCP (Fig. 8). However, the increase was only modest on an absolute basis. The samples had low crystallinity due to rapid cooling applied in this experiment. The slight increase in crystallinity is somewhat unexpected, as most other researchers have observed a decrease in crystallinity [31], probably due to irregularity introduced by the grafted monomer. On the other hand, the crystallinity of grafted isotactic polypropylene (i-PP) depended on anhydride unit concentration [32] and an increase in crystallinity was observed for MA grafted polybutylene succinate (PBS) due to heterogeneous nucleation [33]. PLA is highly

Table 2
Kinetic parameters determined in this study.

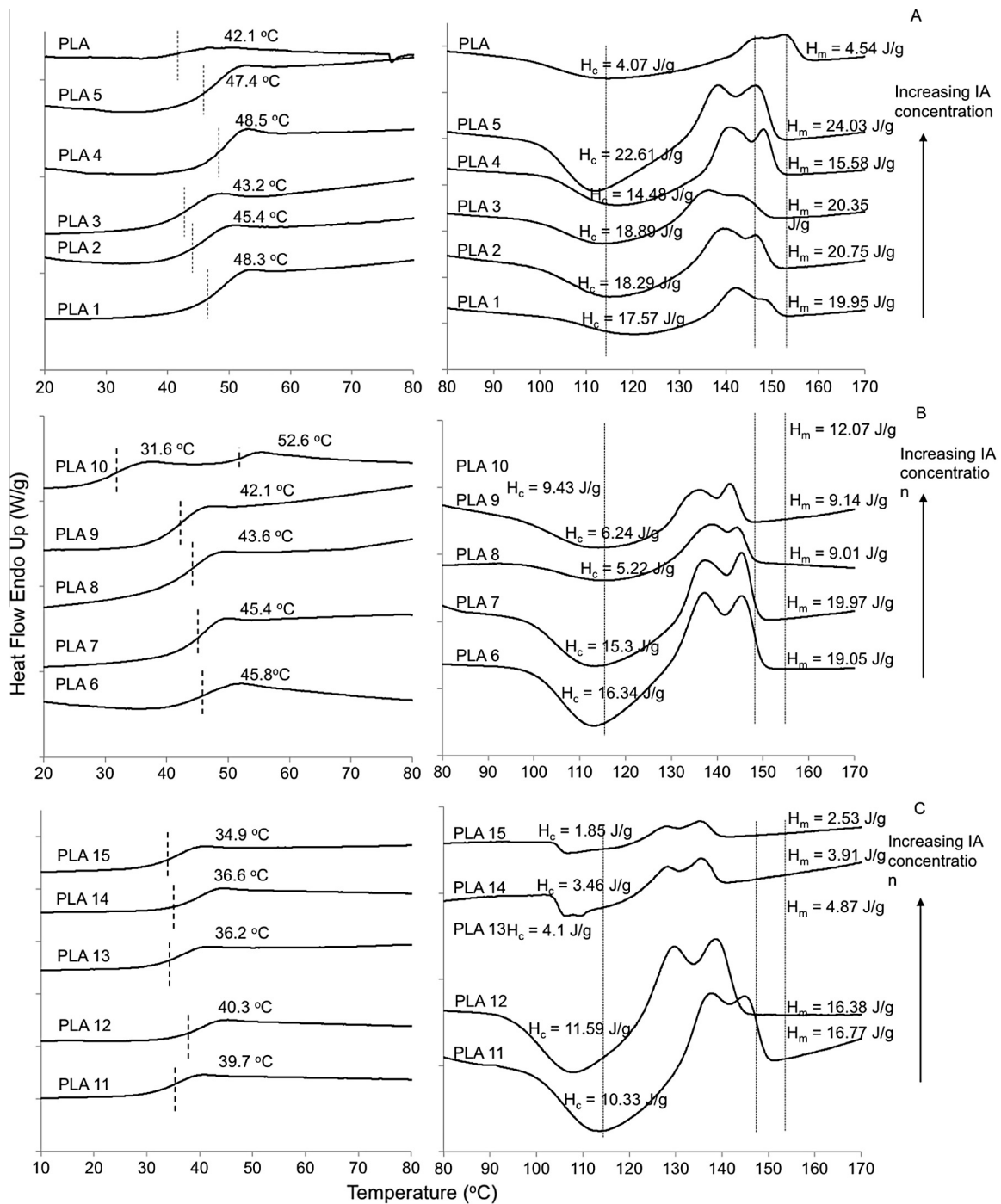| Effective rate constant (l/mol s)$^{1/2}$	Initiator concentration (wt.%)	180 °C	200 °C
$\frac{k_g}{(1+f)\sqrt{k_t}}$	0.5	0.024	0.025
	1	0.027	0.03

Fig. 6. Glass transition temperature (T_g), crystallization peak (T_c) and melting endotherms of PLA and PLA-g-IA at different initiator concentration; 0.5 wt.% DCP (A), 0.75 wt.% DCP (B) and 1 wt.% DCP (C).

amorphous, and a low degree of grafting may lead to similar heterogeneous nucleation.

In other words unreacted monomer, impurities or chain fragments could act as nucleating agents leading to a higher degree of crystallinity. At higher degrees of grafting (high DCP and IA concentration) the irregularity introduced by the grafted groups led to a reduction in crystallinity relative to the other grafted polymers.

3.5.5. Thermal decomposition

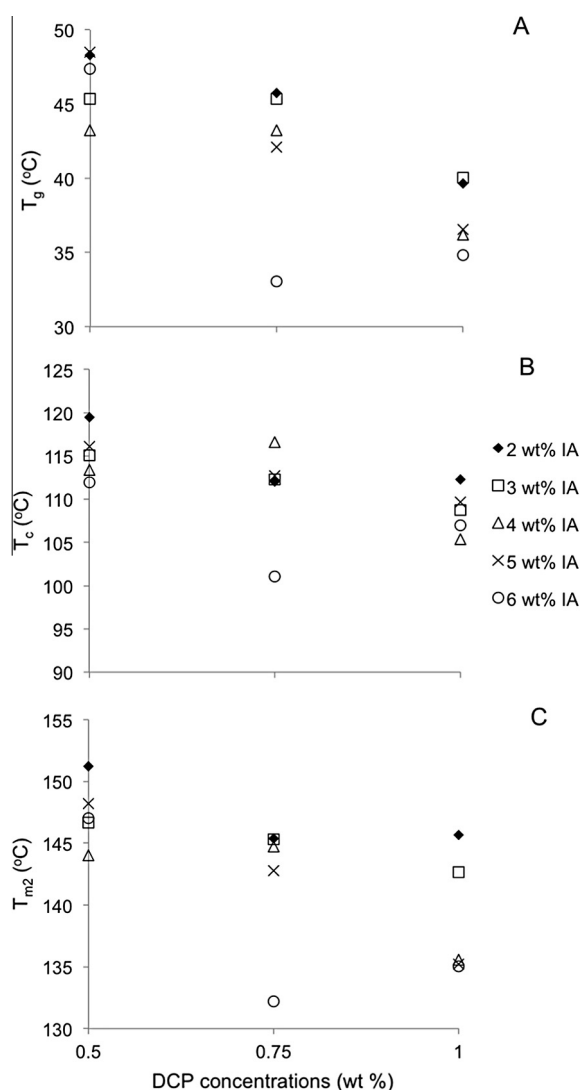All the grafted polymers had a higher thermal stability (rate of maximum mass loss) compared to PLA (Fig. 9, only

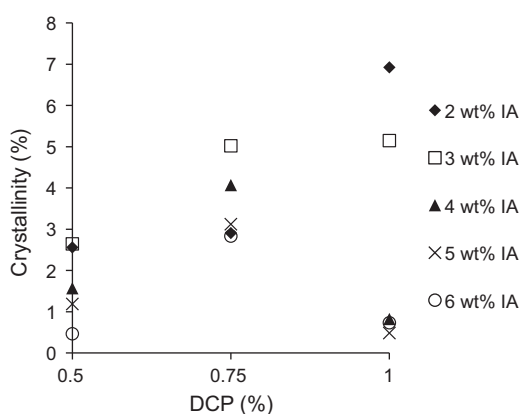Fig. 7. T_g, T_c and Tm_2 vs DCP concentration.

Fig. 8. Crystallinity of PLA and PLA-g-IA at different initiator and monomer concentrations.
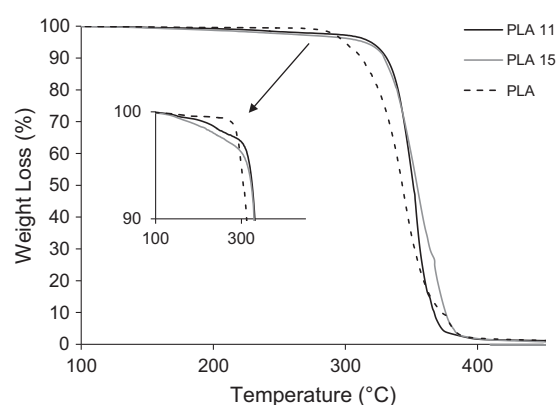

Fig. 9. Thermal decomposition of PLA and PLA-g-IA (PLA 15).

selected data presented). Increased thermal stability could be as a result of many factors such as increased crystallinity or molecular mass or crosslinking. The thermal decomposition temperature for PLA-g-MA decreased due to irregular chain branching of MA onto the PLA backbone, but was also accompanied by a decrease in crystallinity [5,8,28]. The increase in thermal stability would support earlier observations regarding an increase in crystallinity observed using DSC as the molecular weight (intrinsic viscosity) was not increased by crosslinking. A slight increase in mass loss at low temperature was observed, probably as a result of lower molecular fractions forming (chain scission) during grafting.

3.6. Mechanical properties

In general, the mechanical properties of grafted polymers only show minor changes over that of the pure polymer. It depends on the degree of crosslinking, chain scission as well as crystallinity. If grafting exclusively takes place in the amorphous phase, an enhancement in mechanical properties could be observed, however, a higher degree of grafting could also disrupt crystallinity which may reduce the tensile strength and modulus [31].

The mechanical properties of PLA and PLA blended with 2 wt.% PLA-g-IA generally increased, and was dependent on the degree of grafting (Fig. 10). PLA had a tensile strength of 48 MPa and a secant modulus of 3.5 GPa, but have a relatively low elongation at break (~6%). Typical stress–strain displacement curves for PLA and grafted PLA are presented in Fig. 11. The addition of PLA-g-IA had less impact on tensile strength compared to other mechanical properties and varied almost in a similar manner to crystallinity. Blending PLA-g-IA with PLA probably resulted in strengthening the amorphous parts of PLA because PLA-g-IA has a higher crystallinity than PLA. However, when the degree of grafting is too high (PLA10), PLA's crystallinity could be disrupted too much leading to the lower mechanical properties of that sample.

The drop in secant modulus is likely related to the lower T_g associated with the grafted polymer. Adding 2 wt.% IA-g-
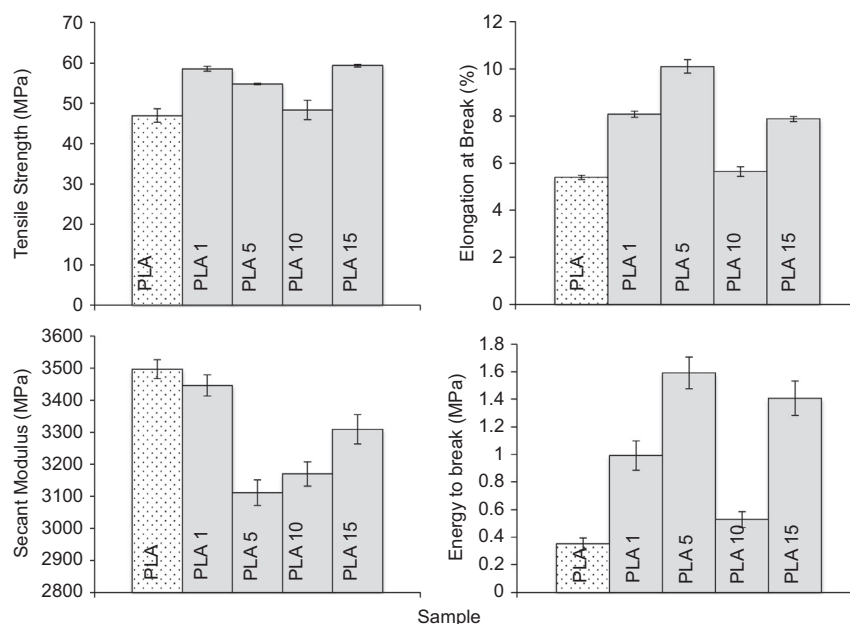
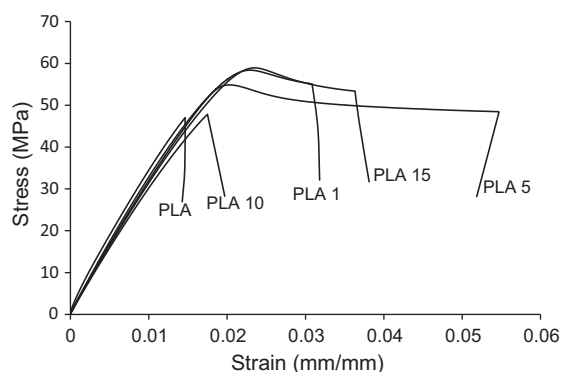**Fig. 10.** Mechanical properties of PLA and grafted PLA.

Fig. 11. Stress–strain curve of PLA and grafted PLA.

PLA would therefore effectively plasticize the PLA matrix, leading to a reduction in stiffness.

4. Conclusion

PLA-g-IA was successfully produced using reactive extrusion. The reaction efficiency depends on the interaction between monomer and initiator concentration, temperature and residence time. These interactions were also found to affect the thermal properties and thermal stability of PLA-g-IA. The thermal properties of PLA-g-IA were significantly altered, leading to a reduction in T_g and an increase in crystallinity, depending on the degree of grafting. Blending PLA-g-IA with pure PLA modified the mechanical properties of the blend, but did not adversely affect its properties and it would therefore be suitable as a compatibilizer in blends of PLA and other polymers.

References

[1] Yuan X, Mak AFT, Kwok KW, Yung BKO, Yao K. J Appl Polym Sci 2001;81:251–60.
[2] Hassouna F, Raquez J-M, Addiego F, Toniazzo V, Dubois P, Ruch D. Eur Polymer J 2012;48:404–15.
[3] Hassouna F, Raquez J-M, Addiego F, Dubois P, Toniazzo V, Ruch D. Eur Polymer J 2011;47:2134–44.
[4] Huneault MA, Li H. Polymer 2007;48:270–80.
[5] Carlson D, Nie L, Narayan R, Dubois P. J Appl Polym Sci 1999;72:477–85.
[6] Mani R, Bhattacharya M, Tang J. J Polym Sci, Part A: Polym Chem 1999;37:1693–702.
[7] Mani R, Bhattacharya M. Eur Polymer J 2001;37:515–26.
[8] Ma P, Jiang L, Ye T, Dong W, Chen M. Polymers 2014;6:1528–43.
[9] Zhu R. Preparation of maleic anhydride grafted poly(lactid acid)(PLA), Doctoral Dissertation. Washington State University; 2011.
[10] Hwang SW, Shim JK, Selke S, Soto-Valdez H, Rubino M, Auras R. Macromol Mater Eng 2012:624–33.
[11] Zhu R, Liu HZ, Zhang JW. Ind Eng Chem Res 2012;51:7786–92.
[12] Nyambo C, Mohanty AK, Misra M. Macromol Mater Eng 2011;296:710–8.
[13] Fischer L, Peißker F. Appl Microbiol Biotechnol 1998;49:129–35.
[14] Sharabasht MM, Guile RL. J Macromol Sc Part A-Chem 1976;10:1039–54.
[15] Okuda T, Ishimoto K, Ohara H, Kobayashi S. Macromolecules 2012;45:4166–74.
[16] Verbeek CJR, Hanipah SH. J Appl Polym Sci 2010;116:3118–26.
[17] Tamboli S, Mhaske S, Kale D. Indian J Chem Technol 2004;11:853–64.
[18] Gaylord NG, Mishra MK. J Polym Sci Polym Lett Ed 1983;21:23–30.
[19] Harris AM, Lee EC. J Appl Polym Sci 2008;107:2246–55.
[20] Zare A, Morshed M, Bagheri R, Karimi K. Fibers Polym 2013;14:1783–93.
[21] John J, Tang J, Yang ZH, Bhattacharya M. J Polym Sci Part A-Polym Chem 1997;35:1139–48.
[22] Ganzeveld KJ, Janssen LPBM. Polym Eng Sci 1992;32:457–66.
[23] Jamshidian M, Tehrany EA, Imran M, Jacquot M, Desobry S. Compr Rev Food Sci Food Saf 2010;9:552–71.
[24] Gromov V, Galperina N, Osmanov T, Khomikovskii P, Abkin A. Eur Polymer J 1980;16:529–35.
[25] Kim B, White JL. Polym Eng Sci 1997;37:576–89.
[26] Cha J, White JL. Polym Eng Sci 2001;41:1227–37.

[27] Jang WY, Shin BY, Lee TJ, Narayan R. J Ind Eng Chem 2007;13:457–64.
[28] Hwang SW, Lee SB, Lee CK, Lee JY, Shim JK, Selke SEM, Soto-Valdez H, Matuana L, Rubino M, Auras R. Polym Testing 2012;31:333–44.
[29] Yasuniwa M, Tsubakihara S, Iura K, Ono Y, Dan Y, Takahashi K. Polymer 2006;47:7554–63.
[30] Yoo ES, Im SS. J Polym Sci, Part B: Polym Phys 1999;37:1357–66.
[31] Bhattacharya A, Rawlins JW, Ray P. Polymer grafting and crosslinking. Hoboken (NJ, USA): John Wiley & Sons Inc.; 2009.
[32] Güldoğan Y, Eğri S, Rzaev ZM, Pişkin E. J Appl Polym Sci 2004;92:3675–84.
[33] Phua Y, Chow W, Ishak ZM. Expr Polym Lett 2013;7:340–54.

Chapter 7

Crystallization of itaconic anhydride grafted poly (lactic acid)

A submitted

manuscript for publication consideration

in

Macromolecular Materials and Engineering

by

K.I Ku Marsilla[1] and C.J.R. Verbeek

[1]As first author of this paper, I prepared the initial draft manuscript, which was refined and edited with consultation with my supervisor, who has been credited as co-author.

Crystallization of itaconic anhydride grafted poly (lactic acid)

K. I. Ku Marsilla[1], C.J.R Verbeek[2]

[1] School of Materials and Mineral Resources Engineering

Universiti Sains Malaysia, 14300 Nibong Tebal, Pulau Pinang

ku_marsilla@hotmail.com

[2] Department of Engineering, School of Science and Engineering

University of Waikato, Hamilton 3240, New Zealand

jverbeek@waikato.ac.nz

Tel +64 7 8384947

Fax +64 7 8384835

Abstract

The effect of annealing poly (lactic acid) (PLA) and PLA grafted with itaconic anhydride (IA) at different temperatures (80-130 ^{o}C) was studied using differential scanning calorimetry (DSC) and wide angle X-ray scattering (WAXS). For PLA, two crystal forms were obtained when annealed between 110-120 ^{o}C, transforming into only the α-form at 130 ^{o}C while a mixture of α' and α-form were obtained in grafted PLA. Grafting accelerated the rate of crystallization of PLA but inhibited the development of large crystallites during annealing, resulting in a lower melting point. Incorporation of a bulky IA functional group slightly increased the lattice spacing by extending the helical conformation of the grafted PLA chain.

Keywords: annealing, crystallization, crystallinity, itaconic anhydride, PLA

114

Introduction

Poly (lactic acid) (PLA) is a biodegradable polymer that is produced from lactic acid and presents great potential for commodity applications due to its good mechanical properties and biodegradability. However, it thermally degrades easily, is brittle and has a low rate of crystallization; these often limit its application. PLA can be modified using free radical grafting, which could be a method to overcome these limitations [1, 2] but may also introduce new opportunities, such as being a compatibilizer in polymer blends [3].

In polymer blends, the crystallization rate of miscible blends is T_g-dependent. Molecular mobility of restricted domains may depress the rate of crystallization, while nucleation is dependent on the blend composition [4]. Additionally, in crystalline/amorphous blends, the amorphous polymer could be completely rejected from the crystal lattice, or be uniformly included (but only to certain amount) due to high viscosity of amorphous material [4, 5]. It is therefore important to understand how a polymer like PLA's crystallization is influenced by grafting, which prepares it for use in blends.

PLA exhibits more than one form of crystalline structure with the same chemical composition (polymorphism). The earliest identified crystalline form of PLA is the α form with 10_3 helical conformations (10 monomeric units are included in the fiber period, turning three times) packed in an orthorhombic crystal system [6, 7]. In the disordered modification, α', the chain conformation and crystal system is looser [8, 9] and is believed to be due to a larger lattice dimension and weaker inter-chain interactions [10, 11]. The α'-type is formed below 100 ^{o}C, and crystallization

above 120 ^{o}C will transform α' to α-crystals; between these, a mixture can be expected.

During extrusion and injection molding of PLA, it is difficult to achieve high crystallinity in a short cooling time due to its low crystallization rate. As a result, PLA is usually amorphous after processing. Crystallization is affected by the presence of a small amount of monomer (copolymer), while chain irregularities (introduced by grafting) reduces the ability of a polymer to form perfect crystal arrangements. A random copolymer can potentially crystallize in two ways. It can form a two phase system of a crystalline phase composed of A-units and a non-crystallizable phase of co-monomer B-units (comonomer exclusion). In the second way, the comonomer B-units produce defects in the crystal lattice of A-units and both phases has the same composition (co-monomer inclusion). Both suggested mechanisms will result in a depression of the crystalline melting point [12, 13].

Nucleation during crystallization could also play an important role [14, 15]. Inclusion of a copolymer sometimes act as a nucleating agent that is usually characterized by an observed increase in crystallization rate. Crystallization of PLA in the presence of starch (1 to 40%) reduced the crystallization half time from 14 to about three minutes,[16] and the effect was even stronger when using thermoplastic starch.[17] In another study, transformation of most original spherullite crystals of PLA into sheaf-like crystals was observed when using a nucleating agent [18].

The slow crystallization rate of PLA can be improved by annealing [11, 19-21]. During heat treatment, semi-crystalline polymers can change their physical and morphological structures as a result of reorganization leading to a state of order with a lower free energy. The quality of the crystal (i.e thickness), however, depends on

116

annealing temperature and time [22]. Another method to improve the crystallization rate of PLA include varying the processing parameters [23-27], which is often accompanied by mathematical modeling of crystallization kinetics [8, 9, 28, 29].

Using natural polymers, such as protein or starch in polymer blends, annealing parameters such as temperature and time are important, e.g. longer annealing time could lead to protein degradation. On the other hand, starch and soy protein were suggested to act as a nucleating agent in PLA blends, [3, 30] but the role of the compatibilizer was not clear.

This study addresses the role of the grafting in the crystallization process of PLA. In our previous work of grafting itaconic anhydride (IA) onto PLA, the degree of grafting strongly affected thermal properties and crystallinity of PLA-g-IA. This study assesses the rate of crystallization and the effect of annealing on the crystallinity of PLA-g-IA using thermally resolved X-ray scattering and differential scanning calorimetry.

Methodology

Materials

Poly (L-lactic acid) (PLA polymer 3051D) in pellet form was purchased from Nature Works. Analytical grade itaconic anhydride (IA), dicumyl peroxide (DCP), chloroform, acetone, potassium hydroxide, hydrochloric acid and phenolphthalein were purchased from Sigma Aldrich and were used as received.

Extrusion

Itaconic anhydride (IA) and dicumyl peroxide (DCP) were dissolved in 20 mL dehydrated acetone and mix with PLA. After the acetone was evaporated completely, the mixtures were compounded using a LTE-20-44 twin-screw co-rotating extruder with a L/D of 44:1 and a screw diameter of 20 mm. The formulations of grafted PLA are listed in Table 1. The barrel temperature was set to 145, 145, 165, 165, 180, 180, 180, 180, 160, 160, 155 °C and the screw speed was maintained at 100 rpm. A vacuum pump was connected to the vent at the 7th heating zone on the barrel to remove vapor generated during extrusion. The extrudate was collected in a water bath and pelletized. Pellets were dried in a convection oven at 80 ^{o}C for 12 h before further analysis. The residence time in the extruder, under this conditions for this study, is 160 s.

Purification

About 2.5 g grafted PLA was dissolved in 40 mL chloroform, and 0.75 mL hydrochloric solution in water (1 M) was added to hydrolyze the anhydride groups into carboxylic acids. The solution was stirred vigorously for 30 min at room temperature. The grafted sample was further purified by drop wise precipitating into cold methanol (200 mL) to remove any homo- and copolymers of IA. A white sponge of filtered precipitate was collected and washed with methanol and distilled water several times and dried in vacuum oven for 24 h. Samples were analysed in triplicate.

Degree of grafting

Purified PLA-g-IA (0.4 g) was dissolved in 20 mL chloroform and titrated to a phenolphthalein end-point using potassium hydroxide in methanol (0.04 M). The grafted sample was completely soluble and did not precipitate during titration.The degree of grafting was calculated using Equation 1.

$$\% \, IA = \frac{N_{KOH}V_{KOH}}{2W_{sample}} \times 130.099 \, \frac{g}{mol} \times 100 \tag{1}$$

where N_{KOH} is the normality (moles per equivalent) of the KOH solution V_{KOH} is the volume (liters) and W_{sample} is the sample mass (grams).

Intrinsic viscosity

The intrinsic viscosity of PLA and grafted PLA were determined by dissolving the polymer in chloroform to concentrations between 0.88 and 8.28 g/dL at a constant temperature of 20 $^{\circ}$C. A Ubbelohde viscometer (Type 1B) was used partially submerged in a temperature controlled water bath. The elution time of the solvent was determined and used to calculate the relative viscosity of each sample for each concentration. The intrinsic viscosity was obtained by extrapolating a plot of concentration vs. relative viscosity to zero concentration.

Table 1: Formulations of grafted PLA

Samples	DCP (wt%)	IA (wt%)	Grafting content (%)	Intrinsic Viscosity (dL/g)	*Molecular weight
PLA	0	0	0	0.63	26 420
PLA-2-IA	0.75	2	0.37	0.57	23 200
PLA-3-IA	0.75	3	0.41	0.55	22 148
PLA-4-IA	0.75	4	0.45	0.47	18 059
PLA-5-IA	0.75	5	0.48	0.36	12 773
PLA-6-IA	0.75	6	0.61	0.33	11 408

* From Mark Houwink equation, using $[\eta] = 2.48 \times 10^{-4} MW^{0.77}$ [31]

Differential Scanning Calorimetry

Differential scanning calorimetry (DSC) was conducted using a DSC 8500 from Perkin Elmer. The specimens (weight approximately 10 mg) were crimp sealed in 30 μ L aluminium pans and run under constant nitrogen purge gas. Thermal history was removed by heating specimens from 0 to 200 ^{o}C at 10 ^{o}C/min, holding for 10 minutes at 250 ^{o}C, followed by cooling to 0 ^{o}C (50 ^{o}C/min). During the first heating cycle, no exothermic peaks were observed between 180-250 ^{o}C, indicating that the grafting reaction was complete (data not presented). The difference between unpurified and purified PLA-g-IA was also considered, and it was found that the DSC curve of purified samples was similar to unpurified; therefore data of unpurified samples were presented. For annealing, samples were heated to the specified crystallization temperature (T_a), and maintained at this temperature for one hour before finally being heated 200 ^{o}C. Annealing temperatures used were 80, 100, 110, 120 and 130 °C.

X-ray diffraction

Isothermal crystallization was carried out using a PANalytical Empyrean X-ray diffractometer at 45kV and 40mA using CuK$_{\alpha 1}$ radiation. Powdered samples were mounted in an Anton Paar CHC Plus chamber with air cooling and scanned between 25 – 200 ^{o}C in 10 ^{o}C increments, controlled by an Anton Paar TCU 110 temperature control unit. The diffraction data was collected in the 2θ range from 5° to 40° with a step size of 0.0131^{o}. A soller slit of 0.04 rad was used, with a fixed 7.5 mm anti-scatter slit. A fixed temperature profile was used to ensure complete removal of thermal history, prior to annealing. Specimens were heated to 200 ^{o}C and immediately cooled to 25 ^{o}C and scanned. Samples were then heated to the annealing temperature (80, 90, 100, 110, 120 and 130 ^{o}C) and scanned every 5 minutes over a 60 minute

isothermal period. After annealing, samples were heated to 200 ^{o}C, cooled 25 ^{o}C to repeat the annealing procedure.

Lattice spacing was calculated using Bragg's law:

$$2dsin\theta = n\lambda \qquad (2)$$

where λ is the wavelength (1.542) and n is positive integer (n = 1).

Results and Discussions

Effect of grafting before annealing

The effect of grafting before annealing (25 ^{o}C isotherm) on the crystallization temperature (T_c) and melting temperatures of PLA (T_mI and T_mII) are shown in Figure 1. These values were obtained from the second DSC scan at different IA concentrations (Table 1). PLA and grafted PLA showed a broad crystallization peak while the double melting peak at around 110 ^{o}C and 135-155°C was barely visible for pure PLA. Multiple melting peaks are typically observed in semi-crystalline polymers due to melt-recrystallization, and for PLA, corresponds to melting of initial lamellae and that of thicker, more perfected crystals formed during heating.[27] It would appear that grafting made this phenomenon a little more prevalent, even before annealing.

Grafting increased the crystallization temperature from 106 ^{o}C (PLA) to 110-116 ^{o}C as the result of increased chain interaction, making it more difficult for these chains to disentangle from each other to crystallize. Grafting also reduced T_m possibly due to IA forcing PLA to form thinner, less perfect crystals that melt at lower temperatures. Imperfect crystals also could be due to poor folding of grafted PLA due to the bulky

121

IA groups attached to the polymer backbone. A higher degree of grafting (higher IA concentrations) led to a greater reduction in T_m, indicating increased disruption to the regularity of PLA crystals.

Side reactions during grafting process, such as chain scission and crosslinking are common, in which excessive chain scission usually leads to lower molecular weight and poor mechanical performance of the polymer while crosslinking may lead to an insoluble polymer. A reduction in molecular weight was observed after grafting, (Table 1). A lower molecular weight would introduce more chain ends that could disrupt crystal structures, leading to a lower melting point [32] as well as increase chain mobility, [33, 34] allowing chains to rearrange into an ordered state more easily by diffusing to lamella growth fronts [35]. This would increase the rate of crystallization. Other work have shown that a graft copolymer can show an increase in the rate of crystallization despite chain irregularities introduced by the grafted monomer [16, 33, 36-38].

In our previous study, grafted PLA has slighty better crystallinity than PLA accompanied by improved thermal decomposition temperature and mechanical properties. Therefore, annealing was conducted in order to further improve the crystallization rate of grafted PLA.

Annealing

Generally, PLA changes its physical properties when annealed at temperatures below the melting point. During annealing between the T_g and T_m, PLA chains can reorganize into a state of lower free energy [22]. Chains with high mobility can rearrange into an ordered state by moving to lamella growth fronts, leading to more

uniform lamellae and regular fold-surfaces [35]. Crystals also eventually thicken and increase in size with longer annealing time, resulting in more ordered crystals [22].

DSC traces of PLA annealed for 1 hour at different temperatures (T_a) are shown in Figure 1. When PLA was annealed at 80 ^{o}C, crystallization was incomplete, resulting in a broad exothermic peak in the subsequent heating scan (ΔH_c =1.92 J/g), not evident in Figure 1 because of scale. When annealed at higher temperatures, the crystallization peak decreased and was absent at higher T_a (120-130 ^{o}C) and is consistent with other research [20, 23, 39].

Two melting peaks were observed when annealed at temperatures lower than 110 ^{o}C, merging into a single peak above 120 ^{o}C. The appearance of T_mI and T_mII depend on the annealing temperature, but the peak position also depends on annealing time (Figure 2). At 110 ^{o}C, T_mII never disappeared, but decreased in intensity over time, while only a single peak was observed at 120 ^{o}C after 60 minutes. If annealed at 130 ^{o}C, the single melting peak was at the highest temperature. Also evident from Figure 2, is the relative size of T_mI and T_mII; as the annealing temperature was increased, T_mII decreased in size relative to T_mI. (i.e. first melting peak increase as annealing temperature increased and peak temperature increased.)
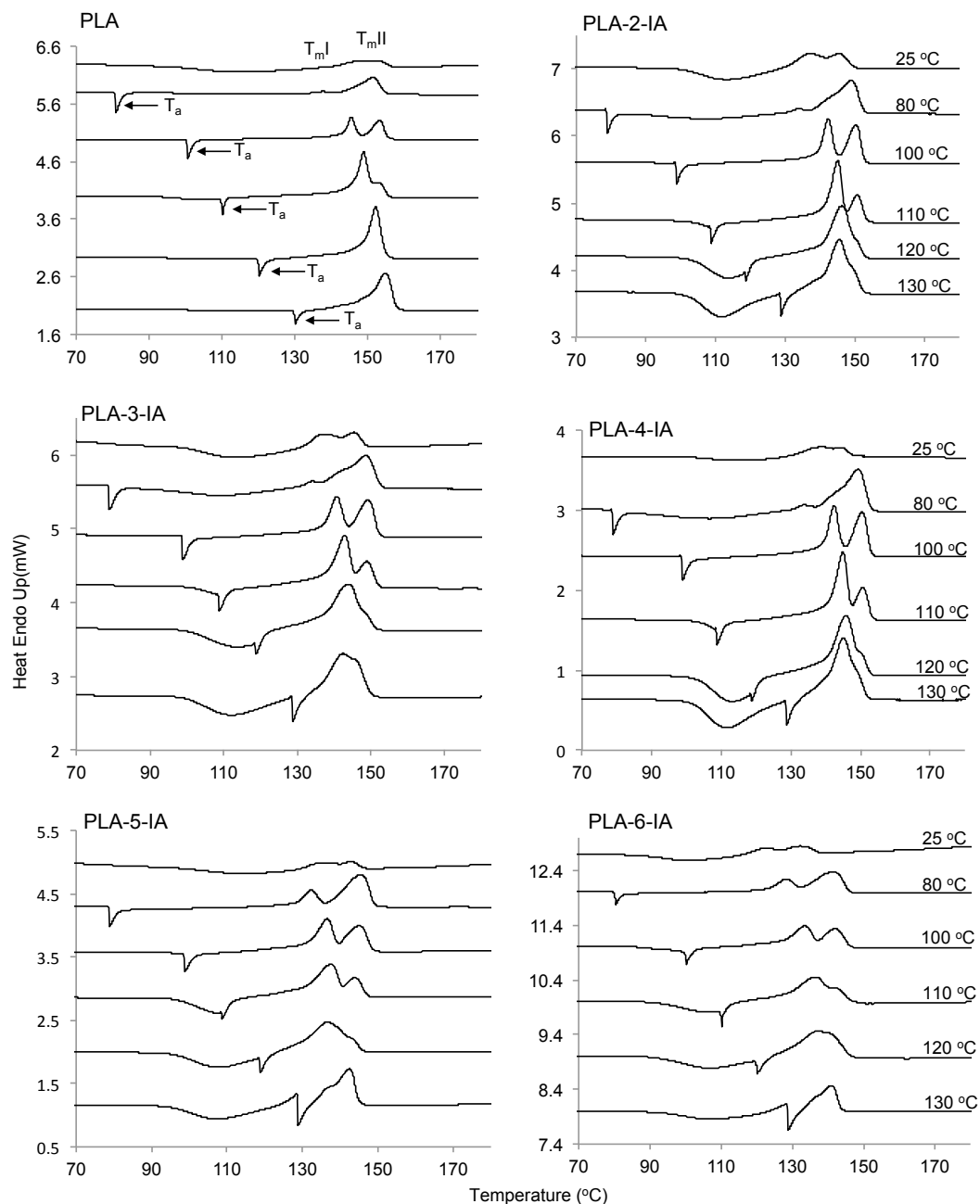
Figure 1: Melting endotherms of PLA and grafted PLA at different annealing temperatures for 1 hour.

The two melting peaks can be explained by melt-recrystallization in which T_mI corresponded to melting of crystals that were formed during annealing and T_mII that of crystals perfected during heating (melt-recrystallisation). When T_a increased to 100 -110 °C, more perfect crystals formed during annealing, evident from a higher melting

point (T_mI), but significant re-crystallization during heating still occurred (T_mII). At 120 - 130 ^{o}C, merging of these peaks indicates that crystallization was completed during annealing.
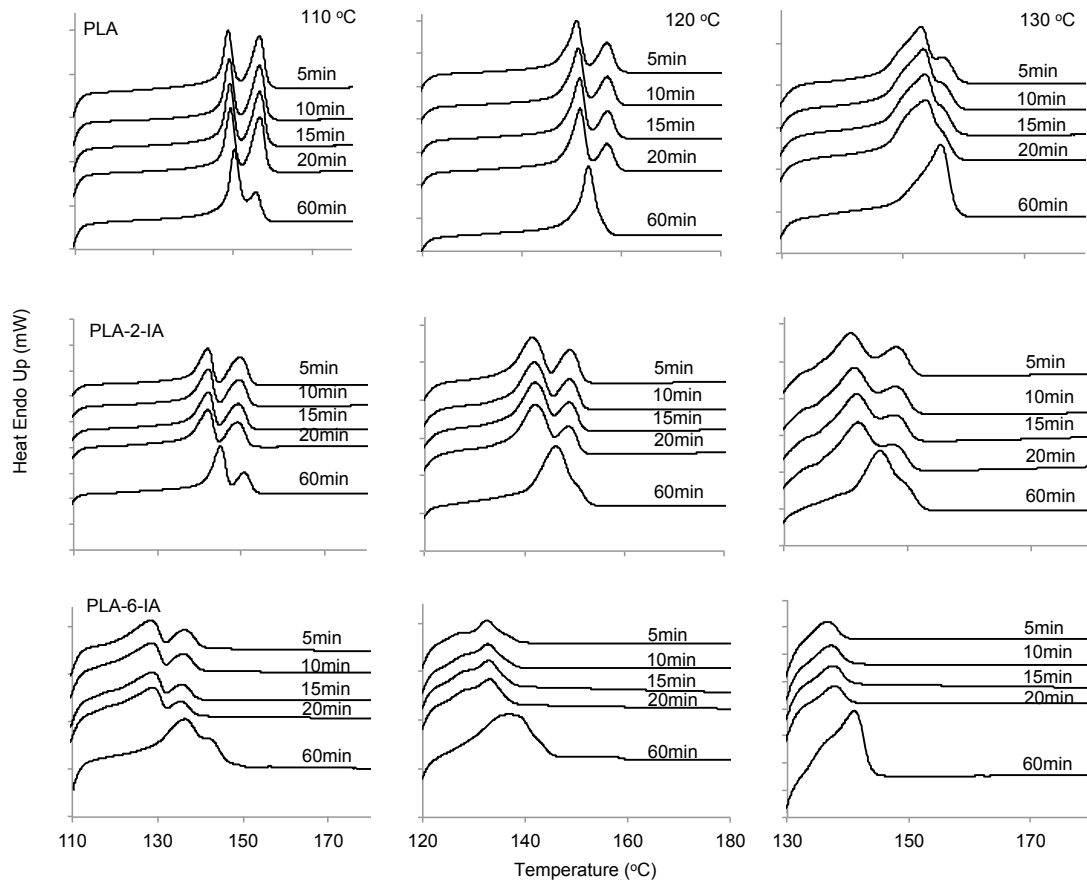

Figure 2: Heat flow of DSC curves at different annealing time temperature a) 110 ^{o}C, (b) 120 ^{o}C and c) 130 ^{o}C

Figure 3 shows the melting temperature and enthalpy of PLA versus annealing temperature. T_mI increased linearly with T_a while T_mII did not change much. It is evident that both melting peaks resolved into one at 110 ^{o}C. It has been suggested that a mixture of α' and α type crystals form in this region [40]. A similar observation was reported elsewhere which concluded that the peak profiles discretely changes at $T_c = 113$ ^{o}C and was ascribed to the difference in crystal structures [41]. It is expected

that the crystallinity or crystal size during annealing increases with increasing T_a ,[42] and as expected, ΔH_m increased almost linearly with T_a. The discontinuity at $T_c =$ 100 - 120 ^{o}C has been observed by others, and was it was postulated that the crystallization mechanism and crystal structure of PLA above and below this point may be different.
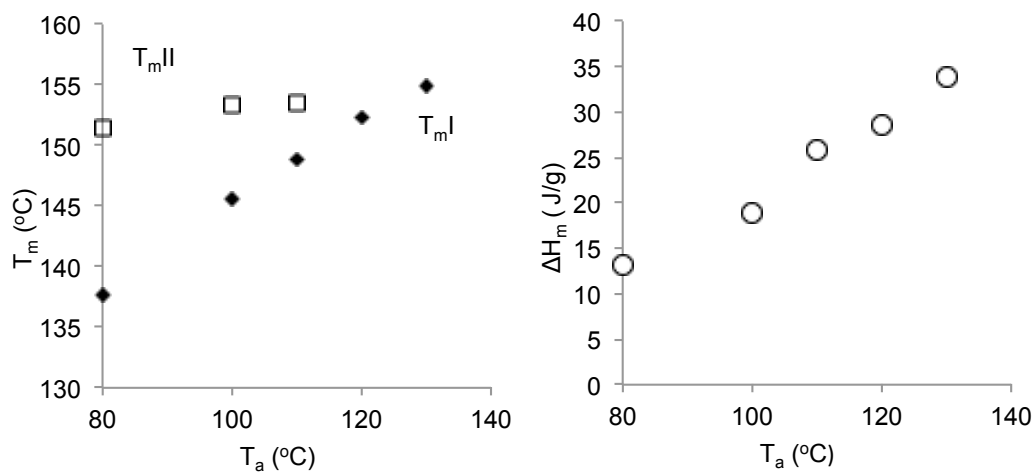

Figure 3: Relationship between T_m and ΔH_m with T_a

Effect of annealing on grafted PLA

In the case of grafted PLA, melt-recrystallization was much more pronounced, even at higher annealing temperatures. For annealing between 110 - 130 ^{o}C, crystallization was observed preceding annealing (T_c approximately 110 ^{o}C). Prolonged annealing scarcely affected crystal structure during a 60 minute annealing cycle (Figure 2); the relative size of T_mI and T_mII stayed approximately constant. However, at high annealing temperature, T_mII was significantly smaller, but never disappeared completely. At a higher degree of grafting (PLA-6-IA), the distinction between the two melting peaks was not as obvious and the melting point was also lower.

T_mI and T_mII versus annealing temperature is shown in Figure 4. The melting peaks did not resolve into one, as observed for PLA. As the annealing temperature

126

increased, T_mI increased but not linearly, as for PLA. T_mI reached a plateau at $T_a = 100\ °C$, while T_mII remained constant (although decreasing with increasing degree if grafting). For grafted PLA, it seems like the more perfected α-type crystal structure cannot be formed to the same extent as PLA.

An exothermic crystallization peak was not observed for PLA after annealing, however, grafted PLA showed significant crystallization preceding annealing, as the sample was heated (Figure 1). Grafting increased the crystallization temperature of PLA to higher temperature as a result of increased chain interaction. However, annealing at different temperatures for 1 hour improved the rate of crystallization of grafted PLA Considering the rate of crystallization of grafted PLA, annealing above $100\ °C$ it is not possible, as significant crystallization occurred at an annealing temperature of $100\ °C$.

Therefore, to calculate the crystallinity of grafted PLA, only values at $100\ °C$ was considered to avoid crystallization during heating. Table 2 showed the enthalphy and crystallinity of grafted PLA at $100\ °C$. After grafting, the enthalphy and crystallinity increased more than half than PLA. This suggested a heterogenous nucleation induced by IA. PLA is highly amorphous and grafting and anenaling probably resulted in acceleration in nucleation of the grafted samples. However, increasing in degree of grafting has slight effect on the enthalphy and final crystallinity.
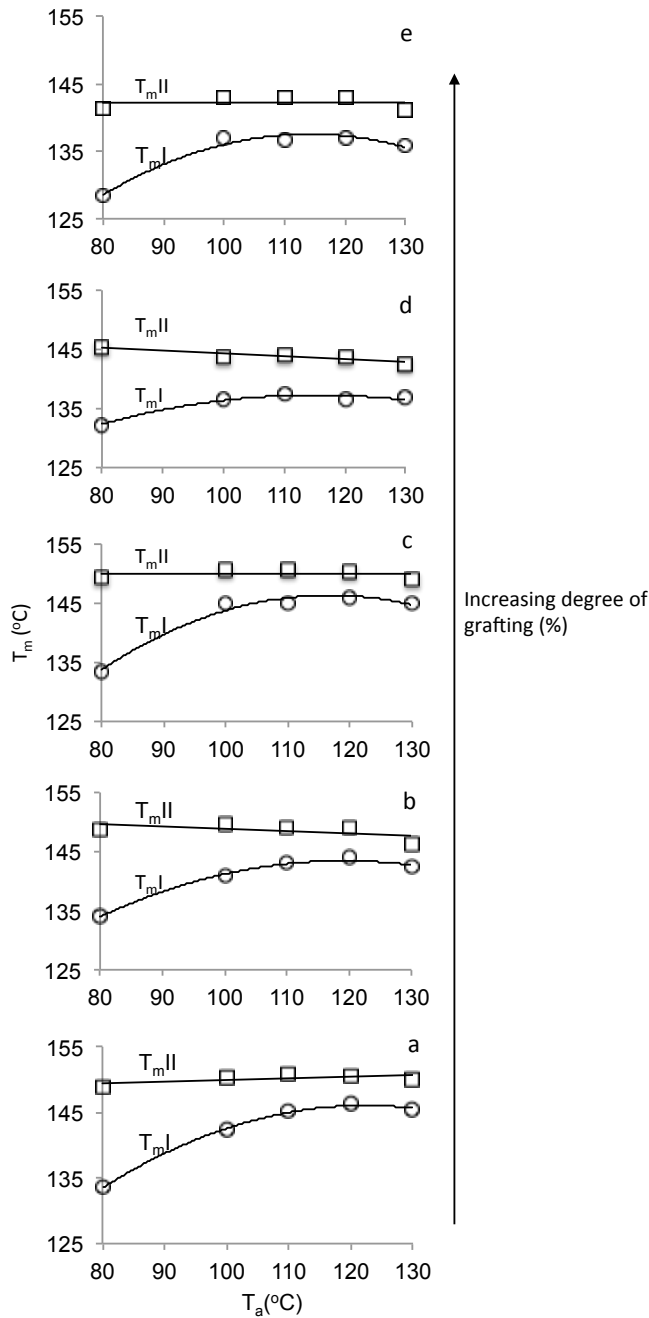
Figure 4: Effect of annealing temperature on melting temperature of grafted PLA (a) PLA-2-IA, (b) PLA-3-IA, (c) PLA-4-IA, (d) PLA-5-IA and (e) PLA-6-IA for 1 hour

It can be concluded that, for PLA, an annealing temperature of 130 $^{\circ}$C was sufficient to obtain maximum crystallinity in PLA. In contrast, for grafted PLA, it is sufficient to conduct the annealing at 100 -110 $^{\circ}$C. It is evident that different types of crystals were formed during heating and annealing and for grafted PLA could not be fully

converted into the, presumably, more ordered α-form crystals. This was confirmed after extending annealing of PLA-6-IA to 120 minutes. At 120 and 130 $^{\circ}$C, PLA-6-IA show similar behaviour and it was thought that 60 minutes was sufficient for annealing grafted PLA.

Plots of relative crystallinity versus time for PLA and grafted PLA are shown in Figure 5. The process of crystallization during annealing for grafted PLA was considered only at an annealing temperature of 100 $^{\circ}$C to avoid crystallization before annealing. X_t is the relative crystallinity at a given time, and is calculated from the integrated area of the DSC curve during annealing from t = 0 to t divided by the total area (Equation 4 and 5).

$$X_t = \frac{\int_0^t \frac{dH}{dt} dt}{\int_0^\infty \frac{dH}{dt} dt} \tag{3}$$

where the first integral represents the heat generated at time t, while the second integral represents the total heat generated up to the end of the crystallization process. By dividing the areas of isothermal DSC curves, the following equation is obtained;

$$X_t = \frac{A_t}{A_\infty} \tag{4}$$

The kinetics of crystallization was analysed using well known Avrami equation:

$$X_t = 1 - \exp(-kt^n) \; or \; \ln\left[-ln\left(1 - X(t)\right)\right] = n \ln t + \ln k \tag{5}$$

where k is the crystallization kinetic constant for nucleation and growth, and n is the Avrami exponent reflecting the mechanism of nucleation and growth. By plotting $\ln[-\ln(1-X_t))]$ versus $\ln t$, the Avrami exponent, n, and the logarithm of kinetic constant, $\ln k$ can be determined.
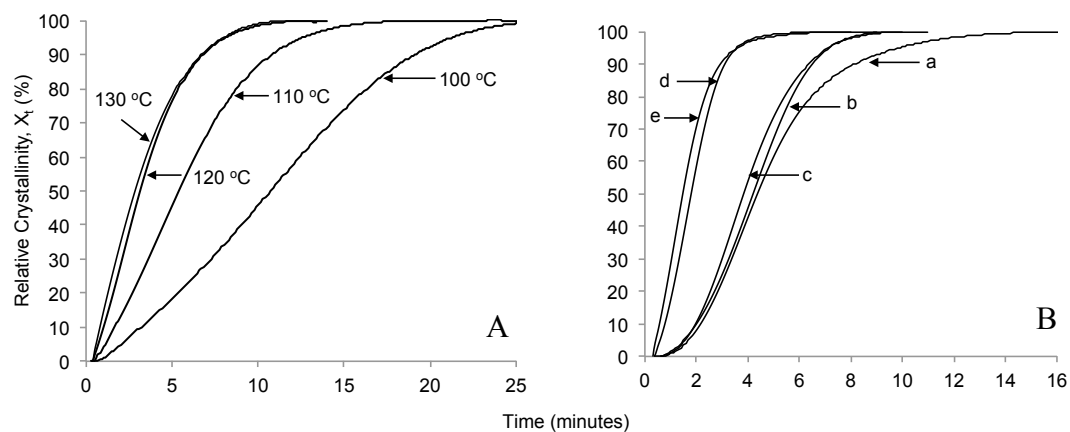

Figure 5: Plots of relative crystallinity as a function of crystallization time for (A) PLA at different temperature and (B) grafted PLA at 100 °C; (a) PLA-2-IA, (b) PLA-3-IA, (c) PLA-4-IA, (d) PLA-5-IA and (e) PLA-6-IA

For PLA, the rate of crystallization increased with temperature and at 130 °C, crystallinity was double that at 100 °C (time to reach 50% crystallinity, Table 2). For grafted PLA annealed at 100 °C, an increase in IA concentration (i.e. higher degree of grafting) increased the rate of crystallization significantly. At low degree of grafting (PLA-2-IA) the time to reach 50% crystallinity was 4.4 minutes while at higher degree of grafting (PLA-6-IA), it was only 1.5 minutes. A large effect on crystallization rate after grafting was observed, evident from the crystallization half time between PLA and PLA-2-IA. The half time of PLA-2-IA was reduced significantly, despite a small reduction of molecular weight (12.8% reduction)

suggesting that grafting had a bigger influence on crystallization rate than chain scission.

The Avrami equation describes how solids transform from one phase to another at constant temperature. It generally considered that the value of n = 0 corresponds to instantaneous or heterogeneous nucleation and 1 to sporadic or homogeneous nucleation. A value of 2 or 3 represents axialites (two dimensional lamellar aggregates) and spherullites (three dimensional aggregates of radial lamellae), respectively. Figure 6 displays the typical Avrami double-logarithmic plots for PLA and grafted PLA annealed at 100 ^{o}C.

The Avrami parameters n and ln$k$ were obtained from the plots with slope n and intercept ln (k) (Table 2). For grafted PLA,the crystallization rate was increased, induced by homogenous nucleation and crystal growth (n >2), producing a two dimensional microstructure. This led to a higher degree of crystallinity and different crystal structure of grafted PLA (discussed in the next section). Crystallization rate generally increase with increased degree of grafting evident from a significant reduction in $t_{1/2}$ (Table 2). However, the formation of new nuclection sites was limited, as the value of n remained less than 3. The value of n would be expected to increase from 2 to 3 if the the nucleation sites increased, indicating a transformation of two dimensional structures to three dimensional structures.

It has been suggested that k is temperature dependant following the Arrhenius equation [43]. Therefore, a decresase in ln(k) would suggest a decrease in activation energy. The results were separated into three groups (Figure 6); PLA, low to medium degree of grafting and those with a higher degree of grafting. Those with a high degree of grafting also had the most significant chain scission. One would thefore

conclude that grafting did reduce the activation energy, but as chain scission became more significant, the effect of shorter chains on the rate of crystallization was more important.

Table 2: Crystallization half times, ΔH_m, X_c, and Avrami constant (n, ln (k) and R values) of PLA and grafted PLA at 100 $^{\circ}$C

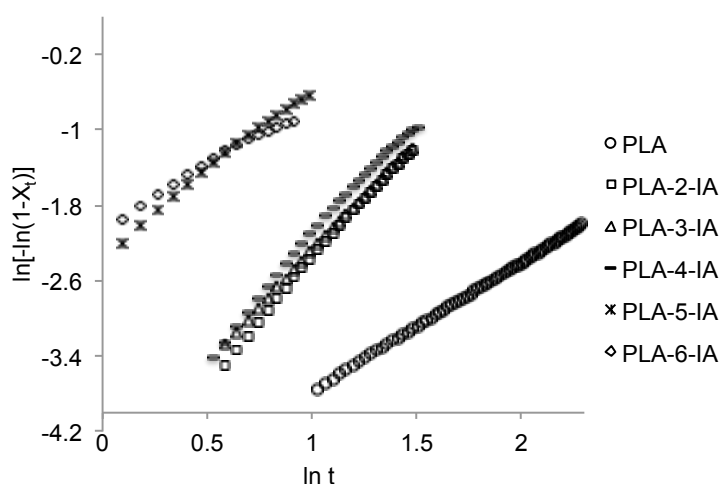| Sample	t ½(minutes)	ΔH_m (J/g)	X_c (%)	n	ln (k)	R values
PLA	10.7	19.04	27.7	1.39	-5.21	0.9987
PLA-2-IA	4.4	40.07	43.09	2.52	-4.93	0.9954
PLA-3-IA	4.2	40.75	43.82	2.41	-4.71	0.9915
PLA-4-IA	3.8	40.29	43.33	2.43	-4.62	0.9879
PLA-5-IA	1.7	42.68	45.9	2.22	-2.48	0.9933
PLA-6-IA	1.5	41.78	44.9	1.91	-2.16	0.9920

Figure 6: Avrami plot of PLA and grafted PLA at 100 $^{\circ}$C

Wide Angle X-ray Scattering (WAXS)

The WAXS diffraction patterns of PLA and grafted PLA at different T_a, annealed for 1 hour are shown in Figure 7. For grafted PLA, similar diffraction patterns were observed for all samples, therefore only the highest grafting degree is shown. The thermal history of samples was removed in order to observe the crystallization behavior at different temperature during annealing. For comparison, all the diffraction patterns given are normalized using the strongest peak corresponding to the (110/200) plane. Indexing of the observed diffractions is based on the crystal structure of α form of PLA [8, 40, 44].

PLA showed seven diffraction peaks, evident from the enlarged diffractogram (Figure 8). A small peak that represent the (110/200) plane appeared at 80 ^{o}C and a peak corresponding to the (203) plane appeared at 90 ^{o}C. A peak representing the (010) plane appeared above 100 ^{o}C. With increasing T_a, all the peak intensities increased dramatically. The transformation of crystal structure from α' to α form can be concluded from the appearance of five characteristic peaks in the α form (above 100 ^{o}C). This results are in good agreement with other research that report growth of α' crystals at low T_c and α modification at high T_a [40, 45]. At a glance, the WAXS pattern of the α' form (100-110 ^{o}C) is similar to the α form, but differ in intensity. The presence of the α-form at 120-130 ^{o}C, as observed using DSC, was confirmed using WAXS and will be discussed in the next section.
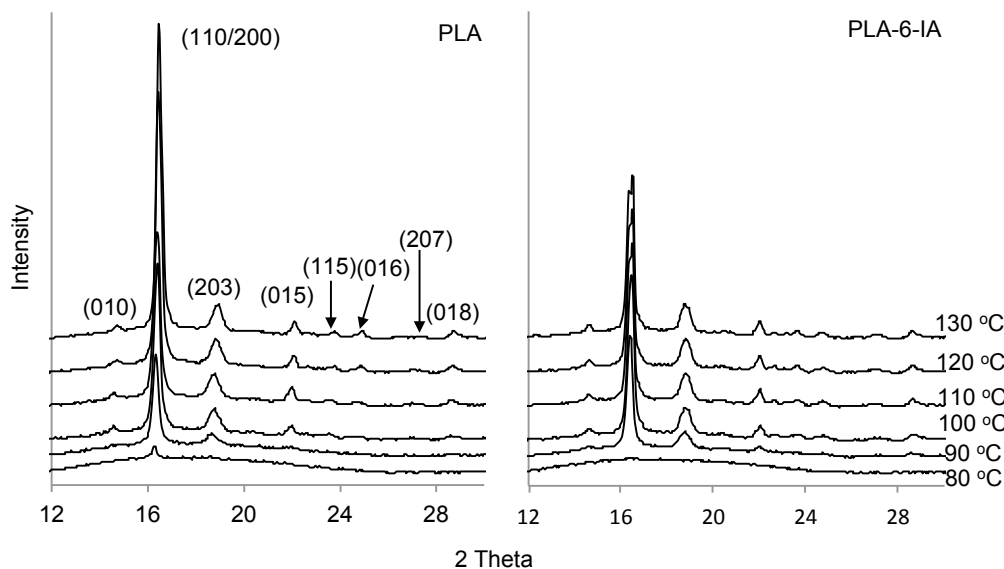
Figure 7: X-ray diffraction profile of PLA and grafted PLA obtained after annealing for 1 hour at different T_a.

For grafted PLA, no peaks were detected at $T_a = 80$ ^{o}C. At 90 ^{o}C, four main peaks were observed and at 100 ^{o}C, a diffraction peak appeared at $2\theta = 26.9^o$ that represents the (207) plane. This peak formed much faster in grafted samples, probably because of increasing rate of crystallization as observed in previous section. Figure 9 shows the effect of grafting on XRD diffractrograms for PLA and grafted PLA at 130 ^{o}C. The peaks corresponding to the (203), (015), (115),(016) (207) and (018) shifted to a slightly lower angle after grafting. This may be explained by inclusion of the bulky IA groups onto PLA backbone expanding the helical structure of PLA.

By considering the molecular weight of semi-crystalline PLA is approximately 26 420 g/mol, the degree of polymerization can be estimated to be around 203. This gives an average of 1 IA molecule for every 123 PLA repeat units (by considering the grafting content is 0.61%). However, grafting is random and a variation in this number is expected around this average. The occurrence of this random pendant group is what disrupts the crystal lattice of PLA.
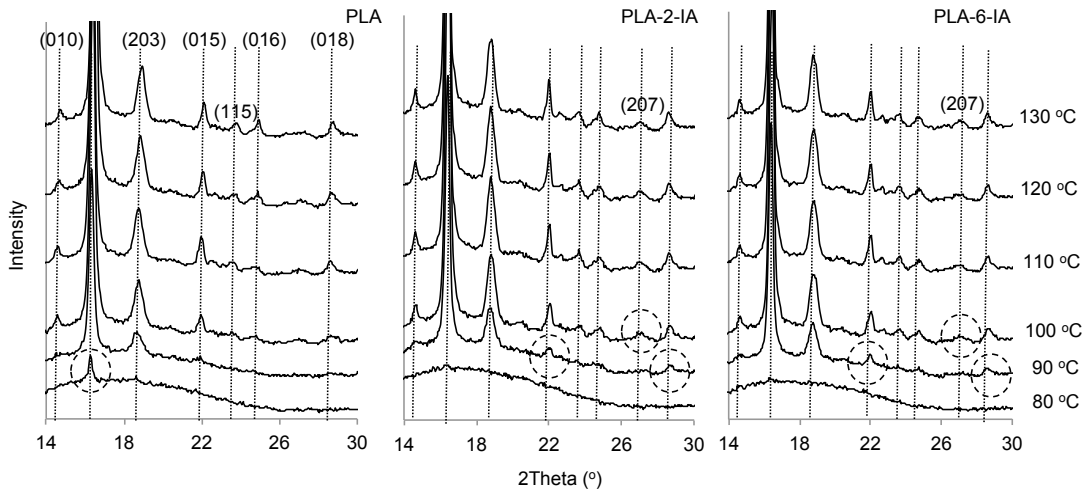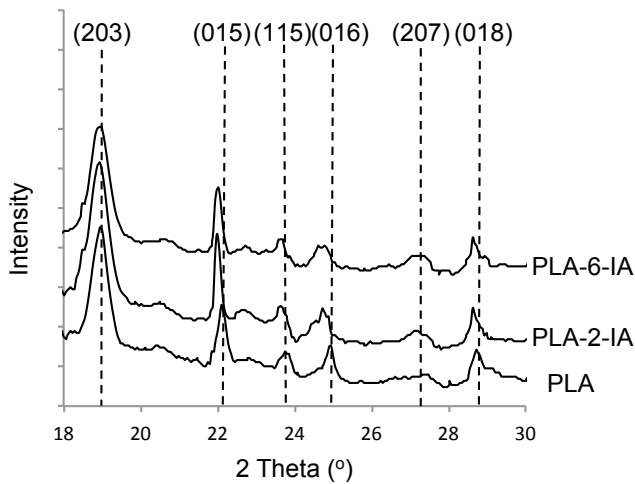
134

Figure 8: Enlarged diffractograms

Figure 9: Enlarged diffractrograms of PLA and grafted PLA at 130 ^{o}C

A closer examination of diffraction intensities at the strongest peak corresponding to the (110/200) plane was carried out in order to observe the differences in crystal structure and is shown in Figure 10. The diffraction angles of the main peak at 90 ^{o}C are marked by dotted lines as a reference to distinguish the shift in the diffraction angle. For PLA, as T_a increased, the peak at 100-110 ^{o}C shifted to slightly higher angles. This indicated that crystals formed at these annealing temperatures are different compared with those formed at $T_c<100$ and $T_c>110$. At 120-130 ^{o}C, the peaks shifted to an even higher angle indicating a more compacted chain structure and

a transformation from the α' to α form crystal structure. Similar observations were obtained elsewhere [11, 45]. This behavior was confirmed in the lattice spacing calculated from the strongest diffraction peak at different T_a, as shown in Figure 11 using Bragg's law.
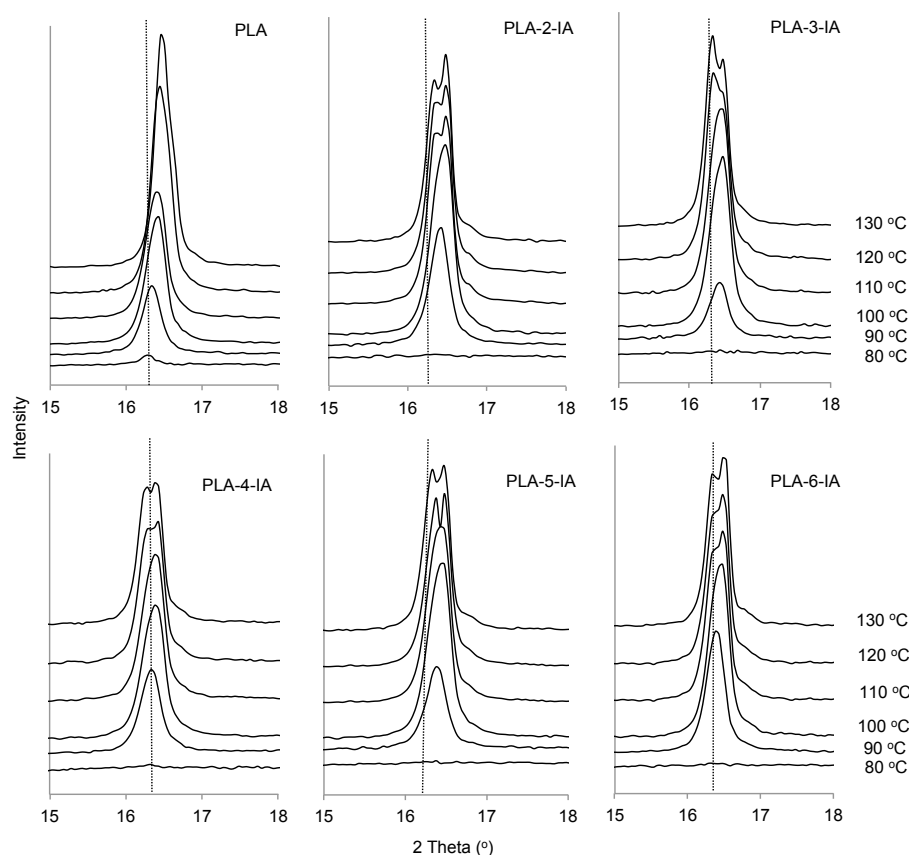

Figure 10: Enlarge diffraction peaks at (110/200)

Diffraction at the (110/200) plane also shifted to higher angles for grafted samples, but also split into two peaks above an annealing temperature of 100 °C. In consideration of grafted PLA could not be converted to more ordered α-form crystals at higher temperature, the appearance of two peaks suggests a different crystal lattice spacing obtained for grafted samples, where the first peak was at a slightly lower angle and the second peak similar to annealed PLA. This suggests a larger lattice

spacing due to incorporation of bulky itaconic anhydride, as schematically indicated in Figure 12.
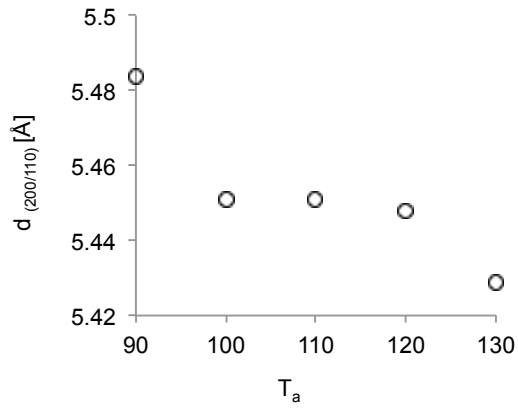

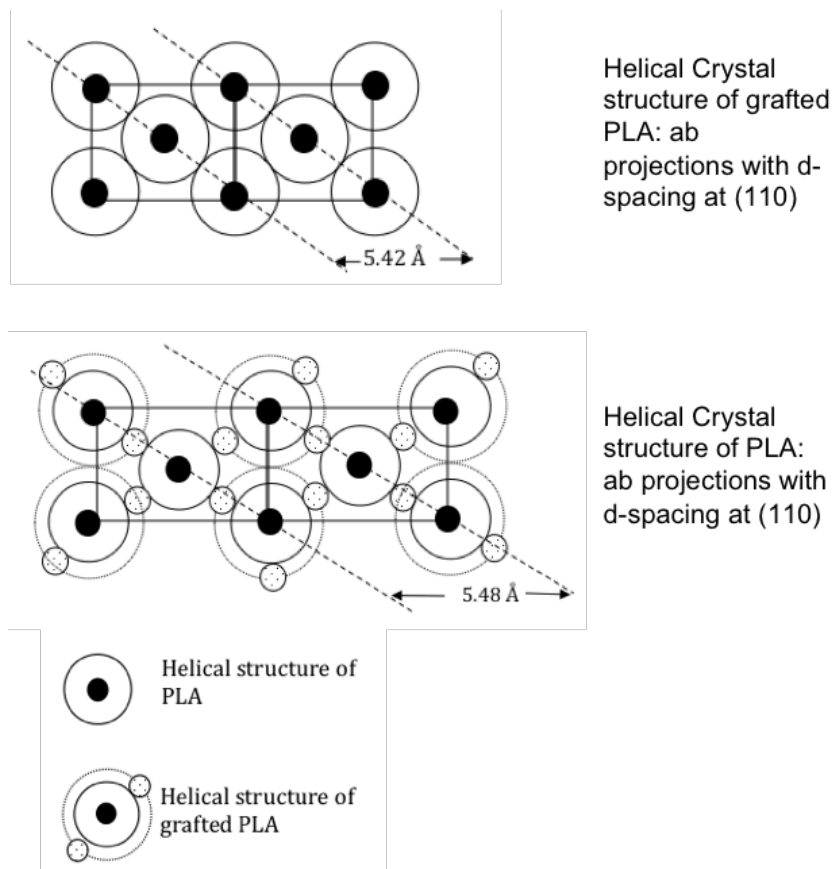Figure 11: Lattice spacing of PLA at different T_a

Figure 12: Illustration of crystal structure of PLA and grafted PLA at ab projections with d-spacing at (110) at 130 °C

The appearance of the five peaks representing the α-form is time dependent and differ for PLA and grafted PLA (Figure 12). For PLA, they are fully formed after 30 minutes annealing, while for grafted PLA (PLA-6-IA), 15 minutes were enough. This would suggest a higher crystallization rate for grafted PLA, supporting previous DSC results. It was thought that the chain conformation after grafting and during annealing are affecting this behavior. Grafted PLA increased the lattice spacing and free volume during annealing, allowing them to crystallize faster.
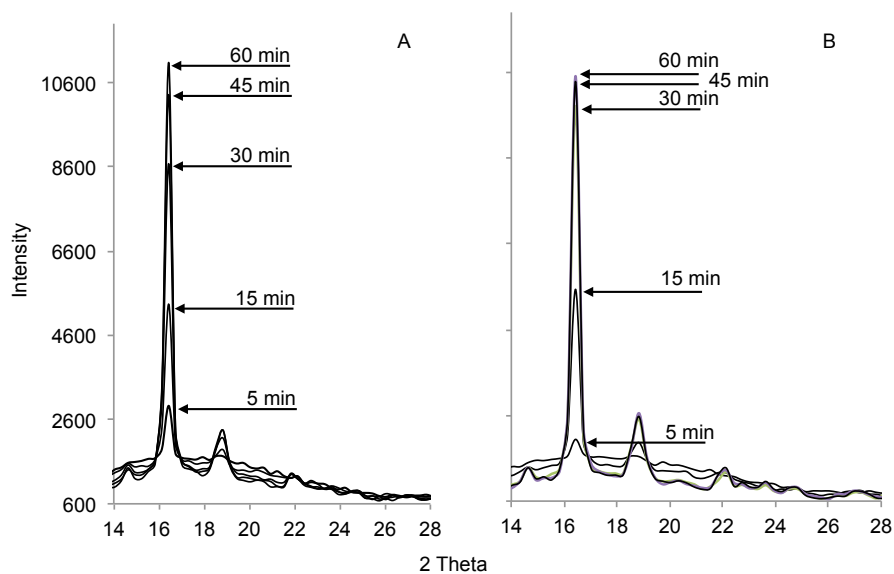

Figure 12: X-ray diffraction patterns of PLA(A) and PLA-6-IA(B) at different annealing time at 100 $^{\circ}$C.

138

Conclusion

In this work, the effect of annealing on PLA at different crystallization temperatures was investigated using DSC and WAXS. Annealing at 130 $^{\circ}$C for 1 hour changed the α'-crystal to α-form while a mixture of both types crystals was obtained for grafted PLA. Incorporation of bulky IA groups increased the rate of crystallization of PLA with increasing in degree of grafting but limits the formation of a larger and more compacted crystals, evident from lower melting point of grafted PLA. Grafted PLA had a more extended helical conformation and a slightly increased lattice spacing. The grafted PLA was thought to crystallize faster due to increase in the lattice spacing and free volume as a result of grafting.

References

1. Hwang, S.W., et al., *Grafting of maleic anhydride on poly(L-lactic acid). Effects on physical and mechanical properties.* Polymer Testing, 2012. **31**(2): p. 333-344.

2. Ma, P., et al., *Melt Free-Radical Grafting of Maleic Anhydride onto Biodegradable Poly (lactic acid) by Using Styrene as A Comonomer.* Polymers, 2014. **6**(5): p. 1528-1543.

3. Hwang, S.W., et al., *Effect of Maleic‐Anhydride Grafting on the Physical and Mechanical Properties of Poly (L‐lactic acid)/Starch Blends.* Macromolecular Materials and Engineering, 2012: p. 624-633.

4. Takeshita, H., et al., *Crystallization and higher-order structure of multicomponent polymeric systems.* Polymer, 2013. **54**(18): p. 4776-4789.

5. Ratta, V., *Crystallization, morphology, thermal stability and adhesive properties of novel high performance semicrystalline polyimides*, 1999, Virginia Polytechnic Institute and State University.

6. De Santis, P. and A.J. Kovacs, *Molecular conformation of poly(S-lactic acid).* Biopolymers, 1968. **6**(3): p. 299-306.

7. Wasanasuk, K. and K. Tashiro, *Crystal structure and disorder in Poly(l-lactic acid) δ form (α′ form) and the phase transition mechanism to the ordered α form.* Polymer, 2011. **52**(26): p. 6097-6109.

8. Di Lorenzo, M.L., M. Cocca, and M. Malinconico, *Crystal polymorphism of poly(l-lactic acid) and its influence on thermal properties.* Thermochimica Acta, 2011. **522**(1–2): p. 110-117.

9. Pan, P., et al., *Effect of crystallization temperature on crystal modifications and crystallization kinetics of poly(L-lactide).* Journal of Applied Polymer Science, 2008. **107**(1): p. 54-62.

10. Kawai, T., et al., *Crystallization and Melting Behavior of Poly (l-lactic Acid).* Macromolecules, 2007. **40**(26): p. 9463-9469.

11. Pan, P., et al., *Polymorphic Transition in Disordered Poly(l-lactide) Crystals Induced by Annealing at Elevated Temperatures.* Macromolecules, 2008. **41**(12): p. 4296-4304.

12. Sanchez, I.C. and R. Eby, *Crystallization of random copolymers.* J Res Natl Bur Stand Sect A, 1973. **77**(3): p. 353-358.

13. Sanchez, I. and R. Eby, *Thermodynamics and crystallization of random copolymers.* Macromolecules, 1975. **8**(5): p. 638-641.

14. Tang, Z., et al., *The crystallization behavior and mechanical properties of polylactic acid in the presence of a crystal nucleating agent.* Journal of Applied Polymer Science, 2012. **125**(2): p. 1108-1115.

15. Jiang, X., et al., *Effect of nucleating agents on crystallization kinetics of PET.* Express Polym Lett, 2007. **1**(4): p. 245-251.

16. Saeidlou, S., et al., *Poly(lactic acid) crystallization.* Progress in Polymer Science, 2012. **37**(12): p. 1657-1677.

17. Huneault, M.A. and H. Li, *Morphology and properties of compatibilized polylactide/thermoplastic starch blends.* Polymer, 2007. **48**(1): p. 270-280.

18. Liang, W. and X. Zhong, *Effect of a novel nucleating agent on isothermal crystallization of poly (L-lactic acid).* Chinese Journal of Chemical Engineering, 2010. **18**(6): p. 899-904.

19. Mohamed, E.-H.A., *The effect of annealing treatments on spherulitic morphology and physical ageing on glass transition of poly lactic acid (PLLA).* Materials Sciences and Applications, 2011. **2**: p. 439.

20. Srithep, Y., P. Nealey, and L.-S. Turng, *Effects of annealing time and temperature on the crystallinity and heat resistance behavior of injection-molded poly(lactic acid)*. Polymer Engineering & Science, 2013. **53**(3): p. 580-588.

21. Wei, Z., et al., *Insight into the annealing peak and microstructural changes of poly(l-lactic acid) by annealing at elevated temperatures*. Polymer, 2013. **54**(13): p. 3377-3384.

22. Fischer, E., *Effect of annealing and temperature on the morphological structure of polymers*. Pure and applied chemistry, 1972. **31**(1-2): p. 113-132.

23. Carrasco, F., et al., *Processing of poly(lactic acid): Characterization of chemical structure, thermal stability and mechanical properties*. Polymer Degradation and Stability, 2010. **95**(2): p. 116-125.

24. Mallet, B., K. Lamnawar, and A. Maazouz, *Improvement of blown film extrusion of poly(Lactic Acid): Structure–Processing–Properties relationships*. Polymer Engineering & Science, 2014. **54**(4): p. 840-857.

25. Luo, Y., et al., *Polylactide foams prepared by a traditional chemical compression-molding method*. Journal of Applied Polymer Science, 2013. **130**(1): p. 330-337.

26. Mihai, M., et al., *Extrusion Foaming of Semi-Crystalline PLA and PLA/Thermoplastic Starch Blends*. Macromolecular Bioscience, 2007. **7**(7): p. 907-920.

27. Pantani, R., et al., *Crystallization kinetics of virgin and processed poly(lactic acid)*. Polymer Degradation and Stability, 2010. **95**(7): p. 1148-1159.

28. Hébert, J.-S., et al., *Morphology of polylactic acid crystallized during annealing after uniaxial deformation*. Journal of Polymer Science Part B: Polymer Physics, 2013. **51**(6): p. 430-440.

29. Bai, H., et al., *New insight on the annealing induced microstructural changes and their roles in the toughening of β-form polypropylene*. Polymer, 2011. **52**(10): p. 2351-2360.

30. Fang, K., et al., *Properties and morphology of poly(lactic acid)/soy protein isolate blends*. Journal of Applied Polymer Science, 2009. **114**(2): p. 754-759.

31. Witte, P.v.d., et al., *Phase behavior of polylactides in solvent-nonsolvent mixtures*. Journal of Polymer Science, Part B: Polymer physics, 1996. **34**(15): p. 2553-2568.

32. Nakaruku, C., *Effects of Molecular Weight on the Melting and Crystallization of Poly(L-lactic acid) in a Mixture with Poly(ethylene oxide)*. Polym J, 1996. **28**(7): p. 568-575.

33. Subramaniam, C., *Morphology, crystallization and melting behaviors of random copolymers of ethylene with 1-butene, 1-pentene and 1-hexene*, 1999, Virginia Polytechnic Institute and State University.

34. Legras, R., J. Mercier, and E. Nield, *Polymer crystallization by chemical nucleation*. Nature, 1983. **304**: p. 432-434.

35. Hsu, S.-T. and Y.L. Yao, *Effect of Film Formation Method and Annealing on Morphology and Crystal Structure of Poly (L-Lactic Acid) Films*. Journal of Manufacturing Science and Engineering, 2014. **136**(2): p. 021006.

36. Hwang, S.W., et al., *Effect of Maleic-Anhydride Grafting on the Physical and Mechanical Properties of Poly(L-lactic acid)/Starch Blends*. Macromolecular Materials and Engineering, 2013. **298**(6): p. 624-633.

37. Orozco, V.H., et al. *Preparation and Characterization of Poly (Lactic Acid)‐g‐Maleic Anhydride+ Starch Blends*. in *Macromolecular Symposia*. 2009. Wiley Online Library.

38. Wootthikanokkhan, J., et al., *Crystallization and thermomechanical properties of PLA composites: Effects of additive types and heat treatment*. Journal of Applied Polymer Science, 2013. **129**(1): p. 215-223.

39. Tabi, T., et al., *Crystalline structure of annealed polylactic acid and its relation to processing*. Express Polymer Letters, 2010. **4**(10).

40. Zhang, J., et al., *Disorder-to-order phase transition and multiple melting behavior of poly (l-lactide) investigated by simultaneous measurements of WAXD and DSC*. Macromolecules, 2008. **41**(4): p. 1352-1357.

41. Yasuniwa, M., et al., *Crystallization behavior of poly(l-lactic acid)*. Polymer, 2006. **47**(21): p. 7554-7563.

42. Yasuniwa, M., K. Iura, and Y. Dan, *Melting behavior of poly (L-lactic acid): Effects of crystallization temperature and time*. Polymer, 2007. **48**(18): p. 5398-5407.

43. Battegazzore, D., S. Bocchini, and A. Frache, *Crystallization kinetics of poly (lactic acid)-talc composites.* Express Polymer Letters, 2011. **5**(10): p. 849-858.

44. Sasaki, S. and T. Asakura, *Helix Distortion and Crystal Structure of the α-Form of Poly(l-lactide).* Macromolecules, 2003. **36**(22): p. 8385-8390.

45. Yasuniwa, M., et al., *Melting behavior of poly (l-lactic acid): X-ray and DSC analyses of the melting process.* Polymer, 2008. **49**(7): p. 1943-1951.

Chapter 8

Concluding Remarks

Concluding Remarks

NTP was blended with LLDPE and PBS with and without compatibilizers, using extrusion and injection moulding. Different types of compatibilizers such as PE-g-MAH, PEOX, and pMDI were used in blending NTP with these polymers. A novel compatibilizer, PLA-g-IA was successfully produced as a potential compatibilizer for NTP/PLA blends.

Generally, blending NTP with other polymers without adding any compatibilizers resulted in an immiscible blend with a mostly rough morphology and poor interfacial adhesion between the two very distinct phases of different polymers. The results were supported by two different T_gs. Addition of compatibilizers improved the adhesion and stabilized the morphology, leading to significant improvements in mechanical and thermal properties, as well as improved water resistance.

The objective to combine the best properties of two different polymers has been met by both LLDPE and PBS/NTP blends. For example, using LLDPE, the blend's elongation at break exceeded that of the raw polymers when using PE-g-MAH as a compatibilizer (at 20-30 % NTP). Increasing NTP content (for compatibilized blends) led to a reduction in mechanical properties, but never dropped below the properties of pure NTP. The hydrophobic nature of LLDPE also improved the overall hydrophobicity of the blend, allowing for better water resistance, but will ultimately compromise compostibility. For PBS blends, the tensile strength of the blend exceeded the tensile properties of pure PBS. Blends containing 50 wt% NTP had a tensile strength of 24 MPa (22 MPa for PBS) and

greatly improved water resistance, without compromising compostibility. However, the cost of using PBS may prohibit large-scale commercial implication.

Assessment of different methods to incorporate the compatibilizers in NTP/PBS blends led to the biggest improvement in tensile strength and secant modulus when two compatibilizers were used (at 50% NTP). Introducing pMDI just before injection moulding, but PEOX during extrusion, allowed for the greatest interaction between phases. Dissolving PEOX during NTP production improved acid-base interactions between PEOX and NTP as well as forming a network of hydrogen bonding between NTP, water and PEOX. pMDI increased bonding between NTP and PBS through reaction between amine terminal-groups from NTP and either the hydroxyl or carboxyl terminal-groups in PBS. PEOX improved the dispersion of NTP and the morphology showed no phase separation between NTP and PBS.

Crystallization of PBS in the NTP/PBS blends increased, which is likely to be due to nucleation effects by NTP or the presence of the compatibilizers, this served as a starting point for subsequent assessment on the rate of crystallization of PLA copolymer (PLA-g-IA).

Production of PLA-g-IA as a potential compatibilizer in NTP/PLA blends was successful, with a maximum degree of grafting of 0.75 wt%, with minimal chain scission. Grafting had a significant impact on crystallization and led to a reduction in melting point. It also increased the crystallinity, thermal decomposition temperature and mechanical properties of PLA, which lead to a similar hypothesis regarding the effect of blending, as observed in NTP/PBS blends. The presence of compatibilizers modified the formation of crystals and led

146

to an increase in crystallization rate in the blends, compared to pure polymers (PLA) or uncompatibilized blends (NTP/PBS).

The effect of grafting on thermal properties of PLA and its copolymer at different crystallization temperatures were investigated using DSC and WAXS. It was evident that the rate of crystallization of PLA increased significantly after grafting but limited the formation of larger and more compact crystals, leading to a lower melting point of grafted PLA. Reduction in T_m was also observed in NTP/PBS blends in spite of the fact that it crystallizes faster. These provide evidence that the rate of crystallization has increased after blending and the compatibilizers promoted crystallization although limited the formation of perfect crystals. Annealing at 100 ^{o}C increased the crystallinity of PLA and PLA-g-IA in short time such that reduces the possibility of NTP degradation to occur in NTP/PLA blends during extrusion. Incorporation of a bulky IA on the PLA backbone disrupted the crystal lattice of PLA by increasing the lattice spacing at the (110) plane (observed at an annealing temperature of 130 ^{o}C), suggesting that the helical structure of PLA was expanded.

Overall, it was found that blending NTP with LLDPE was less complicated compared with PBS. This is really surprising considering PBS is a linear biodegradable synthetic polymer consisting of more terminal groups than LLDPE. The ease of processing for NTP/LLDPE blends could be due to significant numbers of short branches in the LLDPE structure that possibly increased the interactions between the copolymers (PE-g-MAH), LLDPE and NTP. Apart from that, the method of compatibilization mechanisms themselves might also influence the processing. PE-g-MAH was added as copolymer in NTP/LLDPE blends while PEOX and pMDI were added as a third component in

NTP/PBS blends. The difficulties that occurred during NTP/PBS processing in which two-time extrusion is needed as well as two different compatibilizers, might be due to in-situ interactions at the interface of NTP and PBS phases during extrusion.

Blending NTP (at 50wt% or less NTP compositions) with different types of polymers in the presence of compatibilizer successfully produced synergistic combinations of two components such that include higher modulus, toughness (or more accurately referred to as energy to break) and improved water-resistance. However, at higher NTP compositions in the blends, restricted chain mobility after blending was evident and the effect of adding different types of compatibilizer was much less, reducing the toughness of the materials. The restriction in mobility of the molecular chains also affected thermal properties (T_m and T_c) of the blends. The results obtained from this study have laid down an important platform from which to further produce new blends with higher NTP compositions such that can be achieve using completely miscible compatibilizer with a high affinity for both phases. This would make NTP blends more valuable.

On-going research in to NTP/PLA blends using PLA-g-IA as compatibilizer is ongoing at the University of Waikato and includes studies into extrusion and injection moulding processing parameters. NTP/PLA blends have very narrow processing temperature because PLA has a high T_m (180 ^{o}C) while NTP starts degrading at a much lower temperature (~140 ^{o}C). Depending on composition, a suitable processing temperature is needed to process the blends with optimum mechanical properties.

For future work, other interesting topics to explore are the crystallization behavior of NTP/PLA blends and the spherullitic growth. Current work showed that the rate of crystallization increased with increasing of PLA-g-IA contents but limited the formation of perfect crystals. Crystallization can also be affected by addition of NTP. Therefore, a study on crystallization rate of PLA, PLA with PLA-g-IA and NTP/PLA blends as well as morphological development i.e the spherullitic growth will be valuable to manipulate the processing parameters. Furthermore, annealing could also be used to obtain a stable and high performance NTP/PLA blend.

The application of NTP-based blend has potential in the agricultural and packaging industry, especially in foamed products or where high impact resistance is required. Building a large-scale plant to produce NTP in New Zealand is an interesting prospect and blended grades may offer valuable alternatives to current grades of NTP.

Appendix: Copyright Information for Published Chapters

Chapter 3

Title: Properties of Bloodmeal/Linear Low-density Polyethylene Blends Compatibilized with Maleic Anhydride Grafted Polyethylene

Publisher: Journal of Applied Polymer Science

Used with permission with License Number: 3584500603934

Chapter 4

Title: Mechanical Properties of Thermoplastic Protein From Bloodmeal and Polyester Blends

Publisher: Macromolecular Materials & Engineering

Used with permission with license Number: 3584500514824

Chapter 5:

Title: Compatibilization of Protein Thermoplastics and Polybutylene Succinate Blends

Publisher: Macromolecular Materials & Engineering

Used with permission with license Number: 3584500429610

Chapter 6:

Title: Modification of poly (lactic acid) using itaconic anhydride by reactive extrusion

Publisher: European Polymer Journal

Used with permission with license Number: 3703391077853